Using an optical plankton counter to measure fine-scale and seasonal variation in the size-distribution of zooplankton communities.

By

Tomas Joda Bird
B.Sc., University of British Columbia, 2000

A Dissertation Submitted in Partial Fulfillment of the
Requirements for the degree of

MASTERS of SCIENCE

in the Department of Biology, University of Victoria

Supervisor: Dr. John Dower

ABSTRACT

The use of an optical plankton counters in zooplankton ecology requires sampling strategies and hypothesis testing that take into account its ability to collect high-resolution size-structured data, as well as its inability to distinguish zooplankton from detritus. Studies in Saanich Inlet and the Strait of Georgia, B.C. were performed to 1) compare the temporal resolution of OPC and net samples and 2) compare seasonal variation in the zooplankton community size structure against the predictions of biomass size distribution theory. The first part of this work found that OPC samples have finer resolution and require fewer replicates to approximate the mean abundance of zooplankton than net samples at time scales between 20 minutes and 48 hours. However, the OPC is subject to measurement error in high productivity waters. The second section of this work shows that the size-spectrum dynamics of zooplankton in the Strait of Georgia follow the predictions of biomass size spectrum theory. The interpretation of thse data using size-distribution theory suggests that variation in the trophic dynamics of the zooplankton community may be at the root of the observed seasonality.

TABLE of CONTENTS

LIST of FIGURES

CHAPTER 2

CHAPTER 3

APPENDIX 1

LIST of TABLES

CHAPTER 1

CHAPTER 2

CHAPTER 3

LIST of MAPS

ACKNOWLEDGEMENTS

I would like to thank my supervisors for their support, advice and knowledge. John Dower has been invaluable for his ability to locate the kernel of any problem and his clear expression of ideas. Ken Denman has constantly reminded me to think outside of the box and taught me to love programming. The other members of my committee, Dave Mackas and Brad Anholt provided feedback at intervals throughout my degree. Their expertise has been an invaluable resource.

I have had assistance from a diverse collection of people. In the Dower lab, Rob Campbell provided much needed assistance with programming, data collection and general knowledge. Rana El-Sabaawi and Akash Sastri were invaluable for their assistance with planning cruises and collecting data. Sarah Dudas and Gwang-Cheon Kim allowed me to bounce ideas off them and helped make the lab a great place to work.

I also had the pleasure to collaborate with a number of people from the University of British Columbia on the STRATOGEM project. Rich Pawlovicz, Susan Allen, Randall Lee, Shannon Harris, Olivier Riche and Mark Halverson were wonderful to work with on research cruises, despite the unhealthy obsession with donuts.

None of the data presented in this Chapter 3 could have been collected without the officers and crew of the CCG hovercraft *Siyay*. I especially appreciated the proficiency of Captain Ken Brown and his crew on board the MSV *John Strickland*, who worked insane hours to get me the data I needed for Chapters 2 and 3.

My families have given me emotional and logistical support throughout. My parents gave me lodging at the drop of a hat on many of the monthly cruises and helped me maintain a sense of perspective. My parents-in-law, El and Woody Bates made their house open to me as a place to write and a retreat from the chaotic headspace I managed to create in Victoria. Roger Donaldson deserves a special mention for the help he gave me in figuring out size distribution theory. Megan Simmer and Leanna Boyer very graciously put up with me while I wrote up in their house. The rest of my friends have been exceedingly generous with their time, advice, couches, ideas and ears at frequent stages throughout this degree. Pykie also deserves a (mildly) honorable mention: He didn't help much with the thesis, but he sure kept the deer out of our garden.

The last dedication on this page goes to my wife Amanda, who helped make this thing go. Her tireless support as an editor, scientist and partner deserve to be immortalized in words far fairer than these.

CHAPTER 1
INTRODUCTION

1.1 General Introduction

Marine and freshwater zooplankton are patchily distributed in both space and time (Barnes and Marshall, 1958; Haury, 1978, Mackas *et al.*, 1985). These patches persist and vary at all spatiotemporal scales, from minutes and centimeters to centuries and thousands of kilometers (Haury, 1978; Mackas *et al.*, 1985). At mega scales (thousands of kilometers and tens to hundreds of years - *sensu* Haury, 1978), interdecadal climatological oscillations and basin-scale differences in the physical environment cause changes in the biomass and species composition of zooplankton (e.g. Mackas *et al.*, 1998; Gallienne and Roberts, 1998; Rand and Hinsch, 1998; Venrick, 1999). Mesoscale (10^0 to 10^2 kilometers and days to months) variations include phenomena such as seamount effects (Isaacs and Schwartz, 1965; Dower and Mackas, 1996), frontal dynamics (Holligan *et al.*, 1984; Velez-Belchi, 2002), seasonal climatic variations (Arai and Mason, 1982; Nair *et al.*, 1983; Mackas and Galbraith, 2002a; Gaedke, 2004) and eddies (Doty and Ogaru, 1956; Mackas and Galbraith, 2002b).

The bulk of research on zooplankton prior to the 1980's has focused on understanding their distribution with respect to large-scale processes such as those mentioned above (Pinel-Alloul, 1995). Yet many important processes occur at finer scales, including distances of centimeters to hundreds of meters and temporal scales of seconds to days. Understanding how and why fine-scale processes influence the distribution of zooplankton is important for characterizing how individuals interact with their environment. Important biological processes occur at scales of meters to hundreds of meters, including feeding (Conover and Lalli, 1972; DeRobertis *et al.*, 2001; Haberman *et al.*, 2001), swarming (Ambler, 2002; Baumgartner, 2003), migration (Boyd, 1973; Bollens *et al.*, 1992) and reproduction (Lazzarretto *et al.*, 1994; Harris, 2000). As well, fine-scale physical processes can influence the distribution of zooplankton, including Langmuir circulation (Langmuir, 1938; Hamner and Schneider, 1986) small-scale turbulence (Davis *et al.*, 1991; Yamazaki *et al.*, 2002). Fine-scale variation in

zooplankton abundance also has an impact on how their large-scale distribution is perceived. Concentrations of zooplankton can vary by several orders of magnitude overnight due to migration (Rodriguez and Mullin, 1986b), or within meters due to swarming (Ambler, 2002).

However, it was not until after the 1950's that researchers began to accept the idea that fine-scale patches in the distribution and abundance of zooplankton were not simply due to sampling error or random 'noise' (Barnes, 1950; Cassie, 1963; Wiebe and Holland, 1968; Pinel-Alloul, 1995). This is largely due to the inaccuracy of the net based sampling devices that have been the predominant tool used to enumerate zooplankton communities (Wiebe and Benfield, 2003). A net works by filtering a volume of water through a mesh and retaining all the plankton greater than its mesh size. The use of nets makes the implicit assumptions that 1) all organisms greater than the mesh size are retained in the sample, 2) the entire volume of water sampled and, by extension, the water in the immediate vicinity, is relatively homogeneous and 3) the volume of water sampled is known. Yet at fine scales, these assumptions are often violated. Clogging by phytoplankton or detritus reduces the filtration efficiency of nets, altering the 'true' volume sampled and influencing the apparent concentration of zooplankton (Smith *et al.*, 1968; Brander *et al.* 1993). Some species actively avoid nets (Fleminger and Clutter, 1968; Sameoto *et al.,* 1993), or have different retention than other species of the same size (Saville, 1958; Nichols and Thomson, 1991; Gallienne and Robins, 2001). Finally, different net types sample differently and can lead to different approximations of zooplankton abundance within the same community (Fraser, 1966).

Increasingly precise sampling devices such as opening/closing nets (Nansen, 1915; Clarke and Bumpus, 1939; Motoda, 1953), multiple net systems (Tucker, 1951; Wiebe *et al.,* 1976) and Continuous Plankton Recorders (Longhurst *et al.*, 1966; Bruce and Aiken, 1975) have been used to measure patchiness of zooplankton at finer scales. Despite these advances, however, zooplankton ecologists are still limited by the resolution of their sampling gear. It is only in the past 20 years that fine-scale sampling of zooplankton

communities has become feasible, due to the development of automated sampling devices (Wiebe and Benfield, 2003).

1.2 Automated Sampling Devices

Automated zooplankton samplers can be divided in to two categories: optical and acoustic. Acoustic samplers emit ultrasonic pulses that reflect off zooplankton-size particles, which are then recorded in terms of the total volume of backscatter and the signal strength from individual sources (Foote, 2000a). Optical systems generally detect individual particles in a small sub-sample of water and record either images of the particles or an estimate of their size, along with an indication of when and where they were located in the water column (Foote, 2000b). Optical samplers can be further classified as image-forming or particle detecting. Image forming systems include the Video Plankton Recorder (Davis *et al.,* 1996), the "shadowed image particle profiling and evaluation recorder", or SIPPER (Samson *et al.*, 2001), and the holographic zooplankton imager (Knox, 1966; Katz *et al.,* 1999). All of these systems record images of zooplankton as they pass through a pre-defined volume of water, which allows positive identification of each particle encountered. Unfortunately, all require intensive post-sampling analysis which can be just as laborious as analyzing net samples. Particle detection systems such as the Optical Plankton Counter (Herman, 1988, 1992, 1993) or Electronic Zooplankton Counting Device (Boyd, 1973) measure the size and/or shape of particles as they interrupt a beam of light or electrical current within a defined sampling volume. They have the advantage of taking measurements of individual particles *in situ*, which cuts down on post-sampling processing. Particle detection systems are unable to differentiate between plankton and detritus, however, which can introduce significant error into their estimates of zooplankton abundance (Heath, 2001).

1.3 The Optical Plankton Counter

The OPC was developed by Alex Herman in 1988 and has been described in detail elsewhere (Herman, 1988, 1992, 1993). It consists of a rectangular sampling tunnel (2 cm by 25cm aperture) across which a 4 by 20mm (cross section) beam of 640nm LED light is directed at a photodiode array. As the instrument is towed (or lowered vertically),

particles passing through the tunnel interrupt the beam, causing a voltage fluctuation in the array. This voltage fluctuation is proportional to the amount of light blocked by each particle and, hence, to its cross-sectional area. The Equivalent Spherical Diameter (ESD) of each particle is calculated from the magnitude of the voltage fluctuation, assuming that all particles are spherical (Herman, 1988). Because the size of each particle is proportional to the amount of light sensed by the photodiodes, turbid water can influence the perceived size of particles. To correct for this, a measure of light attenuance is calculated from a feedback loop between the sensory array and a separate photodiode. This light attenuance is used to correct the measured size of each particle. The OPC is also equipped with a pressure sensor to record the depth of each particle encountered. It is important to note that, strictly speaking, the OPC cannot distinguish between detrital particles and zooplankton. Because of this, all OPC measurements are hereafter referred to as 'particles' rather than zooplankton.

While the utility of a 'particle' counter to zooplankton ecologists may seem rather limited, the OPC has been shown to provide robust estimates of the abundance of zooplankton (relative to net samples) in a variety of ecological settings (Herman, 1988, 1991, 1992; Huntley *et al*, 1995; Gallienne and Robins, 1998; Sprules *et al*, 1998; Grant *et al*, 2000; Edvardsen *et al,* 2001; Baumgartner, 2003; Nogueira *et al,* 2004). Nevertheless, in practice, OPCs still require validation against better accepted techniques as well as the development of novel analytical techniques with which to make the most of the rich data that they provide. However, the ease with which OPC samples can be collected and analyzed makes this tool an attractive option to researchers wanting greater numbers of samples (or more intense spatiotemporal resolution) rather than detailed species information. As such, the OPC is poised to take a similar place in zooplankton ecology as the fluorometer has taken in phytoplankton research. In other words, it provides a reasonable proxy for the size distribution of zooplankton and can be interpreted either in relation to net samples (*i.e.* as when fluorometer data are directly compared to *Chl* extracted from water samples) or on its own merits (*i.e.* in the same way that phytoplankton ecologists accept the raw voltage output from a fluorometer as a useful proxy for *Chl*).

1.4 Biomass Size-Distribution Theory

The OPC provides a means of collecting data in a form that is directly (and immediately) transferable to size-based models of zooplankton dynamics. Biomass size-distribution theory describes the dynamics of planktonic ecosystems using simple assumptions concerning the way that energy is transferred from small to large size classes. (Sheldon *et al.*, 1972; Kerr, 1974; Sheldon *et al.*, 1977; Platt and Denman, 1977,1978). The theory has its origins in the hypothesis of Sheldon (1972) which asserts that the biomass of plankton in the ocean is approximately equally distributed across logarithmically increasing size classes. From this observation, Platt and Denman (1977, 1978) proposed a partial differential equation to describe the flow of energy through a size-based planktonic ecosystem.

$$\frac{\partial \beta(w)}{\partial t} = -\frac{\partial (g(w)\beta(w))}{\partial w} - u(w)\beta(w) \qquad (1.1)$$

Where $g(w)$ is the weight specific individual growth rate (gC d^{-1}) and $u(w)$ is the population level growth rate (d^{-1}) and $\beta(w)$ is the normalized biomass size distribution (NBSD) such that

$$\beta(w) = \frac{b(w)}{\Delta w} \qquad (1.2)$$

where b is the biomass (gC m^{-3}) in size class (w) and Δw is the weight interval (g C) between logarithmically increasing size classes (Platt and Denman, 1978 – see also Appendix 2 for more detail). Essentially, equation 1.1 predicts that the distribution of biomass (β) in an ecosystem flows from small to large sized organisms over time. Thus, when biomass is added to smaller size classes (*e.g.* the spring phytoplankton bloom), it moves as a pulse through the NBSD to larger size classes (Rodriguez and Mullin, 1986a; Heath, 1995; Gaedke, 2004).

One of the model's interesting features is that the slope of the NBSD:

$$\frac{\partial \ln(\beta)}{\partial \ln(w)} \qquad (1.3)$$

can be used to compare the dynamic states of different plankton communities. If it is assumed that an ecosystem is in steady state and empirical estimates of g and μ are available, then it is possible to derive the slope of the NBSD from the model. Silvert and Platt (1978) found this slope to be around -1.2. Practically speaking, $g(w)$ and $u(w)$ are difficult to estimate in most plankton communities. However, the slope of the NBSD can be measured from field data, albeit with significant effort (e.g. Sprules and Munuwar, 1986; Sprules *et al.*, 1991; Gaedke, 1992; Quinones, 2003). Zooplankton communities have been found to have slopes similar to the predictions of this model (Rodriguez and Mullin, 1986; Ahrens and Peters, 1991b; Gaedke, 1992). Other planktonic communities have been shown to deviate from the predicted -1.2 slope. In some communities, the slope varies seasonally, becoming shallower during the spring and summer and indicating a greater proportion of larger organisms (Gasol *et al.*, 1991; Gaedke, 1992, 1993; Garcia, 1993; Heath, 1995; Cozar *et al.*, 2003; Gaedke, 2004). There is, as yet, no adequate explanation as to why the NBSD slope should vary. Such an explanation would require detailed information on the size distribution of plankton, which is difficult and time consuming to collect with nets. The OPC is ideally suited for generating detailed size-structured data and may thus prove to be invaluable for testing and developing biomass size distribution theory.

1.5 Rationale for this thesis

With the advent of powerful sampling tools such as the OPC comes the potential for new sampling strategies and analyses. There is also a need to validate this new tool against accepted sampling strategies and to develop theoretical approaches to the analysis and interpretation of its data. In terms of its ability to enumerate zooplankton, the OPC has been tested in a variety of situations demonstrating both its versatility in different environments and its precision at describing the size distribution of zooplankton communities (Table 1.1). However, OPC sampling has never been compared to net sampling in terms of its ability to resolve fine-scale variation in zooplankton abundance. Furthermore, the OPC has only been infrequently used in the context of testing size-based models of zooplankton ecology. While there has been some work using the OPC to measure the size distribution of zooplankton, (Heath, 1995; Huntley and Zhou, 1997;

Edvardsen *et al.,* 2001, Nogueira *et al*, 2004), there is much room to use OPC data to test the predictions of biomass size distribution theory.

Given these perceived research needs, the goals of this thesis are twofold:

1) to compare the fine-scale temporal resolution of OPC and net samples and explore short term patterns of variation in zooplankton abundance.

2) to use OPC data to test the predictions of and explore further developments in biomass size distribution theory by measuring seasonal changes in the biomass distribution of the zooplankton community in the Strait of Georgia, B.C..

1.6 Structure of the thesis

In **Chapter 2,** a series of high-frequency OPC and net samples taken in Saanich Inlet, British Columbia are compared to determine the limits of their sampling resolution in terms of:

1) their relative ability to resolve changes in zooplankton abundance over time
2) their relative ability to resolve changes in the zooplankton community composition over time and
3) the sampling effort required to adequately approximate the mean abundance of zooplankton within a given time.

In addition, the short-term (hourly) variation in the zooplankton community structure is evaluated. This is the first study to compare the temporal resolving power of OPC and net samples at fine temporal scales.

In **Chapter 3**, a 1.5 year series of OPC and net samples are analyzed for changes in the size distribution of the zooplankton community of the Strait of Georgia. Evidence is sought for

1) a pulse of biovolume (as a proxy for biomass) moving through the biovolume distribution during the spring bloom
2) changes in the slope of the biovolume distribution before and after the spring bloom

These seasonal observations are related to what is already known about the seasonality of the zooplankton community in the Strait of Georgia. In addition, possible mechanisms for the observed size distribution changes are explored using the biomass size distribution theory of Platt and Denman (1978). This is the first detailed analysis of the seasonal variation in the zooplankton community's size distribution in the Strait of Georgia.

In **Chapter 4**, the utility of the OPC as a sampling tool in zooplankton ecology is discussed, along with some caveats on its use and suggestions of where it will prove to be useful in the future. In **Appendix 1**, evidence is presented of how phytoplankton can have a significant impact on the size measurements made by the OPC. This is the first attempt to quantify this effect from field data. **Appendix 2** outlines in more detail the derivation of biomass size distribution theory.

Study	Location	Sampling Gear Used	Ratio of Measured zooplankton # m^{-3} OPC:OTHER	r^2	Range of Zooplankton Concentration, # m^{-3}
Huntley *et al.* (1995)	California Current	Towed OPC, oblique Bongo nets (155μm mesh)	3:1 to 14:1	0.22 to 0.94	10^1 to 10^3
Labat *et al.* (2002)	Southern Ocean	Vertical OPC hauls, vertical WP2 net hauls (200μm mesh)	3:1	NA	10^2 to 10^3
Gallienne & Robins (1998)	N and S Atlantic	Desktop OPC and in-line 200μm mesh (pumped from sea)	0.94:1	0.55	10^2 to 10^5
Grant *et al.* (2000)	Southern Ocean	Towed OPC, LHPR (200μm mesh)	0.01:1* to 14:1*	0.01* to 0.99*	10^2 to 10^5
Herman *et al.* (1993)	NW Atlantic	Towed OPC, towed acoustic backscatter	2:1	NA	NA
Sprules *et al.* (1998)	Freshwater lakes	Desktop OPC, preserved net samples	0.02:1 to 1:1 *	NA	10^3 to 10^6
Zhang *et al.* (2000)	Cultured *Artemia*	Desktop OPC, known abundances (high detritus water)	0.2:1* to 0.84:1 *	0.57* to 0.94*	10^0 to 10^2
Osgood (1997)	Santa Barbara Basin	Vertical OPC casts, Vertical MOCNESS (333μm mesh)	0.3:1 to 10:1	0.42	10^0 to 10^3
Gallienne *et al.* (2001a)	NE Atlantic	Desktop OPC, live net samples	0.9:1 to 5:1	NA	10^2 to 10^4
This study	Saanich Inlet, BC.	Vertical OPC casts, Vertical SCOR net (233 um)	2:1 to 6:1	0.05	10^3

* OPC data corrected by a regression model

Table 1.1. Studies that compare OPC counts against other measures of zooplankton abundance. (OTHER) refers to an alternate sampling device. The reported ratio of zooplankton abundance as estimated by the OPC:OTHER is given, along with the r^2 value of the linear regression between OTHER and OPC. Some studies used a linear regression model to correct for error in the OPC abundance estimates. These studies are marked with a *. NA indicates a regression was not performed.

CHAPTER 2

Comparing the temporal resolution of an Optical Plankton Counter with traditional net samples.

2.1 Introduction

It has long been recognized that the biomass and size structure of zooplankton communities are variable over spatiotemporal scales finer than those at which field sampling is usually conducted (Yamazaki *et al.*, 2002; Denman and Mackas, 1978). In 1978, Haury *et al.* used a variation of a Stommel diagram to describe the relative amount of variation in zooplankton abundance at different spatiotemporal scales, and suggested that our ability to resolve changes in zooplankton abundance is limited at smaller scales (10^0 to 10^2 m and minutes to days) by the resolution of our sampling techniques. Yet many biologically important processes such as migration, swarming and predation are known to occur at these scales (Haury, 1978). Thus, our understanding of these processes and how they shape zooplankton communities in the field is limited.

Despite their limited accuracy at smaller spatiotemporal scales (Pinel-Alloul, 1995; Denman and Mackas, 1978), nets remain the primary tool used to sample zooplankton. Many researchers have tried to use nets to describe zooplankton communities at small (kilometers and hours) spatiotemporal scales (e.g. Barnes, 1950; Hopkins, 1963; Wiebe and Holland, 1968; Wiebe, 1970; Nair *et al.*, 1983), but the effort required to collect and analyze a sufficient number of samples is usually prohibitive. Consequently, small scale processes are often ignored in favor of more easily detected (e.g. order of magnitude) mesoscale changes.

This broad-scale view of biological oceanography is currently being reshaped by recent technological advances (Wiebe and Benfield, 2003). A number of different automated zooplankton samplers have become available, all of which facilitate rapid, fine-scale enumeration of zooplankton. One such tool is the Optical Plankton Counter® (OPC).

The design and calibration of the instrument has been documented elsewhere (see introductory chapter, also: Herman, 1988; Herman, 1992; Herman *et al.*, 1993). The OPC's primary strengths are its ability to rapidly count and size large numbers of zooplankton. From these data it is relatively easy to construct a size distribution of the zooplankton community being investigated (e.g. Herman, 1992; Sprules, 1998; Gallienne *et al.*, 2000).

Comparisons of OPC and net samples from diverse ocean and lake habitats have shown that measurements of zooplankton abundance from the two techniques are significantly correlated (Huntley *et al.*, 1995; Grant *et al.*, 2000; Pinca and Huntley, 2000; Gallienne *et al.*, 2001a; Labat *et al.*, 2002). However, most of these studies were conducted across broad spatiotemporal scales (10^1 to 10^3 kilometers, weeks to months). OPC and net estimates of zooplankton abundance and community size structure at smaller scales (10^0 to 10^2 meters, minutes to hours) have not been compared. As such, the utility of the OPC at these finer scales remains untested.

Comparing zooplankton abundance estimates from nets and OPC samples at fine scales is difficult and does not necessarily provide an indication of which has greater resolution. The magnitude of error associated with either sampling device may be greater than the magnitude of the natural variation expected in the community. Instead, the resolution of series of net and OPC samples can be compared in terms of the relative amount of autocorrelation present in each series. Early views of zooplankton ecology assumed that zooplankton were randomly distributed in the water column (e.g. Winsor and Clarke, 1940; Silliman, 1946). It is now understood that patchiness exists (and persists) at all spatiotemporal scales in zooplankton communities (Haury, 1978). Nonetheless, in a relatively undisturbed environment, closely spaced zooplankton samples should be more similar than distantly spaced samples. Hence, a higher resolution sampling technique should be able to detect a greater degree of autocorrelation relative to a less sensitive technique.

In practical terms, the resolution of a sampling technique can also be approximated by determining how many samples should be collected in order to adequately approximate the mean zooplankton abundance. Regardless of whether net samples have greater (or lesser) resolution than OPC samples, one of the factors limiting their use is the time required to analyze net samples. Because the OPC requires comparatively little post-sample analysis, it is possible to collect much more data with much less effort. Thus, even if the OPC requires a greater number of samples in order to approximate the mean zooplankton abundance, it may still be cost effective to use the OPC instead of, or to supplement, net samples.

In order to test the relative ability of OPC and net samples to resolve changes in zooplankton abundance at fine scales, the following questions were posed:

(1) Are fine-scale (hours to days) estimates of zooplankton abundance and size structure from an OPC similar to those collected with a traditional plankton net?

(2) What is the fine-scale temporal resolution of OPC and net samples?

(3) What sampling effort is required to approximate the mean abundance of zooplankton in a community using OPC and net samples?

2.2 Methods

2.2.1 Physical and biological oceanography of Saanich Inlet

These data were collected in Saanich Inlet, a 240m deep fjord-like inlet at the south end of Vancouver Island (Map 2.1). The inlet is deep in the middle (240m) and has a 70-80m deep sill at one end that prevents continuous renewal of the deeper areas of the fjord. Saanich Inlet is relatively sheltered, with little tidal or wind mixing (Gargett, 2003; Herlinveaux, 1962). Saanich Inlet experiences strong spring blooms which occur after surface stratification of the water column sets in (Takahashi *et al,* 1977; Gargett, 2003). Mini-blooms sometimes occur in the summer (Anderson and Devol, 1973; Takahashi *et al.*, 1977), fueled by advective exchange of nutrients with turbulently mixed areas outside

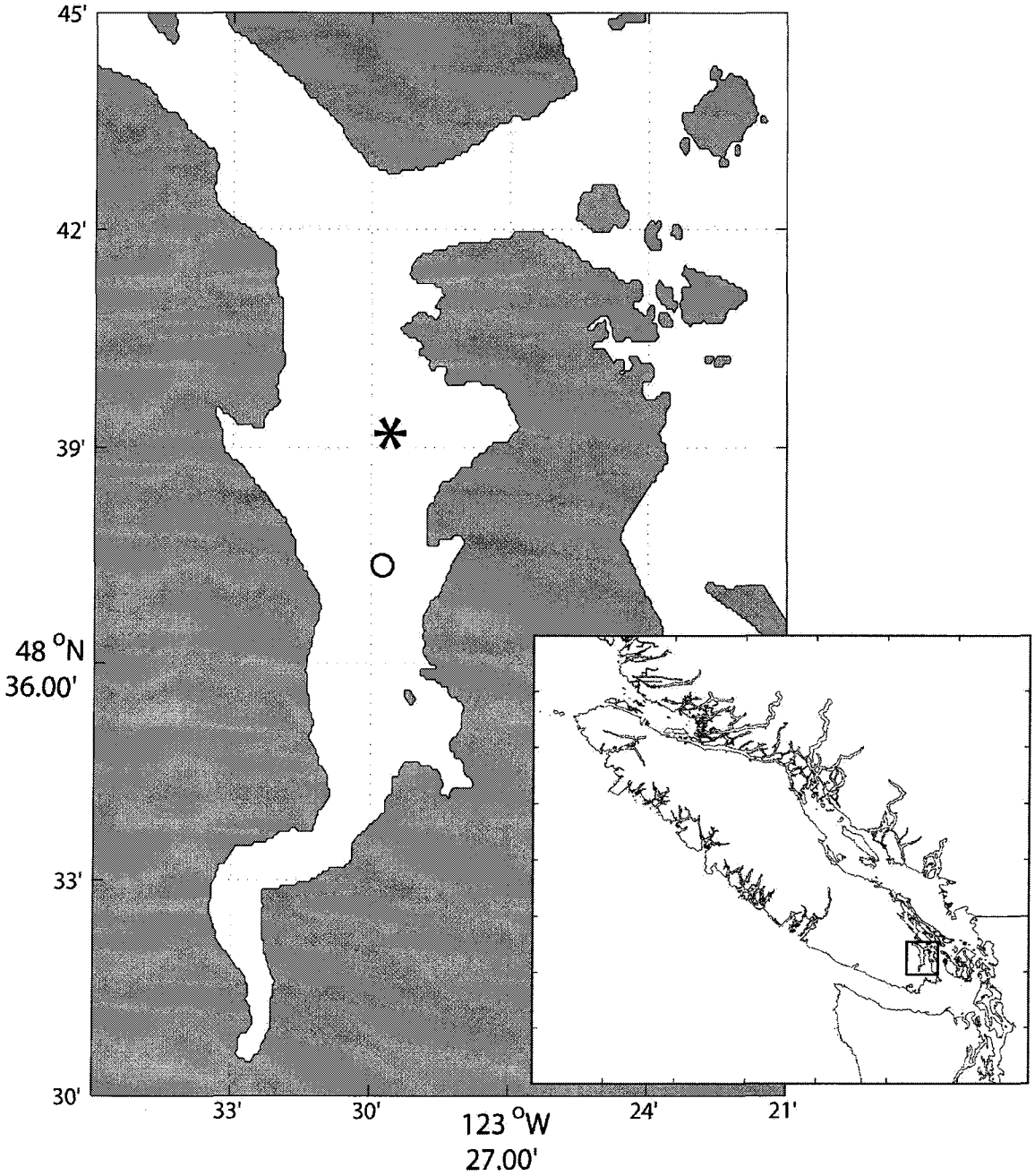

Map 2.1. Map of Saanich Inlet B.C., location of sampling for Chapter 2 of this thesis. Star indicates the sample site used for the six days of sampling between June 18 and 24, 2002. Circle indicates the location of the 220m sample used to examine the depth and size distribution of OPC-measured particles beneath the oxycline.

of the inlet (Gargett, 2003). The presence of a sill at the mouth of the inlet, combined with its depth and the high levels of productivity contribute to a deep anoxic layer which is renewed approximately yearly (Herlinveaux, 1962). The depth of the oxycline varies, but is usually around 110 to 160m.

In terms of abundance, the zooplankton community of Saanich Inlet is dominated by copepods such as *Aetidius divergens*, *Metridia pacifica*, *Calanus* spp., *Pseudocalanus* spp., *Oithona similis* and *Corycaeus anglicus* (Koeller *et al.*, 1979). *Neocalanus plumchrus,* the dominant copepod in the neighboring Strait of Georgia, is notably less abundant in Saanich Inlet. Amphipods such as *Orchomene obtusus* and *Parathemisto pacifica* are common, as are Euphausiids (*Euphausia pacifica)* (Boden and Kampa, 1963; Mackie and Mills, 1983). Gelatinous zooplankton such as jellyfish (*Aglantha digitale*, *Sarsia* spp., *Diphyes* spp., *Obelia* spp., *Phialidium* spp.), pteropods (*Clione limacine* and *Limacina helicina*) and chaetognaths (*Parasagitta elegans*) are an important but understudied component of Saanich Inlet's planktonic community (Larson, 1987; Huntley and Hobson, 1978). The vertical distribution of zooplankton varies both daily and seasonally. Some species undergo a diel migration, such as *E. pacifica, M. pacifica A. digitale* and *S. elegans* (Mackie and Mills, 1983). The lower depth distribution of most organisms is limited by the oxycline, though the amphipod *O. obtusus* has been found feeding below this depth (Mackie and Mills, 1983; DeRobertis, 2001).

2.2.2 Data collection

Data were collected between June 18-24 2002. A high-resolution data series of OPC and net data were collected by sampling repeatedly from the University of Victoria vessel *MSV John Strickland* at a single location (Map 1.1) in the inlet. The vessel anchored in 110 meters of water on June 18 and stayed on site for 48 hours. The sampling package consisted of a Focal Technologies OPC-1T which was mounted on a 100 kg steel frame with a Seabird Electronics 'SEACAT 19' CTD and a Wetlabs 'Wetstar®' fluorometer. Data from the OPC were logged to an on-board computer housed in a submersible pressure casing. The OPC was lowered at a speed of 1m/s to a depth of 100m and only the data from the downcasts were used. Net samples were collected with a traditional

SCOR-type net with a 50cm diameter mouth, 236μm mesh and a TSK mechanical flowmeter mounted in the mouth. Each net cast was towed vertically from 100m to the surface at approximately 0.75m/s. Net samples were preserved in 5% buffered formalin for subsequent analysis. Sampling was conducted every 20 minutes with the OPC and hourly with the net. After the initial 48 hour period, the sampling site was revisited periodically over the next 4 days.

2.2.3 Sample processing

CTD data: Water density (Sigma-t) and chlorophyll *a* (chl *a*) fluorescence (Volts) data for each cast were binned into 1m depth bins. An average chl *a* fluorescence profile from all casts collected during the cruise was calculated to locate the depth at which chl *a* fluorescence was maximum. Time series of water density (Sigma-t) and chl *a* fluorescence were plotted at the depth of the chl *a* maximum for comparison with the surface OPC data. Tide heights were generated using Xtide (Flater, 1998) and plotted along with chlorophyll *a* fluorescence, density and the OPC data.

Net data: The net data used in this analysis included 30 of the 54 net samples that were collected over the 6 day time series. These 30 samples were chosen so as to get the greatest number of pair-wise comparisons at both short (hourly) and long (six day) time separations, without needing to sort all 54 samples. All net samples from the first 12 hours were sorted, then every 3rd sample for the next 12 hours and every 6th sample for the last 24 hours. All the samples from the remaining 4 days were sorted. All net samples were volume corrected using the flowmeter readings. Each sample was split 5 times and all organisms in one split were identified to developmental stage. We calculated the abundance (m^{-3}) for each species in each cast, using towed volumes corrected from the flowmeter readings. For each species (and stage) identified, length was taken from existing zooplankton database maintained at the Institute of Ocean Sciences (courtesy of D.L. Mackas, Institute of Ocean Sciences, Sidney, B.C.).

OPC data: Raw OPC data were imported from the OPC and filtered for incorrect timer, depth and count values. Some OPC data were obviously skewed during collection by

either voltage fluctuations or other equipment malfunction. Each cast was therefore inspected visually and rejected for any of the following reasons: high (>1000 m^{-3}) concentrations of particles in any one 100 μm size bin; whole-cast particle concentrations that were an 1-2 orders of magnitude greater or less than the average; incomplete casts; garbled data. After processing, there were a total of 151 OPC casts taken over the 6 days, with 131 casts concentrated in the initial 48 hours.

The OPC is prone to increased sampling error in high turbidity water such as that found during high primary productivity (Zhang *et al.*, 2001; Sprules *et al.*, 1992; Heath, 2001) such as that observed in Saanich Inlet during the spring/summer. To determine whether phytoplankton had an impact on the OPC data, the surface (0 - 20m) OPC data were visually compared to surface chl *a* fluorescence data. An average depth distribution of counts m^{-1} (i.e. number of particles encountered by the OPC in a one meter vertical section of water) was calculated for small (250 - 500μm) and large (1500 - 3000μm) particles over all casts, as these sizes are most significantly affected by detritus. Time series of the average surface (0 - 20m) zooplankton counts per meter in the small and large size classes were also plotted to compare against the surface chl *a* fluorescence and density data.

To determine whether the OPC was counting primarily detritus below the surface layer, a series of deeper casts were taken in the deepest part of Saanich Inlet. A deep non-renewing layer causes an anoxic layer to develop at about 120m depth in the inlet, below which few zooplankton live (Mackie and Mills; 1983). The OPC should therefore have detected few counts below the oxycline. A series of five casts made in the deepest part of Saanich Inlet over three days were averaged and presented as a single estimate of the depth distribution of all particle sizes. These casts were used to test whether the OPC was detecting zooplankton particles where there should have been none.

The OPC casts used in subsequent analyses are hereafter referred to in terms of two series. OPC_{all} consists of all casts over the 6 days, while OPC_{net}, (a sub-series of the OPC_{all} series) consists of casts collected within 5 minutes of a net sample.

2.2.4 Data analysis

Comparison of net and OPC estimates of zooplankton abundance and zooplankton community structure:

Some zooplankton species are known to be capable of escaping through plankton net mesh that is only 1/3 their prosome length (Gallienne and Robins, 2001b; Brander *et al.*, 1993; Nichols and Thompson, 1991; Yentsch and Duxbury, 1956). In this case, the mesh size of the net was 236 μm. Thus, to ensure that comparisons between the net and the OPC only consider size classes that both sampling devices can sample similarly, all zooplankton with prosome length less than 650 μm (i.e. ~3 x 236 μm) were excluded from the analyses. In addition, because of the small aperture of the OPC sampling tunnel relative to the size of the net mouth (0.005m^2 vs. 0.75 m^2), escapement of larger zooplankton was likely a greater problem in OPC than net samples (Fleminger and Cluter, 1963). In the present study, an arbitrary upper size-limit of 3.0mm was chosen. Thus, subsequent analyses are based on particles spanning the size fraction from 0.65mm – 3.0mm.

Total abundance of zooplankton in the 0.65 – 3.0mm size range was calculated for the OPC_{all}, OPC_{net} and net samples. The mean and the coefficient of variation were calculated for each of the three series and a Spearman Rank Correlation was used to test for a correlation between zooplankton abundance in the net and OPC_{net} samples. The average size frequency distribution for each series was calculated by binning individual counts into 100μm size bins between 650 and 3000μm. The Spearman Rank Correlation between log(abundance) and log(size) was calculated for the average OPC_{net} and net size structures.

Temporal resolution of OPC and Net series: To determine whether there was a correlation between adjacent samples in each series, the temporal autocorrelation in each of the OPC_{all}, OPC_{net} and net series was tested (Legendre and Legendre, 1998). As not all the net and OPC_{net} samples were evenly spaced, we tested the autocorrelation only for

the first fourteen hours. For the net and OPC_{net} series, lags of 1 hour were used while lags of 20 minutes were used to test the OPC_{all} for the first 48 hours.

Ecological Similarities: To determine how the size structure in each series changed through time, the ecological similarity (Percent Similarity Index or PSI) was calculated for all pairwise combinations of samples, and plotted against the time separating each pair. Like other ecological distance measures, PSI is used to describe differences in the species composition (Mackas, 1981; Dower and Mackas, 1996) and size structure (Pinca and Huntley, 2000) of zooplankton samples. It calculates the cumulative difference between the proportional contribution of species in two samples;

$$PSI = 100 - 50 * \sum_{i=1}^{I} \left| P_{xi} - P_{yi} \right| \qquad (2.1)$$

Where P_{xi} is the proportional contribution of species i in sample x. In identical samples, the percent similarity is 1, while orthogonal samples are 0% similar. In the present case, size classes of particles were used instead of species classes. One problem with utilizing size instead of species classes is that the categories used are not independent. In order to address this problem, the PSI was also calculated using logarithmically increasing size bins, so that the mean abundance in each size class was more or less equal. The size of the bins was chosen so as to maximize the average signal to noise ratio in vertical casts. Percent similarity was plotted against the time separating each sample pair. This kinf of plot is called a Structure Function Diagram and is discussed in Mackas (1980).

Mantel Test: To test whether there was a significant decay in PSI with increasing time between samples in each of the three series, a normalized Mantel test (Mantel, 1967; Smouse *et al.,* 1987) was used. The Mantel test determines whether there is a significant correlation between, for example, a similarity matrix (S) and a temporal separation matrix (T). The Mantel test can be based on a two dimensional correlation coefficient (Manly, 1991). The correlation coefficient (r) is first calculated using the original matrices, in this case percent similarity (S) and Time separation (T). Randomized r values are then re-calculated using the original T matrix and a randomly permuted S matrix. This procedure is repeated several thousand times to build a distribution of randomized r values. If the

proportion of randomized *r* values that are greater than the original *r* is smaller than alpha (0.05), then the two matrices are considered to be significantly correlated. In the present study, S was a matrix of Percent Similarities between all possible sample pairs and T was the time separating each pair. The test was also performed between the OPC and Net Percent similarity matrices, to see whether the two sampling types decayed similarly over time.

Comparing sampling effort requirements: A Monte Carlo randomization technique was used to determine the number of samples required to approximate the mean abundance of zooplankton in a community (Manly, 1991). It was assumed that the mean of the first 48 hours in all series represented the 'true' abundance. Sub-samples of a set number were then randomly drawn (with replacement) from the series and the mean re-calculated. If the sub-sample mean was within +/- 10% of the "true" mean, it was counted as being "close". This procedure was repeated 5000 times. The likelihood of approximating the mean was then estimated as the number of "close" occurrences over the number of attempts. This process was repeated for sub-sample sizes of between 1 and 25 for the OPC_{net} and net series.

To estimate the minimum number of samples required to approximate the mean abundance for shorter time periods, the above randomization was performed on the OPC_{all} series for smaller sampling periods. Initially, the minimum number of samples required to approximate the mean of the first two hours (with 95% likelihood) was calculated. This process was then repeated for all sequential two hour periods in the series and the average effort was calculated. This test was performed for periods from 1 to 24 hours. The likelihood of success with a given number of samples over a certain time period was plotted.

2.3 Results

2.3.1 Comparison of OPC data with surface fluorescence and the oxycline

Depth profiles of average fluorescence, density and small and large particle abundance are shown in Figure 2.1. The average fluorescence maximum of between 0.4 and 1.1

volts occurred at approximately 6m. The average OPC depth profile of large particles is similar to the fluorescence profile, with a peak at about 6m. Small particle abundances mirrored the fluorescence peak, with a minimum value of 5-10 counts m^{-1} at 6m. The depth profile of particle abundances shows that the surface layer contained many large particles (Figure 2.2). From the surface to 20m depth, the size distribution was dominated by larger particles. Between 20 and 100m, the size distribution was dominated by smaller (250 - 500μm) particles. Between 100 and 130m, small particle abundances were lower (20-40 m^{-3}), then between 140 and 160m there was another spike in small particle abundances (60-100 m^{-3}). Below this depth, the abundance of most particles dropped off to lower levels than any other depth.

Surface fluorescence values were also periodic in time, though less so than Sigma-t (Figure 2.3). Time series of surface OPC abundance in small and large size classes showed evidence of 12 hour periodicity as well (Figure 2.3). These counts were plotted as the residuals of (series) minus (series average) to show their variation around the mean. The periodicity of OPC counts appeared to be tidal. A diel signal is also possible, though difficult to separate from the tidal signal with the present data set.

2.3.2 Comparison of OPC and Net data

Net samples were dominated numerically by small copepods (*Corycaeus anglicus*, *Oithona similes*, *Microcalanus pigmaeus*), euphausiids (*Euphausia pacifica),* larvaceans (*Oikopleura dioicea*) as well as euphausiid eggs, copepod nauplii and protozoa. These groups constituted 83% of the total abundance in the net samples. Species less than 1mm in size made up almost 75% of the total abundance. The mean, median, maximum and minimum abundances of the dominant taxa are given in Table 2.1.

Neither the net nor the OPC_{net} abundance series showed much in the way of consistent variation, though the abundance of zooplankton in both series seemed to increase slightly at night (Figure 2.4). The net series had an average abundance of 1230 counts m^{-3} and a coefficient of variation of 0.38. The OPC_{net} series had a much higher mean abundance of 2363 m^{-3} and a coefficient of variation of 0.15, while the OPC_{all} series had a mean

abundance of 2515 and a coefficient of variation of 0.11, indicating greater variation in the net series (Table 2.2). On average, the OPC_{net} counted 1.5 times more particles than did the nets. Despite this, the OPC_{net} and net series still shared some common features. Both displayed a period of low abundance (~1500 m^{-3} for net samples, ~2500 m^{-3} for OPC samples) during the first few hours, followed by a period of higher abundance at around midnight on the 18th (~2500 m^{-3} for net samples, ~3500 m^{-3} for OPC samples) followed by a slow decline.

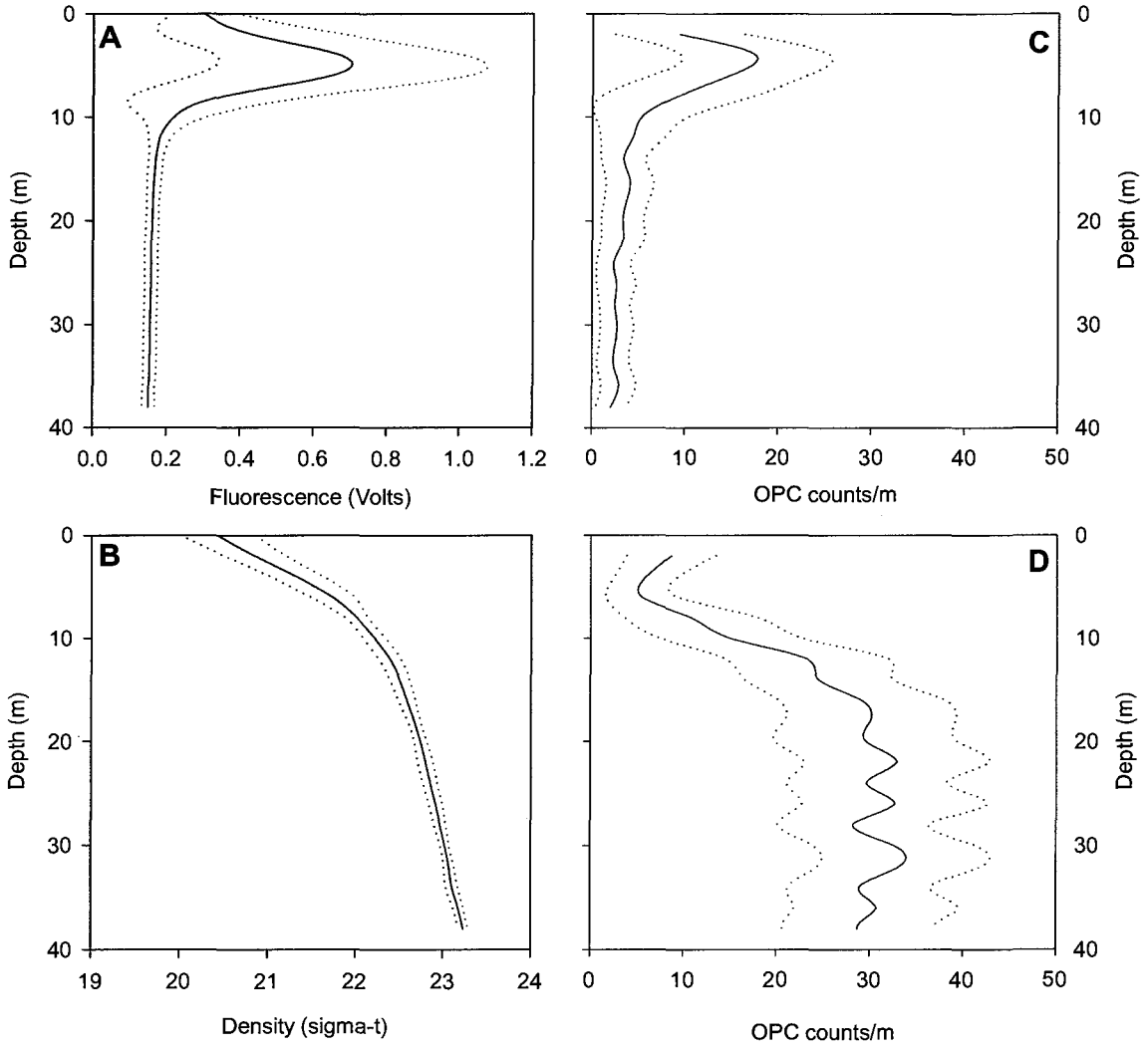

Figure 2.1. Average depth profiles from 48 hour Saanich Inlet OPC and CTD series. **A.** Chlorophyll *a* fluorescence (Volts), **B.** Water density (Sigma-t). Average OPC counts/m with depth for **C.** large (1500 – 3000μm) and **D.** small (250 – 500μm) particles in 48 hour OPC series. Dotted lines indicate one standard deviation around the mean of 131 casts. Note the similarity between the profiles for chl *a* fluorescence and large particle abundance.

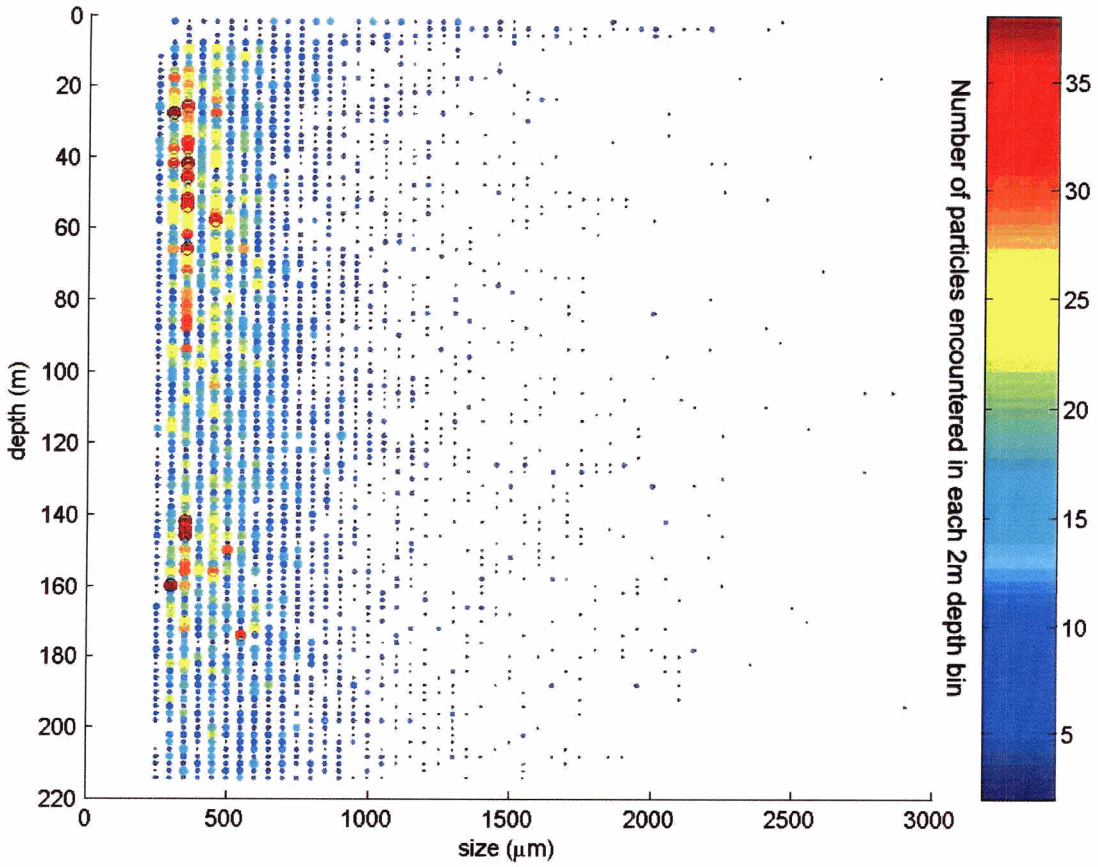

Figure 2.2. Depth profile (0 - 220m) of the size distribution of particles in Saanich Inlet. Profile represents the average of five daytime casts taken between June 21 and 23. Vertical resolution = 2m. The color and size of each dot indicates the number of particles encountered in each 2m depth bin. Note the concentration of small particles between 140-160m, around the depth of the oxycline.

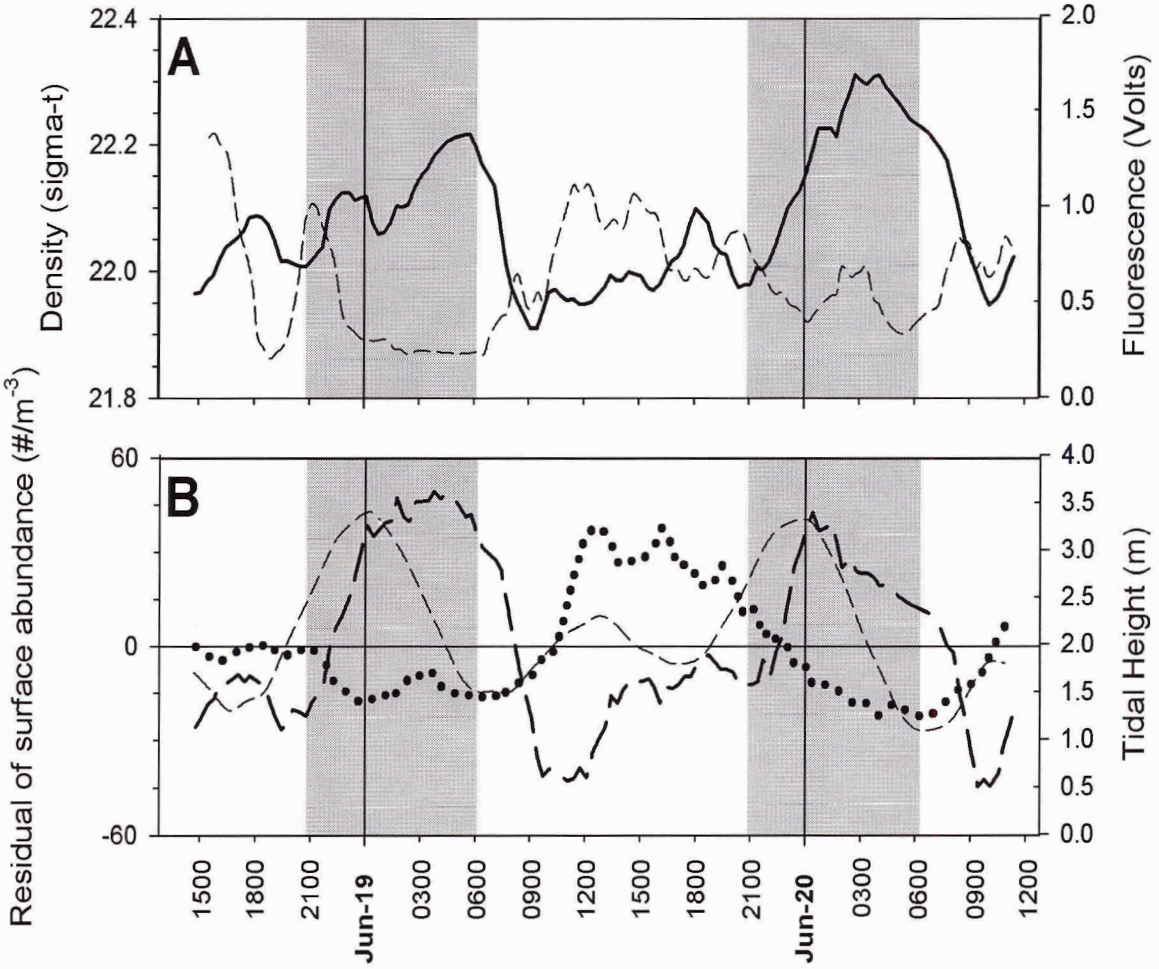

Figure 2.3. Time series of density, chl *a* fluorescence and OPC counts/m in the surface 20m between June 18 and 24, 2002 in Saanich Inlet (Pacific Standard Time). Shaded areas indicate night time. Vertical CTD and OPC hauls were taken every 20 minutes for the whole 48 hours **A.** Water density (solid line) and chl *a* fluorescence (dashed line) at 6 meters, the average depth of the highest chlorophyll values. **B.** Residuals of (abundance minus the series mean) for large (>1500 μm, dotted) and small (250 – 500μm, long dash) particles. Thin dashed line in the bottom panel indicates tidal height.

There was no significant correlation between OPC and net derived zooplankton abundance in the 0.65 to 3.0mm size range ($p > 0.05$, r=0.06, df=30). Particle size was significantly correlated with log(abundance) ($p < 0.0001$, $r = -0.99$, df=25) in the OPC_{net} casts (Figure 2.5), with little variation around each size class, except in the larger ones. Particle size was also significantly correlated with log(abundance) in the net samples at ($p< 0.01$, $r = -0.64$, $df = 25$).

The OPC_{all} abundance series was significantly positively autocorrelated for lags of up to 6 hours (Figure 2.6). The OPC_{net} series, on the other hand, was only significantly correlated for lags of up to 2 hours. The Net series was not significantly autocorrelated at all, though there was some evidence of periodicity in this series on the order of 4 hours. There was no evidence of periodicity in either of the OPC series.

2.3.3 Temporal resolution of OPC and Net samples

There was a significant decrease in the Percent Similarity Index as the time separating pairs of samples increased in each of the OPC_{all} ($p < 0.001$, $r = 0.61$, n = 17 030 comparisons), OPC_{net} ($p < 0.001$, $r = 0.707$, n = 870 comparisons) and Net ($p < 0.01$, r = 0.451, n = 870 comparisons) series. In addition, there was a weak but statistically significant relationship between the OPC_{net} and Net PSI matrices ($p < 0.01$, $r = 0.23$, n = 870 comparisons) (Table 2.3). A Loess smoothing curve was fitted through the scatterplot (smoothing estimated by minimizing the residuals around the smoothing line – Cleveland, 1985). From these smoothing lines, the "background similarity" (i.e. the similarity between pairs of samples taken the shortest possible time apart) among the OPC_{all} samples was 97% and decayed to a minimum of 83% in an inverse parabolic shape (Figure 2.7). The Net series had a background PSI of 82% and a minimum of 65% and the loess curve increased in the first 30 hours then decayed almost linearly.

Taxon	Total abundance	% contribution to total abundance	Mean abundance	Median abundance	Max abundance	Min abundance	length (mm)
Corycaeus anglicus	16335	23	435.22	411.33	833.40	0.00	0.5 - 0.64
Euphausia pacifica eggs	8295	12	196.00	178.19	395.91	37.04	0.7 - 0.94
Oithona similis	7213	10	198.71	157.62	415.88	83.35	0.9
Oikopleura dioica	5949	8	198.16	142.46	457.59	0.00	4.6
Microcalanus pygmaeus pygmaeus	4565	7	111.97	119.34	197.71	0.00	0.8
Pseudocalanus spp.	3188	5	103.39	87.85	278.66	30.50	0.9 - 1.3
Mollusc velligers	3035	4	87.19	60.09	252.25	7.33	0.5 - 0.8
Calanus pacificus	2754	4	78.93	74.65	238.62	18.40	1.8 - 2.2
Cirripedia nauplii	2996	4	94.82	82.44	176.66	29.32	1.0
Paracalanus parvus	2308	3	78.25	51.35	427.17	8.54	0.74
Diphyes sp.	2115	3	43.15	31.78	169.77	0.00	1.0
Cirripedia cyprids	1191	2	34.83	32.46	77.95	7.79	2.5

Table 2.1. Dominant zooplankton taxa in 0 - 100m vertical net hauls in Saanich Inlet between June 18 and 24, 2002. In total, 30 net samples were taken over the 6 days.

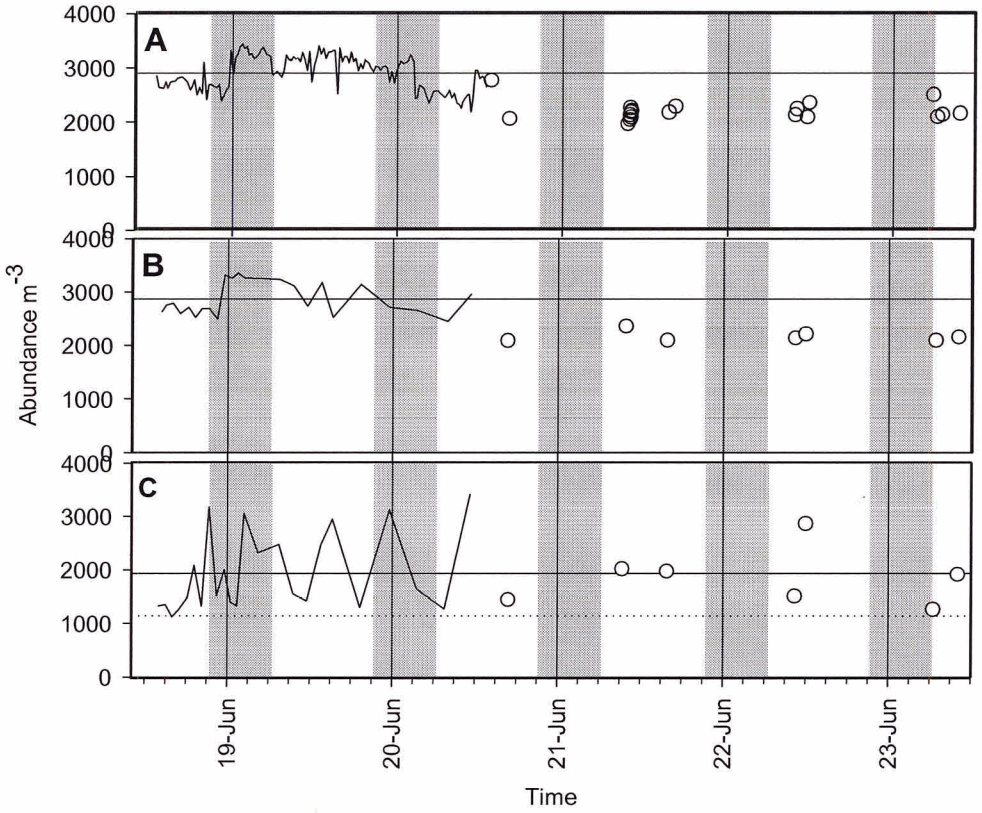

Figure 2.4. Time series of total zooplankton abundance (# m^{-3}) in the 0.7 to 3.0mm size range from 0 - 100m vertical OPC and net casts taken in Saanich Inlet between June 18 and 24, 2002 (PDT). **A.** OPC_{all} series (i.e. all OPC samples over the full 6 day series = 152 casts), **B.** OPC samples taken within 5 minutes of net samples (OPC_{net}, = 30 casts) and **C.** Net samples (30 casts). Grey areas indicate night time. Mean (solid), minimum and maximum (dotted) values in each series are plotted. Open circles represent samples taken at irregular intervals in the four days following the 48 hour series.

Series name	Total samples over the 6 days	Samples in first 48 hrs	Mean # m^{-3}	Coefficient of Variation of mean # m^{-3}	Max # m^{-3}	Min # m^{-3}
OPC_{all}	152	131	7080	0.105	8260	5420
OPC_{net}	30	25	6540	0.113	7840	5420
Net	30	25	1920	0.34	3400	1140

Table 2.2. Summary statistics of OPC_{all}, OPC_{net} and net series. Note that the coefficient of variation for the net series is three times that for either of the OPC series.

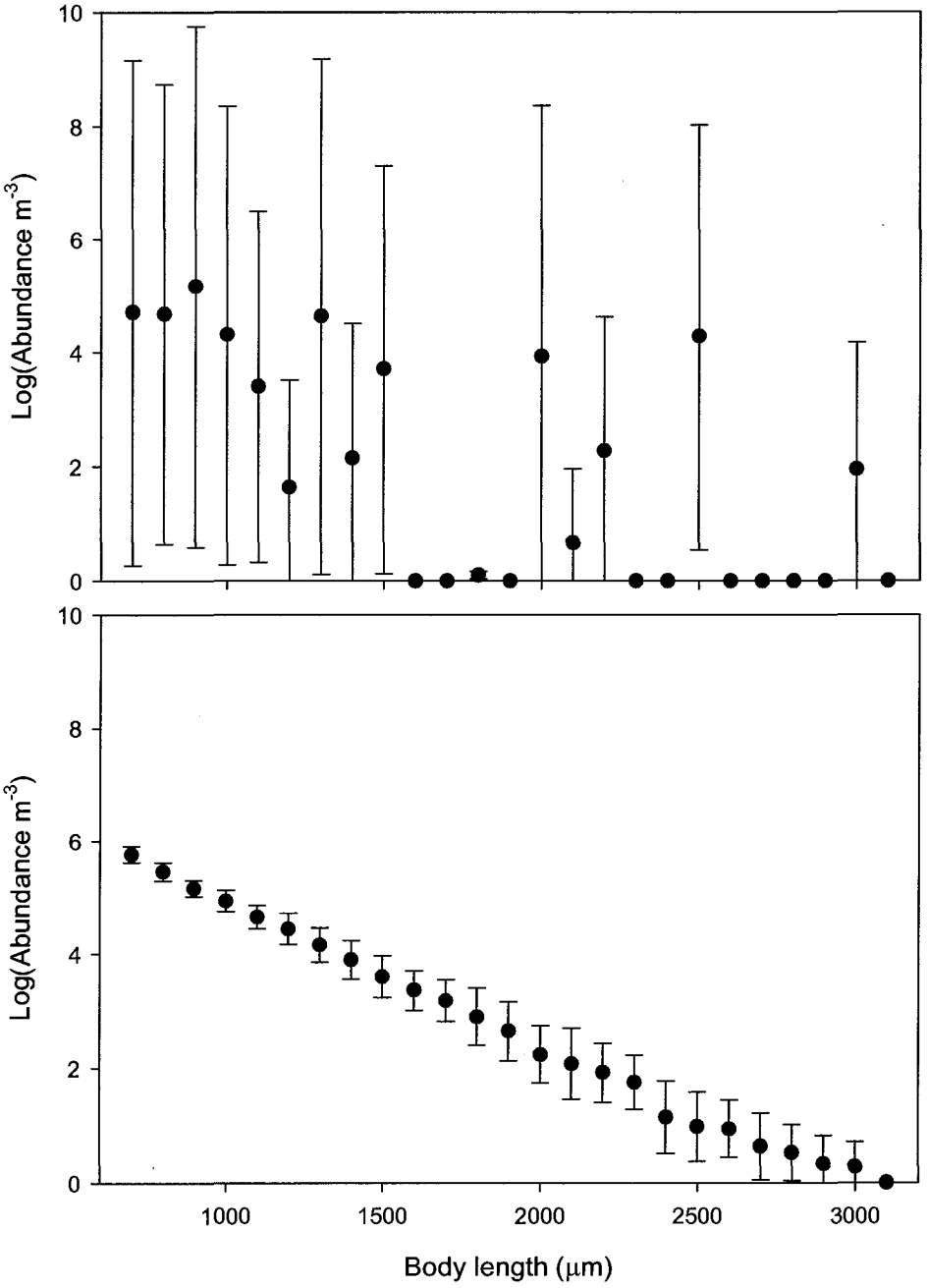

Figure 2.5. Average size distributions of zooplankton in OPC and net data from a total of 25 net and OPC casts. Top Panel: 0 - 100m net hauls and Bottom Panel: 0 - 100m OPC_{net} hauls. Error bars are one standard deviation around log(average abundance) in each size class.

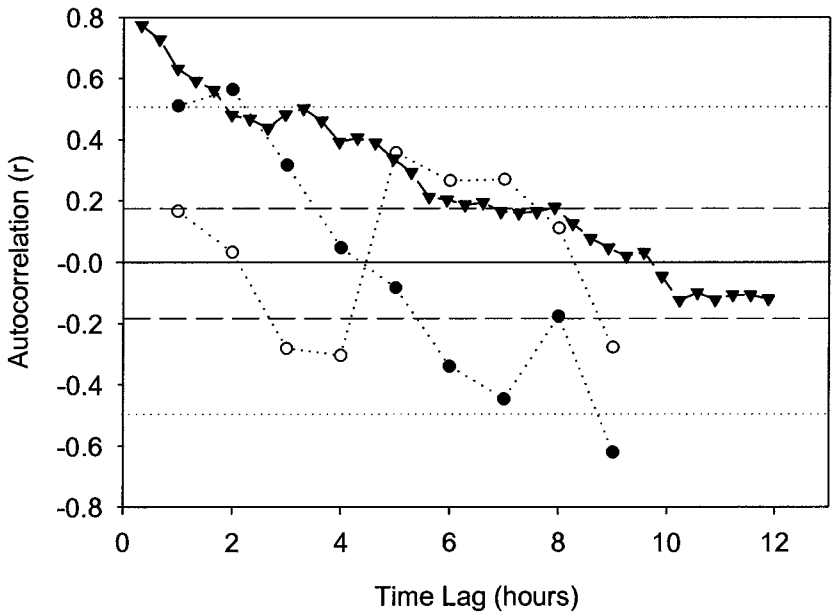

Figure 2.6. Temporal autocorrelation for the first 18 hours of OPC and net abundance data. Shown are the OPC_{all} (▼, n=42), OPC_{net} (●, n=18) and NET (○, n=18) series. Horizontal lines show the 5% significance levels of the autocorrelation (i.e. points above these lines are significantly autocorrelated) for OPC_{all} series (dotted line) and OPC_{net} and net series (long dashed line).

Test	Size of matrices	Iterations	*r*	*p*
OPC_{all} vs. Time	151x151	5000	-0.61	< 0.001
OPC_{net} vs. Time	30x30	5000	-0.71	< 0.001
Net vs. Time	30x30	5000	-0.45	< 0.01
OPC_{net} vs. Net	30x30	5000	0.23	< 0.01

Table 2.3. Results of Mantel randomization test of the correlation between distance matrices and similarity matrices from OPC and net series. *r* is the correlation between a similarity matrix and its distance matrix, *p* indicates the probability that, when randomized, the two matrices, have a degree of correlation greater or equalto *r*.

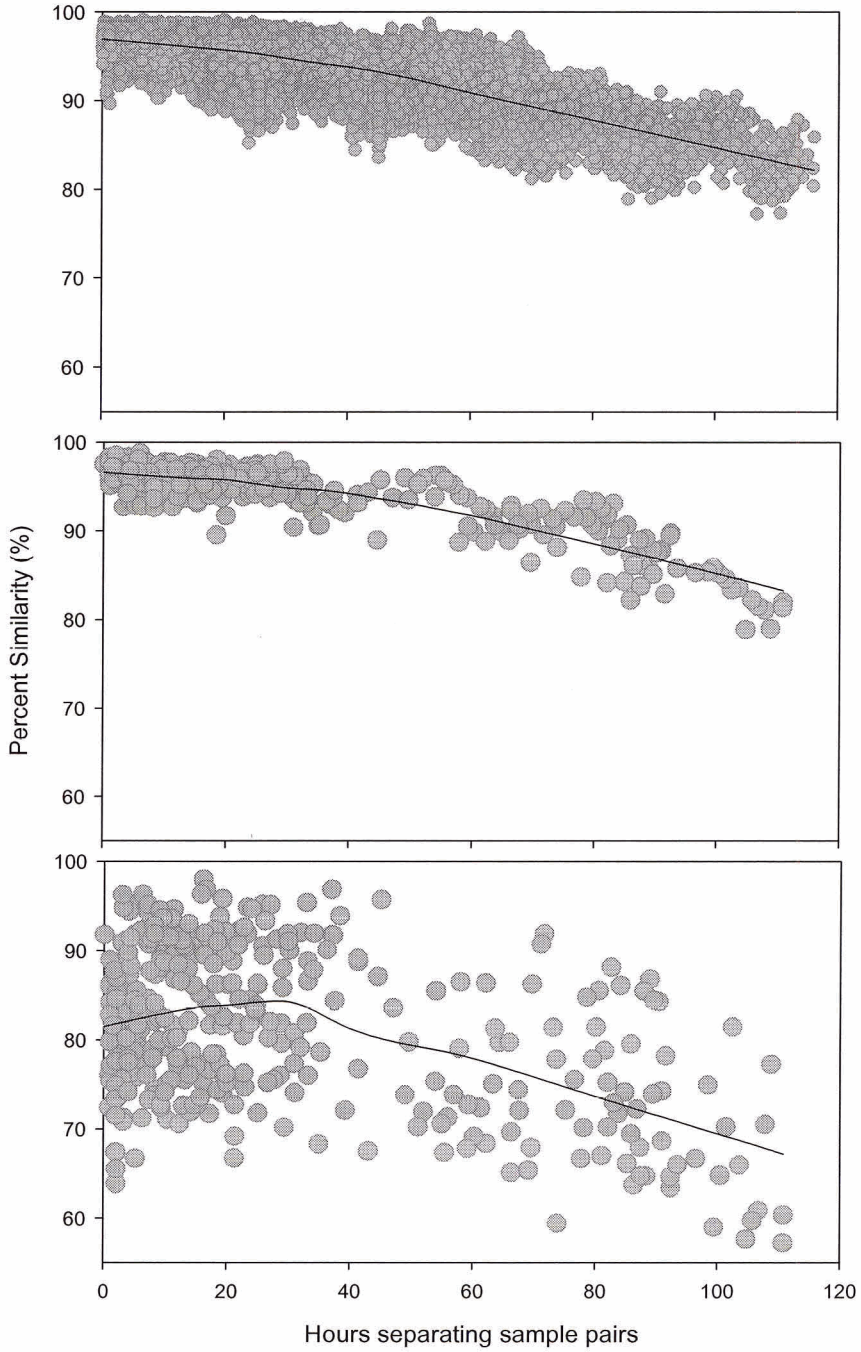

Figure 2.7. Percent similarity index for all pair-wise comparisons of the zooplankton size distribution within the OPC_{all}, OPC_{net} and net series, plotted against the time separating each sample pair. **A.** OPC_{all} series (17 030 comparisons), **B.** OPC_{net} series (870 comparisons) and **C.** net series (870 comparisons). Solid lines are Loess smoothing curves (quadratic degree = 1, smoothing coefficient = 0.7).

2.3.4 Sampling effort

There was a higher likelihood of approximating the mean abundance of the OPC_{net} series than the net series with all sampling efforts (Figure 2.9). There is a 95% probability of approximating the OPC_{net} mean abundance with as few as 5 OPC samples, whereas even with 25 net samples there was still only a 80% likelihood of approximating the mean abundance of the net series. The average sampling effort required to approximate the mean abundance in the OPC_{all} series generally increased with the length of the sampling period (Figure 2.10). However, some sampling periods require relatively greater sampling effort per unit time. Six hour sampling periods required a greater sampling effort per unit time than any of the other sampling periods.

2.4 Discussion

2.4.1 Are fine-scale OPC and net estimates of the abundance and size structure of the zooplankton in a community similar?

OPC and net samples of a zooplankton community do not provide equal estimates of the community structure or the abundance at fine scales. The OPC_{net} abundances were consistently 1.5 times greater (and far less variable) than were the abundance estimates from the net samples. Also, the average size structure of net and OPC samples differed greatly. The decay of similarity between pairs of net samples and pairs of OPC samples followed roughly the same pattern, though pairs of OPC samples had higher similarity than pairs of net samples. Finally, it appeared that the high levels of primary productivity in Saanich Inlet during the period of this study may have cause problems in both the OPC and net samples.

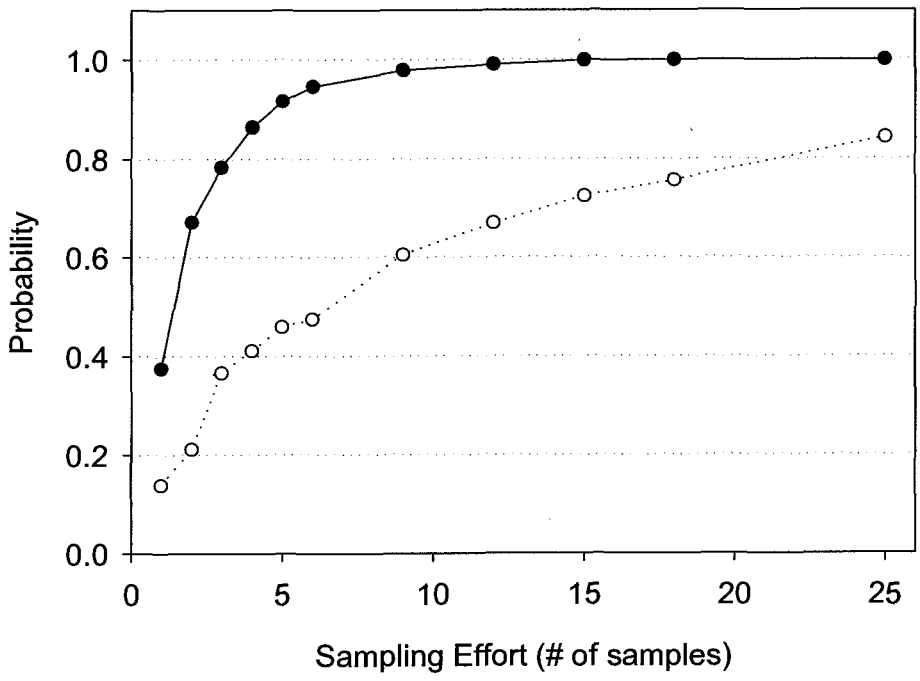

Figure 2.8. Probability of approximating the 'true' mean abundance zooplankton in the first 48 hours of the OPC_{net} (filled circles) and net (open circles) series, with a given number of samples. Probability levels were calculated using a randomization test.

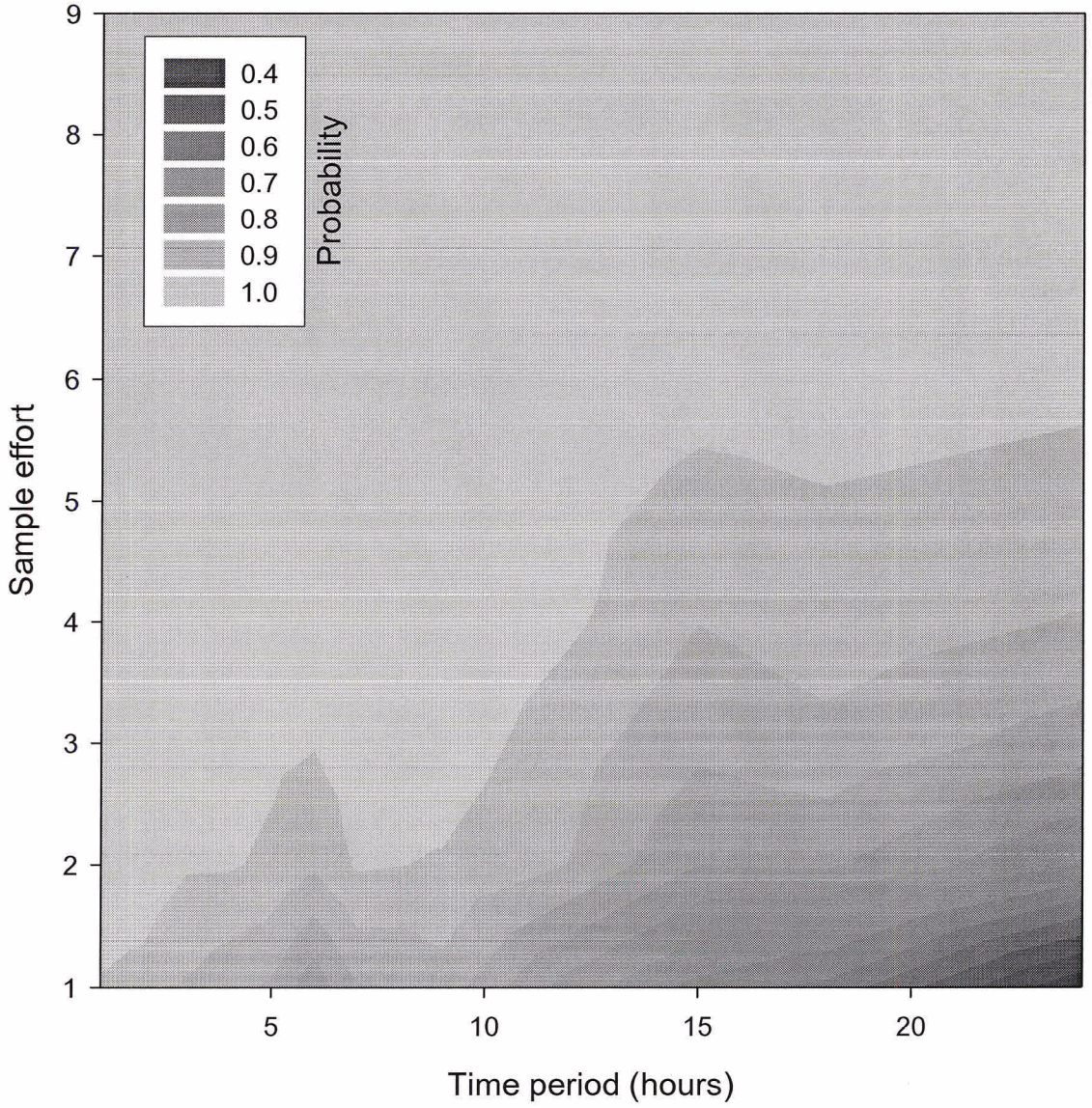

Figure 2.9. Surface describing the likelihood of approximating the mean zooplankton abundance within a given time period with a certain number of OPC samples. The shading of contours denotes the likelihood levels. Probability levels were calculated using a randomization test on the OPC_{all} 48 hour series.

In this study, the surface depth distribution of large OPC particles was almost identical to that of chlorophyll *a* fluorescence and appeared to follow a strongly tidal period. The distribution of small particles mirrored the chl *a* fluorescence profile. In addition, the periodicity of the surface fluorescence closely reflected that of the surface abundance of small and large particles, and the average particle size closely followed the chl *a* fluorescence level. This indicates that coincident counting was likely responsible for much of the observed surface distribution. Coincident counts occur in the OPC when two or more particles enter the sampling tunnel within the same 5ms period. As a result, groups of small particles are recorded as individual large particles, thereby skewing the resultant size distribution towards larger sizes. According to the OPC manufacturers, this problem is supposed to be corrected automatically by an internal record of light attenuance measured by the OPC. However, the OPC's measurement of light attenuance differs greatly from that of a transmissometer (Appendix 1). Therefore, the OPC's correction factor used to control for coincident counts may be unable to cope with high particle concentrations.

While the depth distribution of chl *a* fluorescence suggests that coincident counting was not a problem below 20m, it is possible that aggregates of diatoms raining down from the surface may have contributed significantly to the observed zooplankton size structure. However, without a true measure of their distribution and/or the true water clarity, it is impossible to quantify this effect. Estimates of the true concentration and size distribution of diatom flocs are difficult to obtain, given their fragility. However, phytoplankton, and diatoms in particular, are known to sink constantly and slowly from the surface in Saanich Inlet, so numerous small (~50 - 250 μm) particles may also have been present at depth (Timothy *et al.*, 2003). Their size distribution tends to be steeper than that of zooplankton (Jackson, 1995), so it is unlikely that the distributions observed here were entirely dues to detritus. However, it is difficult to say exactly how this detritus may have affected the OPC particle distribution.

The presence of a low-oxygen layer in the inlet provided an opportunity to test whether the OPC was influenced by background noise. Mackie and Mills (1983), using the PICES IV submersible, noted that few zooplankton venture below the oxycline, with the exception of certain amphipods and euphausiids. They also noted that zooplankton often aggregated just above the low oxygen layer. Though no measurements of oxygen were available for this study, past measurements indicate that the anoxic zone is typically encountered between 100 and 160m (Mackie and Mills, 1983; Anderson and Devol, 1973; Herlinveaux, 1962). The depth distribution of particle counts in the 220m casts suggests aggregations of zooplankton at around 140m. Assuming that this depth represents the top of the anoxic layer, the presence of counts in all particle sizes below this depth indicates that there was likely a background of detritus interfering with the OPC's estimate of zooplankton abundance.

However, the large amount of variation in the net samples was also responsible (in part) for the disparity between the net and OPC data. The primary cause of variation in net samples (asides from natural variability and patchiness) is from clogging, which contributes to variable retention of smaller zooplankton (Brander *et al.,* 1993; Nichols and Thompson, 1991; Yentsch and Duxbury, 1956). Phytoplankton likely had a significant and variable clogging effect in the present study, given the amount of phytoplankton ooze present on the nets after each cast. A further source of clogging was likely gelatinous zooplankton. There was a significant ($p<0.05$, $r^2=0.75$) and positive relationship between the abundance of jellyfish and small (<0.8 mm) zooplankton. This suggests that the error in net samples was a function of both the concentration of phytoplankton and the community composition of the zooplankton.

Given that both estimates of zooplankton abundance were prone to different kinds of error due to phytoplankton, this study highlights both the difficulty of sampling in high productivity areas, and the importance of utilizing alternative estimates in such conditions. The different types of error experienced by each techniques indicates that net and OPC samples should be interpreted differently in order to maximize their utility and minimize the amount of error introduced by sample processing. As such, it is

important that OPC samples be interpreted on their own merit, rather than trying to approach them as a kind of digital net.

2.4.2 Do series of OPC or net samples have greater temporal resolution?

As measured by the OPC, the 'background' size structure of the zooplankton community was less variable than that measured from the net samples (Figure 2.7). The reason for this difference is unclear. One interpretation is that the size structure of particles sampled by the OPC remained relatively constant over the whole series, changing only slightly (but significantly) over periods of less than four days. However, this general shape of the structure function is to be expected, with samples collected closer together in time being more similar (Mackas, 1980). It indicates that there was consistency in the OPC samples that decayed regularly over time. In contrast, the shape of the structure function derived from the net samples is more variable, suggesting less coherence in the size structure of the zooplankton community over time. This is also confirmed by the large amount of variation observed in the size distribution relative to that found in the OPC samples.

The 'background' size structure of the zooplankton community, as measured by the OPC, was less variable than that measured from the net samples (Figure 2.7). The reason for this difference is unclear. One interpretation is that the size structure of zooplankton sampled by the OPC remained relatively constant over the whole series, changing only slightly (but significantly) over periods of less than four days. However, this general shape of structure function is to be expected, with closer samples being more similar (Mackas, 1980). It indicates that there was consistency in the OPC samples that decayed regularly over time.. In the net samples, The shape of the structure function is more variable and suggests less coherence in the size structure of the zooplankton over time. This is confirmed by the large amount of variation observed in the size distribution relative to that found in the OPC samples.

A second interpretation of the PSI results is that the OPC may have been measuring small particulates (*e.g.* phytodetritus) as well as zooplankton *per se*. If the OPC was indeed measuring a constant background level of particle noise, this noise could have

overwhelmed any variation in the "true" zooplankton community structure. The presence of particles in all size classes below the oxycline in the deep OPC casts indicates that detritus may have been an important component of the observed particle size distribution. In addition, Herman (2001) noted that the smallest mesh size that should be used to compare between net and OPC samples is 80μm. Mesh sizes greater than this allow for significant escapement of copepods and other long, narrow zooplankton. This raises the problem of net clogging, however, as such a fine mesh would clog much faster than the 236μm net used in the present study. Without some independent measure of the size distribution of particulates, it is impossible to say to what extent the OPC was measuring the 'true' zooplankton distribution. A potential solution might be to use Video Plankton Recorder technology (Davis *et al.*, 1996) to assess the distribution of small particles and zooplankton for a small subset of the total series. The VPR has been used successfully in other situations to produce *in-situ* estimates of the abundance and size-structure of zooplankton communities. Its primary drawback is that the data analysis tends to be time-consuming and covers only a very small volume of water. Despite this (and despite the obvious drawback of trying to compare three different sampling techniques!), however, the use of a VPR might allow a better estimate of the relative error of the net and OPC samples in high productivity waters.

2.4.3. What sampling effort is required to approximate the mean abundance of zooplankton in a community using OPC and net samples?

Fewer OPC casts than net casts were required to approximate the mean abundance of zooplankton over the whole series. This is likely due to the greater short-term variation observed among net samples. In the OPC_{all} series, some sampling periods required a proportionally greater number of samples. For example, the six hour period required more samples than the ten hour period. This matches the temporal autocorrelation scale of the OPC_{all} series and suggests that a large proportion of the variation seen in the OPC_{all} abundance series was due to tidal fluctuations.

These results indicate that OPC samples may provide a greater degree of spatiotemporal resolution at a lesser sampling effort than nets. They also point to a way in which

zooplankton sampling strategies can be optimized in order to take advantage of the strengths of both sample types. The OPC may be used to obtain an initial assessment of the dominant spatiotemporal scales of variation in the zooplankton. Net samples may be then strategically spaced in order to sample the maximum variation in abundance with the minimum number of samples. In order to maximize the accuracy of sampling at any given location, replicate samples should be taken. The data presented here indicate that four or five net samples will approximate (to within 10%) the mean abundance with a 50% probability of success.

Yet the question remains as to whether the OPC and net samples measured the same thing. The main reason for the disparity between them seems to be the presence of small particulates (e.g. phytoplankton aggregates and other detritus). There are two possible remedies to the problem. The first is to simply take independent measures of water clarity along with the OPC samples. Those sections of OPC data associated with turbid water can be removed from the series, or treated independently. The second solution is to derive a model of how the perceived abundance of different size classes varies in water of different detritus concentrations. These data indicate that the propensity of the OPC to overestimate zooplankton abundance in the field is directly related to the concentration of detritus in the water. Zhang *et al.* (2001) showed this for lab samples and demonstrated that it is possible to correct OPC abundance data for background counts due to detritus. Sprules *et al.* (1998) also demonstrated that it is possible to correct for coincident counts, using a model based on a Poisson distribution of particle abundances. A correction model using an independent measure of water clarity (such as a transmissometer) could be developed to help interpret field OPC data taken in areas of high primary productivity.

In spite of the uncertainty around what particles the OPC actually measured, the present study does indicate that it was able to do so with greater temporal resolution than the net samples. Because of its greater resolution, the OPC can be used to investigate a different suite of questions than is possible using traditional plankton nets. For example, Baumgartner (2003) used the OPC to search for aggregations of *Calanus finmarchicus* with repeated OPC casts near the feeding sites of gray whales. Pinca and Huntley (2000)

used an OPC to link the spatial distribution of particulates in the California current to physical features of the current. Edvardsen *et al.* (2002) employed size distribution theory to develop method of calculating size-specific growth rates from OPC data. Noguiera *et al,* (2004) showed that OPC and net estimates of the slope of the zooplankton size-distribution were the same, within a restricted size range. Therefore, based on the growing body of literature on the use of the OPC, there is every reason to believe that the OPC can provide a rapid and fine-scale assessment of the zooplankton community in relatively clear water.

The present work demonstrates the feasibility of using the OPC to elucidate fine-scale patterns in zooplankton abundance and the size structure of zooplankton communities. However, it also indicates that the OPC may be prone to considerable error in high productivity waters. It is therefore important that OPC data be accompanied with independent estimates of water clarity, fluorescence, and the zooplankton community composition in order to know exactly what might be influencing OPC counts. However, this work also indicates that traditional net samples are prone to at least as much (if not more) error. As such, it is recommended that OPC data be interpreted with caution in such situations, but that they also be interpreted on their own merits rather than forcing reconciliation between OPC and net estimates (which may be a classic example of comparing apples and oranges). Used appropriately, the OPC has the potential to help address long-standing questions concerning the fine-scale distribution of zooplankton.

CHAPTER 3

Seasonal variation in the size distribution of zooplankton in the Strait of Georgia.

3.1 Introduction

3.1.1 General Introduction

Planktonic food webs are complex and difficult to characterize with generalized trophic models (Olsen *et al.*, 2001). However, underlying patterns for the distribution and abundance of those communities have been proposed. One dominant pattern is that the biomass of a community which is in a steady-state tends to be evenly distributed between logarithmically increasing size classes (Sheldon *et al.*, 1972). This observation led to the first size-based models of community dynamics (Kerr, 1974; Sheldon *et al.*,1977; Platt and Denman, 1977, 1978; Silvert and Platt, 1978). These models described the flow of energy from small to large sized organisms based on the assumptions (i) that the biomass of small zooplankton is transferred to larger sizes via growth and predation and (ii) that a certain amount of biomass is lost from the system through non-predation mortality and respiration.

The equation derived by Platt and Denman (1978) is:

$$\frac{\partial \beta(w)}{\partial t} = -\frac{\partial [g(w)\beta(w)]}{\partial w} - u(w)\beta(w) \qquad (3.1)$$

Where $g(w)$ is the weight specific growth rate (gC d^{-1}), $u(w)$ is the population level growth rate (d^{-1}) and $\beta(w)$ is the normalized biomass size distribution. Normalized biomass refers to the biomass within a weight interval $w_1 \rightarrow w_2$ divided by the weight interval $\Delta w = w_1 - w_2$ (see introductory chapter or Platt and Denman, 1978). The normalized biomass distribution is also displayed using logarithmically increasing size classes.

Planktonic size distributions are usually expressed in units of grams of Carbon per m^3. However, if the density of plankton is assumed to be relatively constant, then the Normalised biovolume size distribution (NBSD) can equally be considered in terms of

the total volume of living organisms (Biovolume, denoted in this paper as $mm^3\ m^{-3}$) and will be expressed as such for the rest of this paper. Equation 3.1 provides a simple framework from which to explore the organization of zooplankton communities and how that organization changes in space and time.

Platt and Denman's model predicts that if the biovolume in smaller size classes increases, this increase will propagate upward through the system (i.e. to larger size-classes) as a coherent damped wave (Silvert and Platt, 1978). The spring phytoplankton bloom which occurs in temperate marine ecosystems in response to the onset of surface stratification can be thought as one addition of biovolume. This spike in phytoplankton production propagates through the NBSD from small to large organisms via growth and predation. Since the model framework was established, field research has focused on characterizing the form of the NBSD of planktonic ecosystems (Sprules *et al.,* 1983; Sprules and Munuwar, 1986; Gaedke, 1992, 1993; Garcia, 1993; Kobayoshi *et al.*, 1998; Quintana *et al.*, 2002; Cozar *et al.*, 2003), and pulses of biovolume moving through the size distribution of plankton communities have since been documented (Rodriguez and Mullin, 1986; Heath, 1995; Edvardson *et al.*, 2002).

Another feature of the NBSD model is that it allows researchers to compare the dynamic properties of different planktonic communities based on the slope of their size distributions. Using empirical estimates of $g(w)$ and $u(w)$, Platt and Denman (1978) predicted that the slope of the normalized *biomass* size distribution of an oligotrophic plankton community in steady-state should be about -1.22. Subsequently, planktonic size distributions in oceans, lakes, marshes and river plankton communities have all been shown to have biomass size distributions with slopes close to this prediction (Rodriguez and Mullin, 1986a; Sprules *et al.,* 1983; Sprules and Munuwar, 1986; Ahrens and Peters, 1991). In contrast, empirical measurements of the normalized *biovolume* (i.e. as opposed to biomass) size distribution have shown it to be close to -1.0 (Sprules *et al.,*1983; Rodriguez and Mullin, 1986a; Gaedke, 1992). The size distribution of a zooplankton community has been related to its trophic transfer efficiency (TTE) (Havens, 1998). Trophic transfer efficiency refers to the total production of consumers (i.e.

herbivorous zooplankton) divided by the production in primary producers. In the context of the biovolume distribution, TTE can be thought of as the biovolume in one size class divided by the biovolume in the size class of its food source. If the TTE of a community is high, then greater biovolume can be supported in higher levels (Sprules *et al.,* 1991; Havens, 1998; Gismervik *et al.,* 2002). The TTE of an ecosystem has also been related to its productivity: oligotrophic ecosystems tend to have lower TTEs (Lindeman, 1942; Gasol *et al.,* 1991; DeBruyn *et al.,* 2003). Therefore, a community in which production levels vary seasonally should have a varying biovolume distribution slope (Sprules and Munuwar, 1986; Gaedke, 1992, 1993; Garcia, 1993; Gaedke, 2004).

Platt and Denman's model (Equation 3.1) provides a way by which to explore possible mechanisms for environmentally-induced variation in the NBSD. The slope of the biovolume distribution can be approximated as the loss rate divided by the growth rate:

$$\frac{\partial \ln(\overline{\beta})}{\partial \ln(\overline{w})} \cong \frac{\overline{u}}{\overline{g}} \qquad (3.2)$$

where the overbar symbol denotes a time average (Huntley and Zhou, 1997). Therefore the average slope of the biovolume distribution should become shallower when $g(w)$ increases or when $u(w)$ decreases. As yet, there have been few studies exploring possible mechanisms by which environmental factors could cause the slope of an ecosystem's planktonic size distribution to increase or decrease. This is likely due to the difficulty in calculating $g(w)$ and $u(w)$ in the field, and to the effort required to adequately measure the size distribution of an entire planktonic ecosystem from bacteria to meso-zooplankton.

By focusing on a narrower range of sizes and using automated particle counters, zooplankton researchers have been able to more accurately test the predictions of size distribution theory. In particular, the optical plankton counter (OPC) developed by Herman (1988, 1992, 2001) has been used to relate field observations to patterns predicted by the theory. Heath (1995) used the OPC to track a pulse of biovolume moving through the biovolume distribution of a Scottish loch. In addition, Heath was able to calculate growth rates of the zooplankton community in the loch based on size distribution theory. His work was extended by Huntley and Zhou (1997) and Edvardsen

et al. (2001) to develop size-specific calculations of growth rates from serial observations of a zooplankton community. More recently, Nogueira *et al* (2004) used the OPC to measure the slope of the zooplankton size spectrum, which compared favorably with net derived estimates of the size spectrum. Therefore, the OPC can provide a way to relate size distribution theory to field measurements of zooplankton community dynamics.

In order to use size distribution theory in a field setting, it is important to have a working knowledge of the ecosystem or community being studied. Rodriguez and Mullin (1986b) cautioned that while the theory can be applied to many broad patterns in ecology, there are important behavioral and trophic aspects of zooplankton ecology which cannot be explained by size distribution theory alone. For example, the ontogenetic migration of some zooplankton species can have a large impact on community size structure. In addition, knowledge of the species composition of a community can provide information on the behavior, life cycles and seasonal distribution of many zooplankton species which could not be easily explained using size distribution theory. For practical considerations, it is therefore preferable that the community being studied have a relatively predictable pattern of variation.

3.1.2 Physical and Biological Oceanography of the Strait of Georgia, British Columbia

The Strait of Georgia (SoG hereafter) provides an excellent system within which to study variation in the size distribution of a zooplankton community (Map 3.1). The hydrography and biological oceanography of the SoG have been previously described (Legare, 1957; Waldichuck, 1957; Thomson, 1981; Leblond, 1983; Harrison, 1983). The SoG is a semi-enclosed inland sea, open at the north and south ends. Channels to the north (i.e. Johnstone Strait) are quite restricted and southern access to the Juan de Fuca Strait (hereafter referred to as JdF) and the Pacific Ocean occurs via a network of passages between islands and shallow sills. The Fraser River is the main source of freshwater input, with a maximum discharge of 10^4 m^3 s^{-1} during June and a minimum of 10^2 m^3 s^{-1} for most of the rest of the year (Waldichuk, 1957). This freshwater input causes a low salinity layer that can cover much of the SoG to a depth of 2-10m. This results in a net positive estuarine circulation out of the JdF, the main thoroughfare for ocean

exchange. A compensatory inward flow of coastal shelf water occurs below 20m to replace the surface outflow (LeBlond, 1983). The flushing time of the SoG through the JdF is on the order of 400 days (Waldichuk, 1957), though different parts of the Strait may have different renewal times (Samuels, 1979). The relatively shallow (80m) sills in the JdF prevents frequent deep-water exchange with the Pacific, though deep-water. renewals of nutrient rich water do periodically occur in the late winter and summer (Waldichuk, 1957; Masson, 2002).

The plankton ecology of the SoG has been reviewed byLeGarre (1957), Harrison *et al.* (1983, Figure 3.1) and Parsons *et al.* (1970). The Strait is dominated by a strong spring bloom, similar to the blooms experienced in Saanich Inlet. During winter, light limitation keeps phytoplankton levels low. Around April each year, stratification of the water column and increased light levels result in a rapid and dramatic spring bloom. Although factors controlling the stratification are widely held to be tied to the timing of the Fraser river freshet (Yin *et al.,* 1996, 1997), more recent evidence suggests that the timing of the freshet is less important than previously thought (SE, Allen, University of British Columbia, *pers comm*). The main bloom usually lasts about a month and is often followed by a series of "mini-blooms" which can continue late into the summer and early fall (Takahashi *et al.*, 1979; Yin *et al.*, 1996, 1997).

Much of the research on zooplankton ecology in the SoG has focused on the dominant copepod, *Neocalanus plumchrus,* due to its large size, abundance and potential importance as a food source for fish stocks (Figure 3.1; Campbell, 2003; Harrison *et al.,* 1983; Fulton, 1973). *N. plumchrus* spends most of the year overwintering at depths below 200m as fifth stage copepodites (CV), before spawning at depth in December-January. Nauplii rise to the surface in February or March, usually preceding the spring bloom by a month or so. By early June, the nauplii have progressed to the CV stage and descend to their overwintering depth after laying down significant stores of lipids. The degree of overlap between the timing of the bloom and the arrival of *N. plumchrus* can determine whether the bloom remains strong and persistent or is rapidly grazed down by copepods (Yin *et al.,* 1996; Harrison *et al.,* 1983). Because it is the dominant

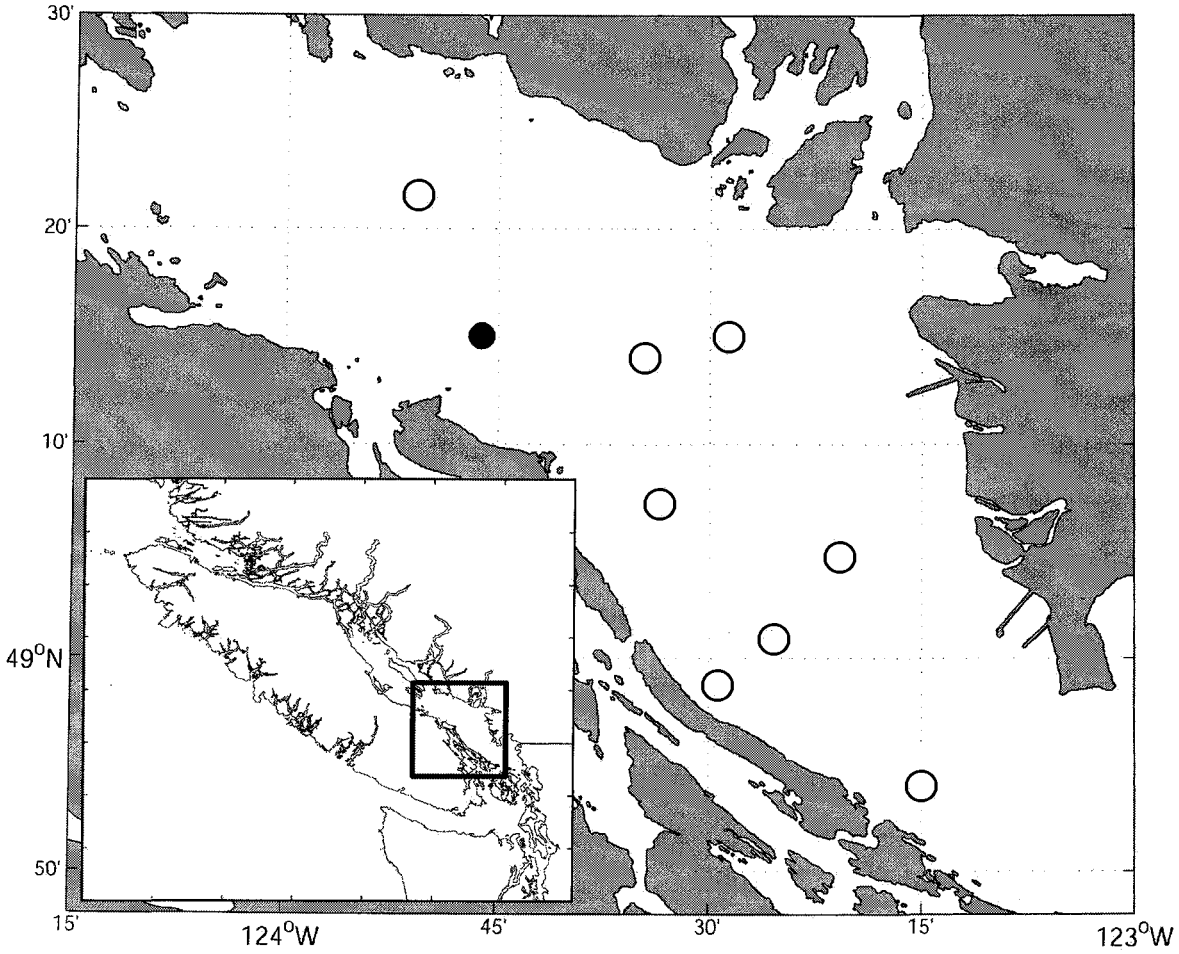

Map 3.1. Map of the Strait of Georgia, British Columbia. Open circles indicate sites at which OPC data were collected during monthy STRATOGEM cruises. Filled circle is station S4-1, where both OPC and net samples were collected.

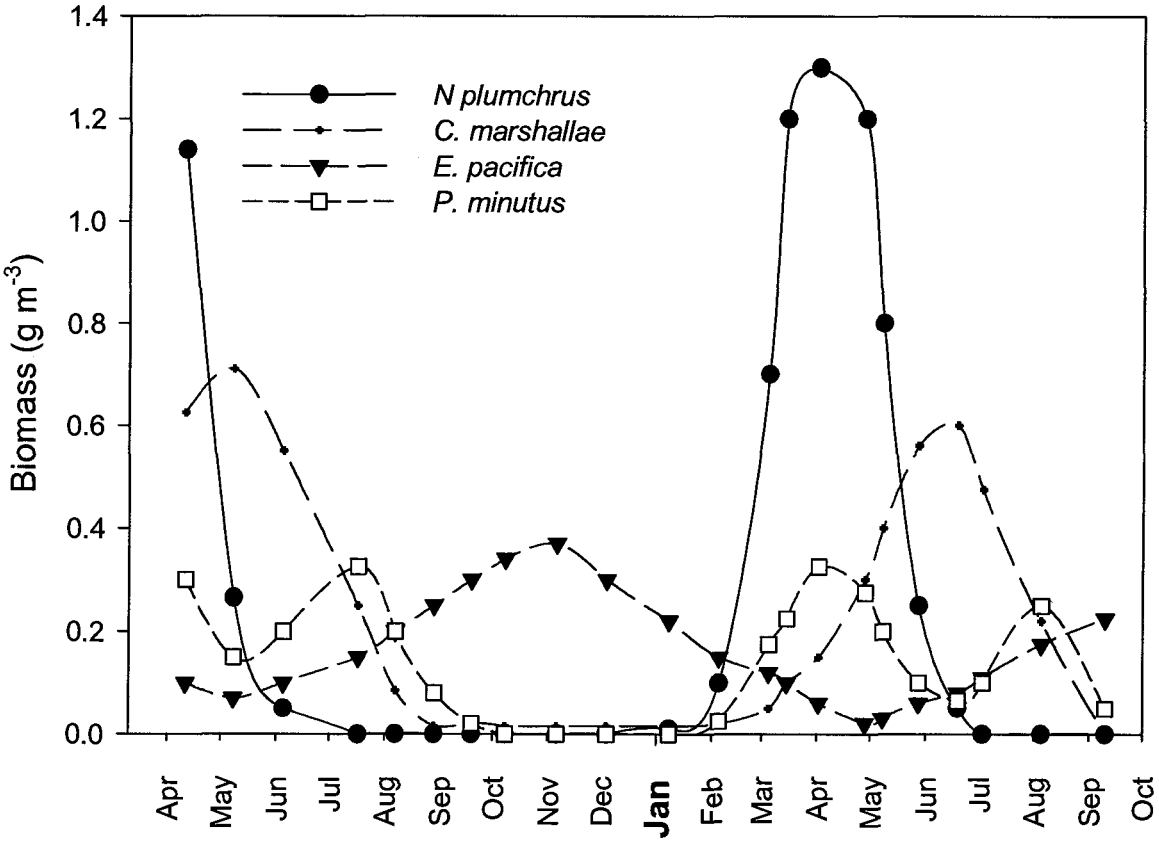

Figure 3.1. Classical view of seasonal patterns in zooplankton biomass and species succession in the Strait of Georgia. Note the high biomass of *N. plumchrus* in April. Redrawn from Harrison *et al.* (1983).

zooplankton species in the SoG, the life cycle of *N. plumchrus* is an excellent one with which to study the flow of biovolume through the NBSD.

Other zooplankton species also comprise a significant portion of the total biomass in the Strait. Calanoids such as *C. finmarchicus* and *C. marshallae* can be abundant (Gardner, 1977). Euphausiids (*E. pacifica*) are abundant at depth and migrate to the surface to feed during the night. Numerous small calanoids are present year round (such as *Oithona, Pseudocalanus, Microcalanus, Metridia*) (Harrison, 1983; Gardner, 1977). Jellyfish such as *Aurelia* and *Aglantha digitale* are abundant in the spring and summer, as well as siphonophores, ctenophores and chaetognaths (Arai and Brinkman -Voss, 1980; Arai and Masson, 1982;). Pteropods (*Limacina helicina* and *Clione Limacina*) are also known to occur high abundance (Gardner, 1977; Mackas, *pers comm*). The role of these gelatinous zooplankton is likely significant but remains poorly studied.

The Strait of Georgia, with its complex but relatively predictable cycle of biophysical interactions, is an excellent place for the application of size-based models to field-based observations of zooplankton community dynamics. With this in mind, the objectives of this study are:

1) to relate the seasonal variation of the zooplankton community size distribution to the community composition dynamics in the SoG using an Optical Plankton Counter and net samples.

2) to use size distribution theory to generate hypotheses on how seasonal changes in rate processes such as growth and loss could have influenced the slope of the NBSD.

3.2 Methods

3.2.1 Data Collection

Data were collected from April 2002 to September 2003 as part of the Strait of Georgia Ecosystem Monitoring Project (STRATOGEM), a multi-year collaborative program

designed to model the ecosystem dynamics of the Strait of Georgia. This study presents data from the first 18 months of STRATOGEM sampling. Each month, nine stations within the Strait were visited in one day (Map 3.1). During the spring bloom of 2003 (late March through June), additional cruises were conducted at weekly intervals (for 8 weeks) to bracket the period of greatest change. Data were collected from the Canadian Coast Guard hovercraft *Siyay* and included vertical profiles with a Seabird 25 CTD, OPC (Focal Technologies), transmissometer, oxygen sensor (Seabird SBE 43®) and a Wetstar® fluorometer (Wetlabs). In addition, bottle samples were taken at five depths (0, 5, 10, 15 and 30m) at each station. All combined OPC/CTD profiles were taken from the surface to within 10 meters of bottom. Zooplankton samples were also collected using a 236μm SCOR – type net (volume corrected with a flowmeter), towed vertically from 100 to 0m at one station (S4-1) on each cruise. Samples were preserved in 5% buffered formalin. For some cruises, net samples were not available due to weather conditions. In those cases, additional samples from S4-1 (collected by R. Campbell) were used to fill in the gaps in the series. In all, 158 OPC/CTD casts and 20 net tows were collected over 22 cruises.

3.2.2 Data Analysis

CTD Data: CTD data are maintained online on the STRATOGEM web site by Rich Pawlowicz (University of British Columbia, www.stratogem.ubc.ca). Chlorophyll *a* (chl *a*) fluorescence values were translated from units of volts to units of μg chl *a* L^{-1} using bottle samples to calibrate the fluorometer (analysis done by S. Harris, University of British Columbia). For each cast, CTD and fluorometer data (temperature, transmissivity and fluorescence) were averaged into 2m depth bins. To give an idea of the average environmental conditions in the Strait of Georgia (and for later comparison to OPC profiles), these profiles were averaged across all stations within a cruise (usually nine per cruise). Contour plots of transmissivity (%tx) and chlorophyll *a* fluorescence (μg chl *a* L^{-1}) were made. These plots were compared visually to the OPC contour plots.

Net Data: Net samples were available for April 2002 through July 2003. Samples were split (typically 5 or 6 times) using a Folsom plankton splitter and then sorted to species

and (where possible) to stage. The length (mm) and dry weight (μg) of each species and stage were drawn from an existing database (courtesy of D.L. Mackas, Institute of Ocean Sciences). Zooplankton that were too small (smaller than 0.25mm) or too large (greater than 6.0mm) to be accurately counted by the OPC were ignored. For each cruise, the average dry weights of individual zooplankton was calculated, as well as the total dry weight of the numerically dominant species. All species were then classed as either a small (less than 1mm) or large (greater than 1mm) size class and the dry weight (mg m^{-3}) in both classes was calculated.

OPC data: All OPC casts were binned into 5m depths. This size of the depth bin was chosen so as to maximize the amount of "signal" apparent over the "noise" that is inherent to the OPC data. To increase the total volume of water sampled at each depth, all casts in a cruise (which were generally collected in less than 10 hours) were then binned into one "average" profile. It was assumed that samples taken at different stations did not differ enough to be distinguishable from the background "noise". Comparison of the size structures of the individual OPC casts from a single cruise using the percent similarity method described in chapter 2 (section 2.2) showed that there was no statistically significant relationship between the spatial separation and the PSI between any pair of samples (Figure 3.2). Furthermore, a linear regression through the resulting structure function plot showed no significant decay of similarity with increased geographic distance between samples. In addition, most stations were not far enough apart to be considered isolated communities over the time separating cruises. All OPC particle counts were classed as either smaller or greater than 1mm equivalent spherical diameter (ESD). These two size classes are referred to as OPC_{small} and OPC_{large}, respectively. The biovolume (mm^3 m^{-3}) of each particle was calculated from its ESD, assuming that all particles were spheres (see chapter 1 for a more complete introduction to the OPC).

To track the depth distribution of zooplankton throughout the year, contour plots of average (over all stations) abundance m^{-3} in 5m depth bins were plotted for OPC_{small} and OPC_{large} size classes. Because high transmissivity water is related to greater average particle sizes (Sprules *et al.*, 1998; Appendix 1), contours of the average size ESD, (mm)

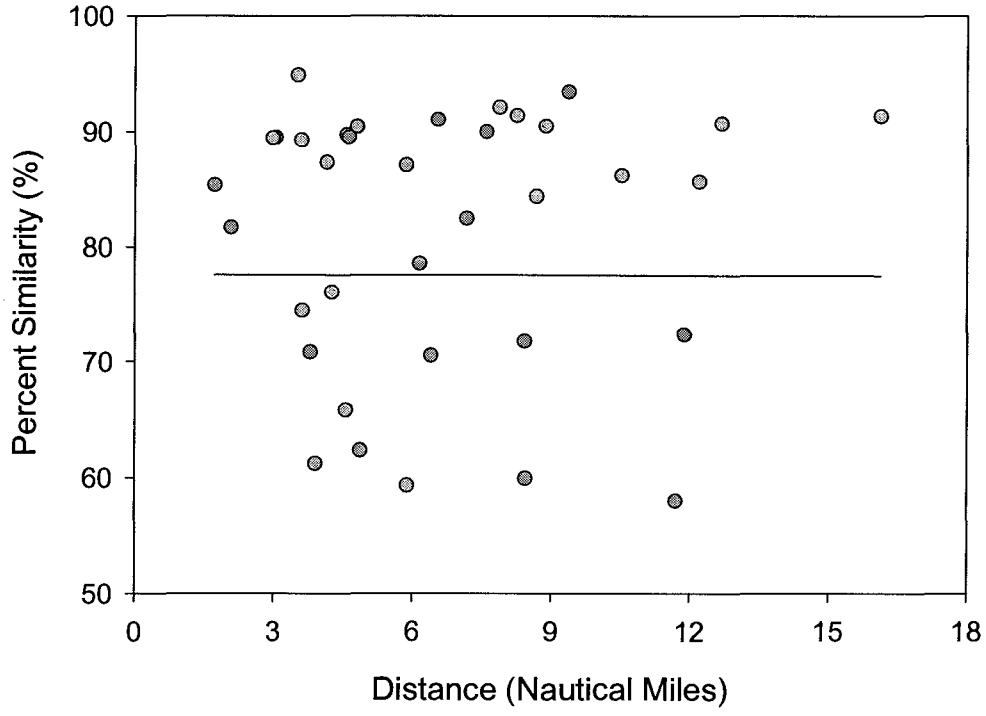

of

Figure 3.2. Structure function diagram showing the percent similarity between pairs of OPC casts in a single cruise plotted against the geographic distance separating each pair. Solid line is a linear regression with slope not significantly different to 0 (t-test, $p = 0.55$). Similar plots were made for each of the other STRATOGEM cruises, with a similar outcome. This indicates that the size structure of the zooplankton community does not differ significantly among the samples within a given survey in the Strait of Georgia.

particles in each 5m depth bin were also plotted. The average ESD plot was compared (by eye) to the transmissivity and fluorescence contour plots to determine where high average ESDs corresponded with water that had low transmissivity and high phytoplankton concentrations (see discussion of this topic in section 2.4 and Appendix 1). For comparison to the 0 - 100m net data, the average biovolume per m^{-3} (mm^3 m^{-3}) in the OPC_{small} and OPC_{large} size classes and the average individual body volume was calculated for both the OPC data between 0 and 100m.

Comparison of net and OPC data: A Spearman Rank Correlation was used to determine whether the biovolume (mm^3 m^{-3}), abundance (# m^{-3}) and average individual particle volume (mm^3) in the OPC samples followed a similar pattern to the total biomass (mg m^{-3}), abundances (# m^{-3}) and average individual dry weight (μg) in the net samples. These analyses were performed separately on the small (<1.0mm) and large (>1.0mm) particle size classes.

Comparing dry weights from net samples to biovolumes from the OPC samples may be inappropriate (*i.e.* another instance of apples and oranges). Also, because the net likely undersampled small particles relative to the OPC (Nogueira *et al*, 2004; Herman, 2001, Gallienne and Robins, 2001b) while the OPC likely undersampled large particles relative to the nets (Heath, 2001), it may be inappropriate to compare the two types of samples over the entire possible range of sizes. Therefore, the OPC and net samples were compared in terms of the *total* biovolume sampled by each for particles between 0.65 and 3.0mm. A time series of biovolumes in the net and OPC estimates of particle abundance was plotted and a Spearman's rank correlation used to test the relationship between them.

Biovolume size distribution: The OPC-derived biovolume size distribution of zooplankton in the entire water column was plotted for each cruise. Particles were binned into log_2 sizes based on their volume, then the total volume in each bin was plotted for each cruise. Note that this distribution was not normalized by the size of the

weight interval as in the normalized biovolume size distribution. This size distribution was calculated for all particle sizes between 0.25 and 6.0mm. To represent the biovolume of particles that were likely sampled equally by the OPC and net samples, the size distribution for particles between 0.65 and 3.0mm was also plotted.

For each cruise, the slopes of the normalized biovolume size distribution (NBSD) were calculated from the OPC and net data using a linear regression of log(normalized biovolume) against log(size). To obtain body volumes for the net zooplankton, their body lengths were used to calculate a body volume assuming one of three general shapes approximating the body shapes of zooplankters (sphere, oblate spheroid or cylinder) (Lawrence *et al.,* 1987; Kobayashi *et al.,* 1998). Formulae for calculating the volumes of different organisms based on their body lengths are listed in Table 3.1. To resolve depth-related differences in the size distribution from the OPC data, NBSD slopes were calculated over four different depth strata (0 - 25m, 25 - 100m, 100 - 200m and 200 - 400m). In addition, the slopes of the NBSD averaged over 0 - 400m was calculated. Time series of NBSD slopes for each cruise were plotted and average slopes over all cruises calculated. The average slopes were compared to the -1.0 slope found empirically in other studies (e.g. Sprules *et al.*, 1983; Rodriguez and Mullin, 1986a; Gaedke, 1992; Noguiera *et al*, 2004).

To demonstrate the evolution of the NBSD through the year the cumulative probability distribution (CPD) approach of Vidondo *et al.* (1997) was combined with the use of residuals (Quinones *et al.* 2003) to clarify the source of variation within the zooplankton size distributions. Cozar *et al.* (2003) examined variation in the size distribution of an aquatic community by calculating the average biovolume size distribution over the duration of their study, and then calculated the residuals of the biovolume distribution for each cruise as:

$$\text{Residuals} = \log\left(\frac{\beta_{cruise}}{\beta_{average}}\right) \qquad (3.4)$$

where β_{cruise} is the NBSD for a single cruise and $\beta_{average}$ is the NBSD averaged over all cruises. In the present study, a cumulative probability distribution was substituted for the

NBSD. One common problem with plotting the NBSD is that it requires binning individual organisms into size classes, resulting in a significant loss of information. Instead, a cumulative probability distribution can be used to display biovolume distribution data (Vidondo *et al.*, 1997; Quintana, 2002). This amounts to taking each particle and finding the proportion of the whole sample that is of greater or equal size. In this way, each particle provides one piece of information to the resulting size distribution and greater resolution is preserved. The CPD was calculated for all four depth strata in each cruise. The average CPD for all cruises was then calculated and the residuals for each cruise were plotted sequentially to demonstrate the change in shape of the NBSD through time.

Group	Body Shape	Length (mm) to biovolume (mm^3) conversion
Copepods	Oblate Spheroid	$v = \frac{4}{3}\pi(L)\left(\frac{L}{3}\right)^2$
Euphausiids	Oblate Spheroid	$v = \frac{4}{3}\pi(L)\left(\frac{L}{4}\right)^2$
Chaetognaths	Long Cylinder	$v = L \times \pi\left(\frac{L}{20}\right)^2$
C. limacina	Cylinder	$v = L \times \pi\left(\frac{L}{10}\right)^2$
L. helicina	Sphere	$v = \frac{4}{3}\pi\left(\frac{L}{2}\right)^3$
Larvaceans	Sphere	$v = \frac{4}{3}\pi\left(\frac{L}{2}\right)^3$

Table 3.1. Formulae used to convert length measurements (mm) from zooplankton in the net samples to volumetric equivalents (mm^3) . L indicates the body length of an individual.

3.3 Results

3.3.1 Temperature, chl a fluorescence and transmissivity

Temperature in the surface 0 - 25m varied from a high of 16°C to a low of 8°C (Figure 3.3). Below 20m the average temperature rarely exceeded 10°C. Chlorophyll *a* fluorescence values in the Strait of Georgia followed a typical spring bloom pattern (Figure 3.4). Peak values (which occurred in April of both years and ranged from 4-20µg chl *a* L^{-1}) were limited to the top 20m, with occasional intrusions down to 40m. Winter values ranged between 0.2 and 1.2µg chl *a* L^{-1}. The average surface (0 - 25m) fluorescence was high, around 20µg chl *a* L^{-1} for an extended period in 2002, until late October. The bloom in 2003 was of shorter duration, with a peak value of 14.3µg chl *a* L^{-1} in May before dropping to winter levels by the end of August. The lowest surface transmissivity values (>63%) occurred primarily in the top ten meters in May-June of both years (Figure 3.5). Below 20m transmissivity was generally >85%, except during October 2002 when a pulse of low transmissivity water was recorded between 50-200m.

3.3.2 Net data

Copepods were the numerically dominant group in all net samples, with the 22 species found in this study comprising 58% (by abundance) of the zooplankton sampled over the whole series. Also present were cnidarians, chaetognaths, polychaetes, molluscs and other arthropods such as decapod larvae, euphausids, isopods and amphipods. A list of dominant taxa and their summary statistics are presented in Table 3.2.

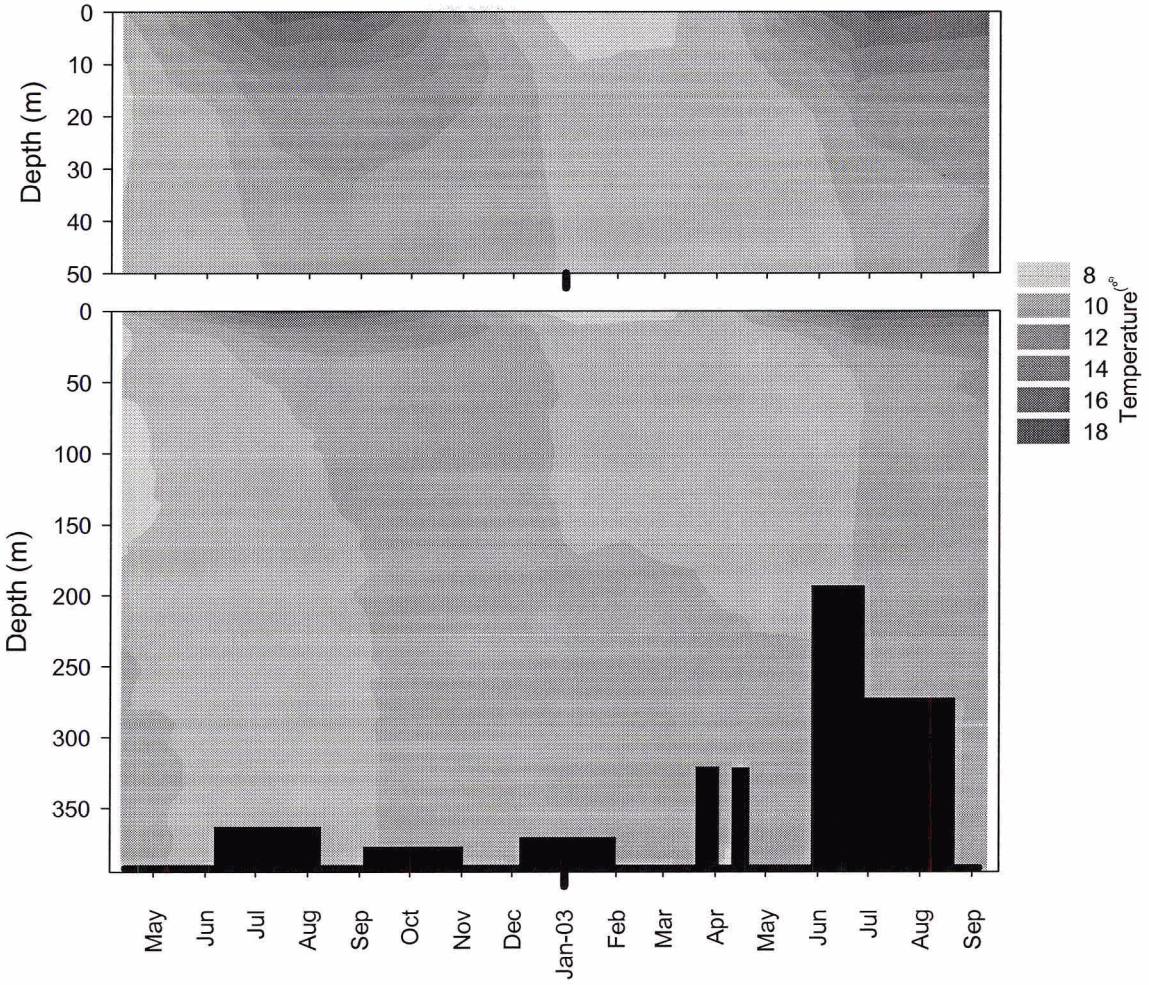

Figure 3.3. Contour plot of temperature (°C) from the STRATOGEM series between April 2002 and September 2003. For each cruise, all casts were averaged to produce one profile. Top panel: 0 - 50m (Depth scale exaggerated to show detail). Bottom panel: 0 - 400m. Black areas indicate no data at that depth.

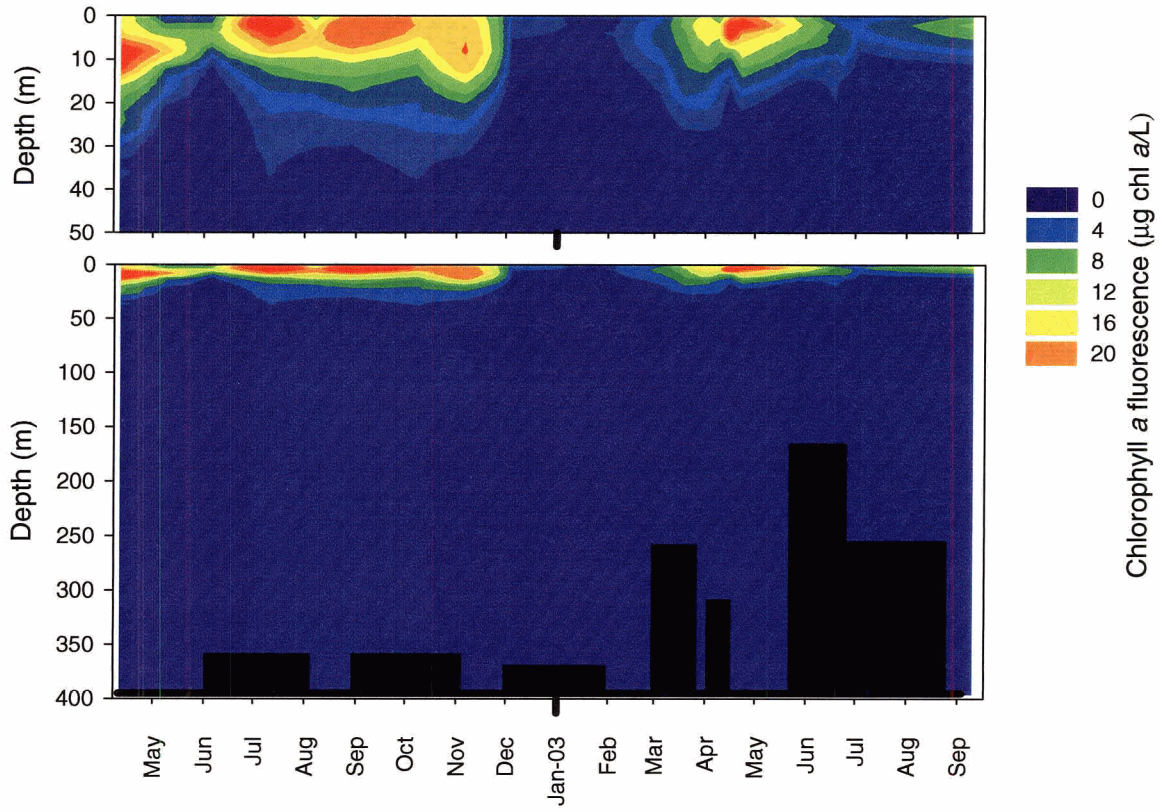

Figure 3.4. Contour plots of chlorophyll *a* fluorescence (µg chl *a* L^{-1}) averaged over 2m depth bins in the 0 - 50m (top panel) and 0 - 400m (bottom panel) depth strata. Data are from April 2002 to September 2003 in the Strait of Georgia. Profiles for each cruise represent the average of all casts on that cruise. Note that high chlorophyll fluorescence values are confined to the top 25 meters. Black areas indicate no data.

Pteropods (*Clione limacine* and *Limacina helicina*) dominated the biomass in both years, with total dry weights of up to 1000 mg m^{-3} (Figure 3.6). Among the crustaceans, *Metridia pacifica, Neocalanus plumchrus* and *Euphausia pacifica* dominated the biovolume of large (>1mm) zooplankton. *Oithona similis, Oithona atlantica, Paracalanus parvus, Pseudocalanus minutus, Pseudocalanus moultoni* and *Oncaea borealis* were also abundant, but their smaller size meant that their relative contribution to total biovolume was small (Figure 3.6). There were two distinct pulses in the small size ranges: one during and one after the spring bloom. The first, in April 2002, consisted primarily of *Acartia* spp., *Oithona* spp., *P. minutus* and euphausiid eggs. In July/August, there was a resurgence of *Acartia* spp. and *O. similis*, as well as an increase in *P. parvus*. In March 2003, *P. minutus* and *P. parvus* preceded the bloom by several weeks, followed by *Corycaeus anglicus*, euphausiid eggs and *Acartia* spp. in April at the start of the bloom. In May, all species decreased and in July the dry weights of *C. anglicus*, *P. minutus, Acartia* spp. and *P. parvus* increased again.

Because the dry weights in some net casts were dominated by the pteropods *C. limacine* and *L. helicina* (which contribute disproportionately to measures of dry weight due to their shells), average size and total dry weight in each cruise were re-calculated with the pteropod fraction excluded. The dry weight of zooplankton in the small and large size classes from net tows was highest in the spring of both years (Figure 3.7). This period of high biomass lasted about three months in both years, starting in April. The removal of the two pteropods species from the net data had a marked effect on both size classes, resulting in an eight-fold decrease in total dry weight in some of the spring-time net tows. The average dry weight (μg) of individual zooplankters was also strongly seasonal, with the greatest average weights occurring between April - July 2002 and March - June 2003 (Figure 3.12). In addition, there was a marked increase in average size in January 2003. The removal of pteropods from the average weight calculation reduced the average weights by a factor of 2 or 3, but the same overall pattern of variation persisted.

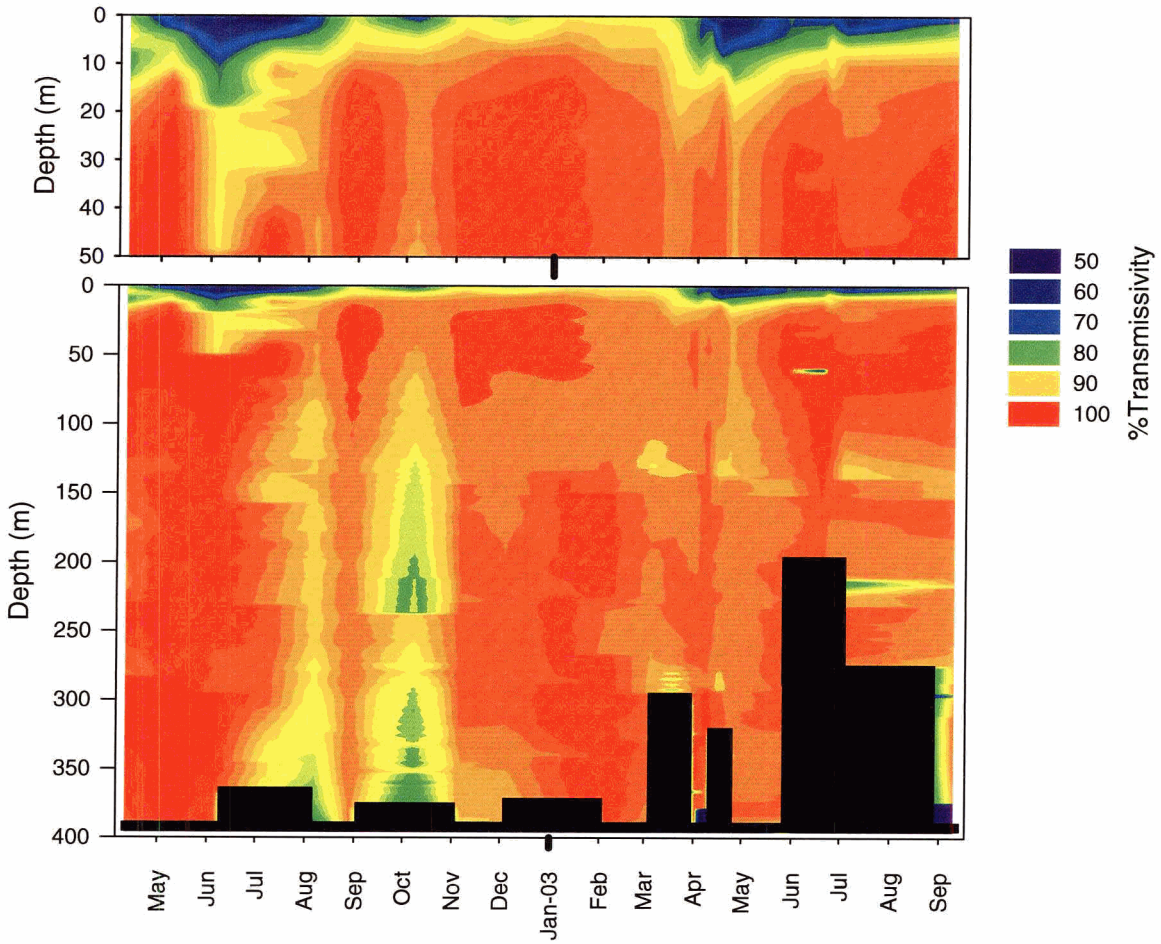

Figure 3.5. Contour plot of water transmissivity averaged over 2m depth bins in the 0 - 50m (top panel - depth scale exaggerated for detail) and 0 - 400m (bottom panel) depth strata between April 2002 and September 2003 in the Strait of Georgia. Profiles for each cruise date represent the average profile of all casts taken within a cruise. Note that low transmissivity values (indicating cloudy water) are confined to the 0 - 25m surface layer. Black areas indicate no data. The discontinuity in October at 230m is likely due to the way in which the casts were averaged over the whole cruise

Species	Body Length (mm)	Dry Weight (µg)	% Contribution to total number	Total mass in all samples (mg)	Median #/m^3 per tow	Max #/m^3 per tow	Mean #/m^3	Standard deviation of mean
Copepods								
Oithona atlantica CIV-CVI	0.8 - 1.4	2.0 - 3.0	12.6	38.7	44.7	454	30.7	117.7
Metridia pacifica CI-CVI	0.1 - 1.4	12.0 -13.6	10.8	45.0	38.2	282	8.2	87.3
Oithona similis CV-CVI	0.6 - 0.9	0.5 - 1.5	7.9	1.6	38.7	209	8.2	64.5
Paracalanus parvus CIV-CVI	0.6 - 0.7	2.9 - 6.5	4.6	3.4	1.6	216	79.0	58.1
Corycaeus anglicus CV-CVI	0.5 - 0.6	2.5 - 5.0	4.3	2.8	4.8	217	14.4	65.5
Copepod nauplii	0.2	0.3	4.2	0.2	0.0	383	33.4	95.7
Pseudocalanus minutus CIII-CVI	0.5 - 1.4	1.8 - 2.1	4.0	4.3	9.9	194	29.0	47.7
Oncaea borealis CVI	0.7	0.3	2.8	0.1	0.9	158	18.3	46.4
Pseudocalanus moultoni CIV-CVI	0.8 - 1.3	1.8 - 18	2.5	4.1	8.6	93	9.0	27.0
Neocalanus plumchrus CI-CV	0.9 - 3.8	7.0 - 55.0	2.0	61.4	0.0	163	91.9	40.0
Scolecithricella minor CV-CVI	0.8 - 1.1	5.0 - 11.0	1.2	1.5	7.0	31	57.7	7.8
Acartia hudsonica CVI	0.8	7.0	1.1	1.2	0.0	90	31.2	21.8
Acartia longiremis CV-CVI	0.8 - 1	3.5 - 7.0	1.1	1.2	0.0	90	20.1	21.8
Euphausiids								
Euphausiid eggs to protozoa	0.25 - 1.4	1.0 - 4.5	8.5	2.8	0.4	603	43.5	145.1
Euphausia pacifica Zoea to Adult	3-4.7	40 - 160	6.0	49.5	0.0	675	61.6	153.3
Chaetognaths								
Parasagitta elegans	3 - 7.5	8.8	3.1	40.0	2.1	116	22.7	34.9
Pteropods								
Clione limacina	3 - 7.5	3500	2.3	1191.2	0.0	228	17.0	50.9
Limacina helicina	0.5 - 1.2	38	2.1	195.6	0.5	152	15.2	35.9
Larvaceans								
Fritillaria borealis	1	10	1.4	2.1	0.0	203	10.4	45.3
Oikopleura dioica	4.6	10	1.0	1.5	0.0	76	7.5	19.3

Table 3.2. Dominant zooplankton species in STRATOGEM 0 - 100m vertical net hauls,. In all, 20 net hauls were taken between April 2002 and September 2003.

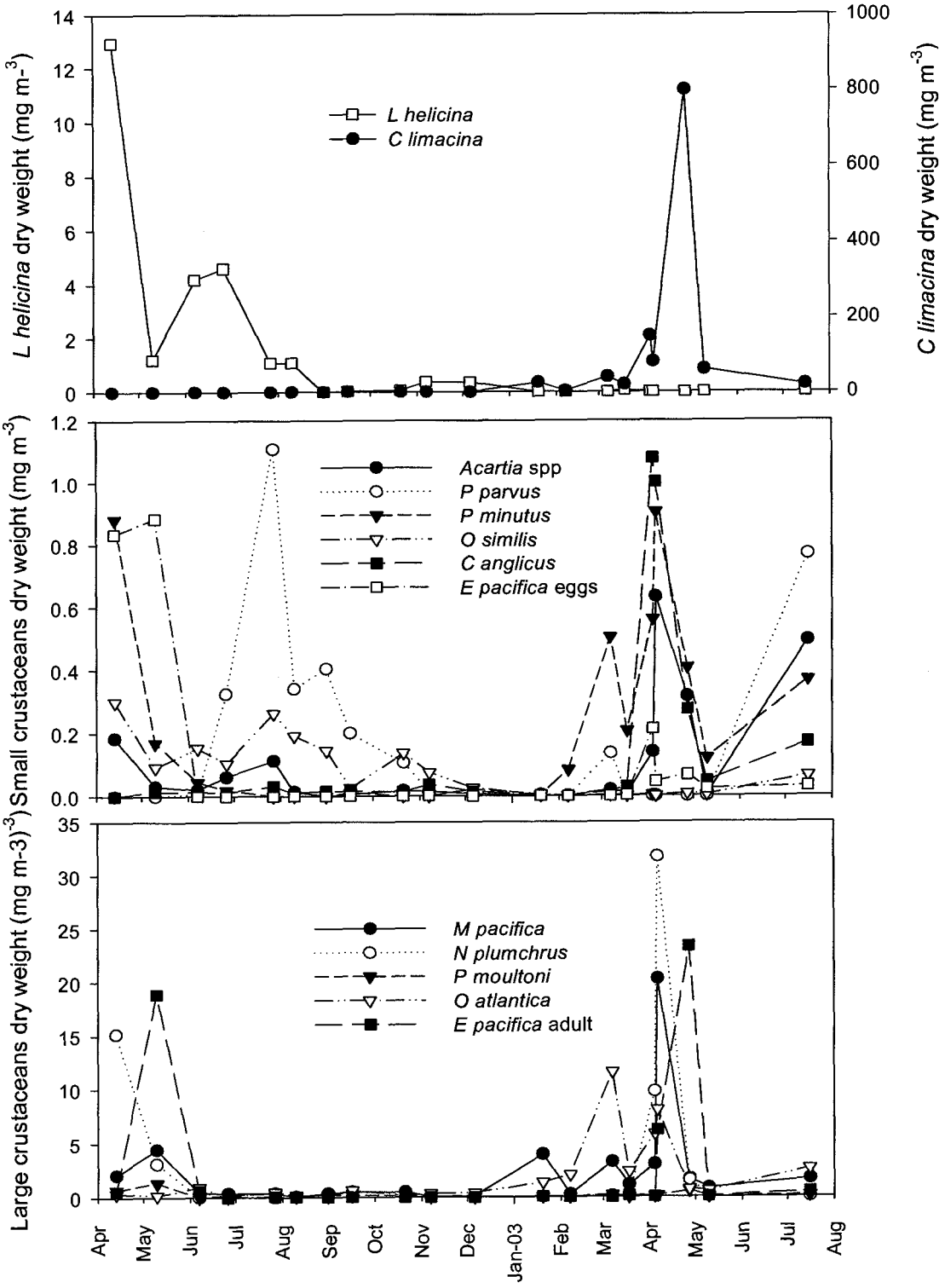

Figure 3.6. Dry weight of numerically dominant zooplankton species in 0 - 100m vertical net hauls in the SoG between April 2002 and September 2003. Top panel: Pteropods. Middle panel: other zooplankton >1.0mm in length. Bottom panel: other zooplankton < 1.0mm in length.

3.3.3 OPC data

The OPC particle abundance contour plots reveal a rich pattern of spatiotemporal variation in the distribution and abundance of zooplankton over the 18 months of this study. Small particles were most abundant (up to 3500 ind. m^{-3}) at the surface 0 - 25m and at depths between 300 - 400m for most of the series (Figure 3.8). In mid-water depths (25-300m), small particles reached concentrations of between 2500 to 3000 ind. m^{-3} in July - August 2002, November 2002 - January 2003 and March 2003. Large particles were abundant (~150 ind. m^{-3}) in the surface between May -July 2002 and May - August 2003 (Figure 3.9). Below this (100-300m), large particles were abundant in May-August 2002 between 100 and 400m. Between July 2002 and February 2003 and below 250m large particles were present in abundances of up to 100 ind. m^{-3}. There was another patch of abundant (300 ind. m^{-3}) large particles during July - August 2003 at 200m.

The average ESD of particles measured by the OPC was highest (> 0.75mm) in the surface between April - September 2002, and March - July 2003 (Figure 3.10). Average ESD was also high (0.6 - 0.675 mm) below 300m between August 2002 - February 2003. There were two further patches, one at 250m between April - July 2002, another at 200m in July - August 2003. Comparison of the average ESD contour plot with the plots of transmissivity and chlorophyll *a* fluorescence show that in the surface, average particle ESDs are highest during the spring when chl *a* fluorescence is high and transmissivity is low. Below 25m, there were no sections of data in which the OPC data appeared to have been affected by low transmissivity water.

From the contour plots of chlorophyll *a* fluorescence (Figure 3.4), transmissivity (Figure 3.5) and average particle ESD (Figure 3.10), it appeared that the surface (0 - 25m) OPC data was contaminated by phytoplankton. The small and large biovolumes and average individual biovolume were therefore calculated for the 25 - 100m as well as the 0 - 100m OPC strata. In the surface 0 - 100m, the biovolume (mm^3 m^{-3}) in the small and larger

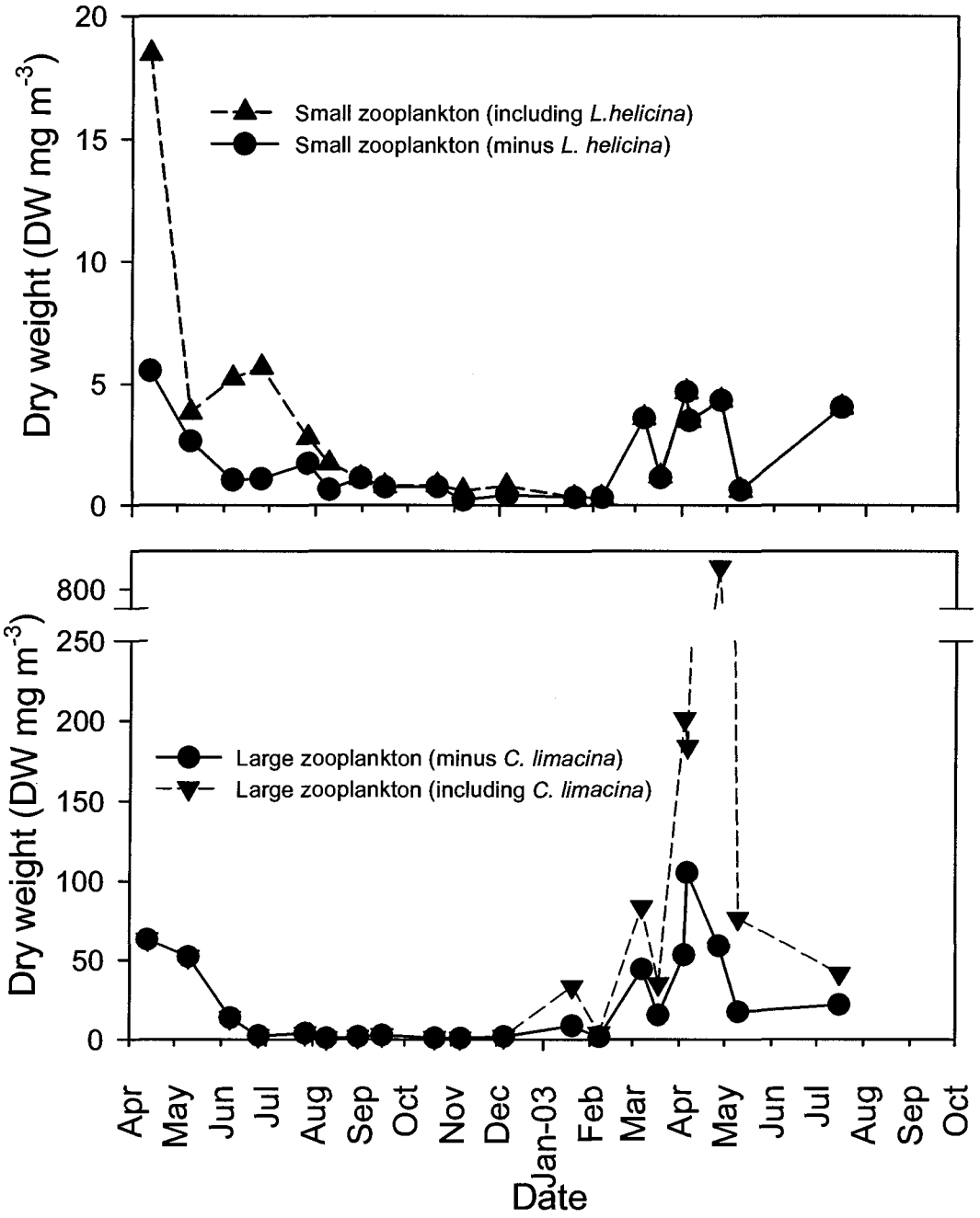

Figure 3.7. Dry weight (mg m^{-3}) of small (<1mm, top panel) and large (>1mm, bottom panel) zooplankton in 0 - 100m vertical net hauls between April 2002 and September 2003 in the SoG. Dashed lines indicate dry weights including pteropods, solid lines indicate dry weights with pteropods excluded.

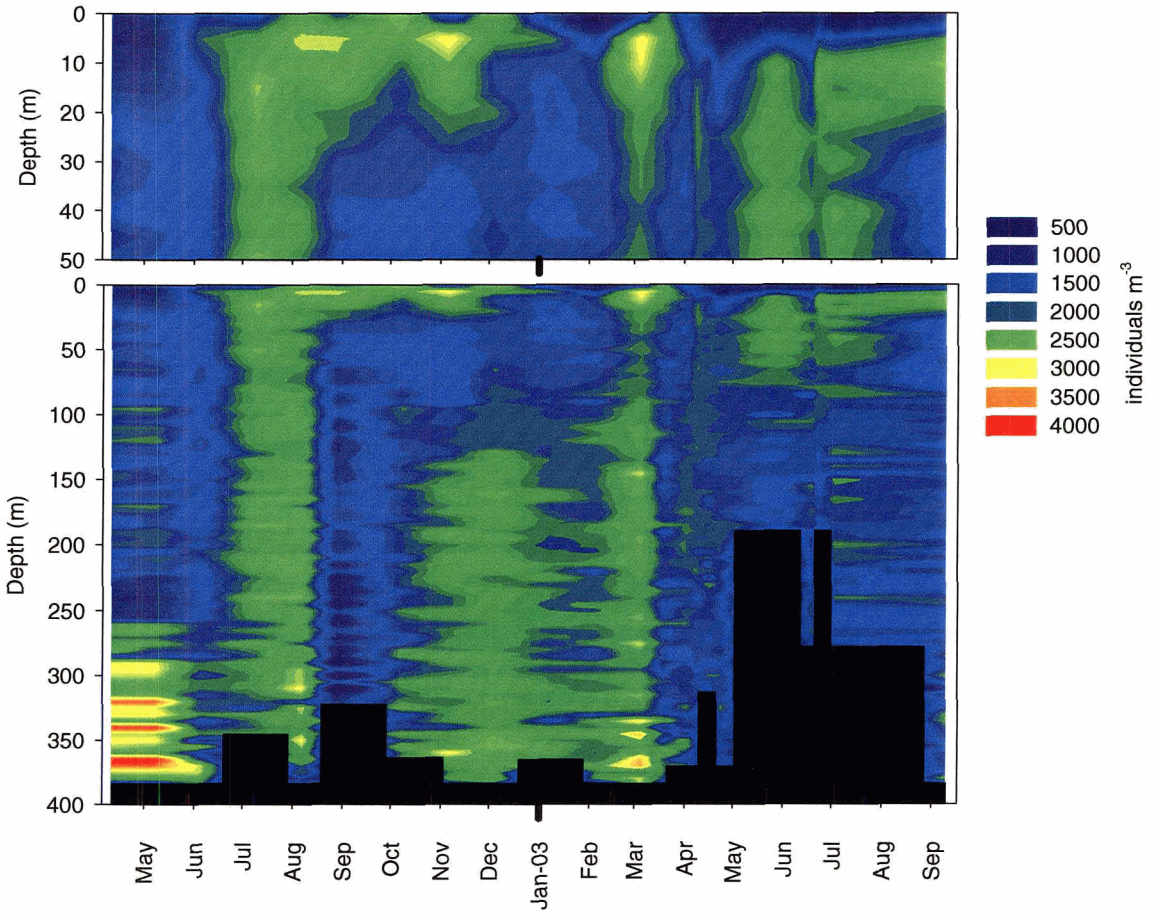

Figure 3.8. Contour plots of small particle (< 1.0mm ESD) distribution over depth and time from vertical OPC casts between April 2002 and September 2003 in the Strait of Georgia. Vertical resolution is 5m. Top panel: 0 - 50m (depth scale exaggerated to show detail), Bottom Panel: 0 - 400m. Black areas indicate no data.

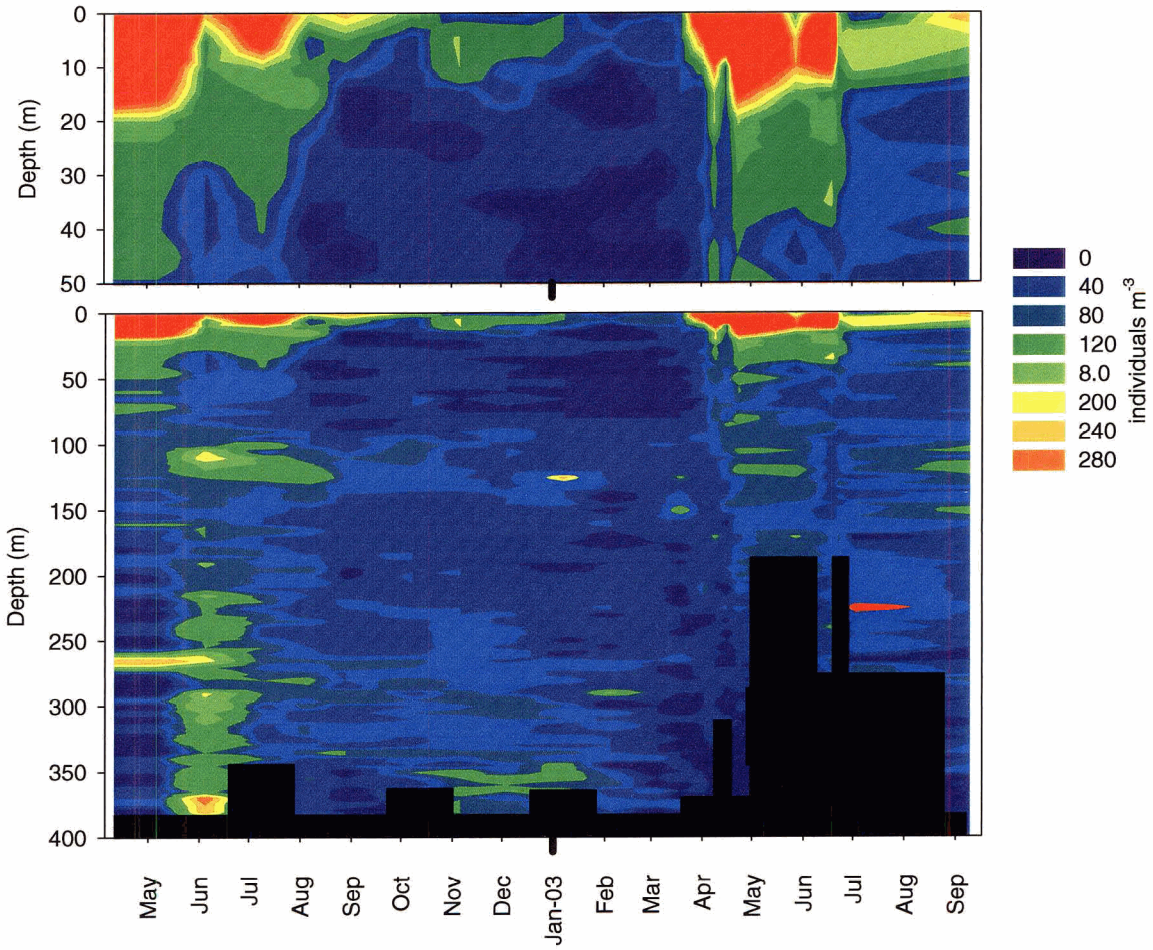

Figure 3.9. Contour plot of large particle (> 1.0mm ESD) distribution over depth and time from between April 2002 and September 2003 in the Strait of Georgia. Vertical resolution is 5m. Top panel: 0 - 50m (depth scale exaggerated to show detail), bottom panel, 0 - 400m. Black areas indicate no data.

size classes varied in the same way as the dry weight (mg m^{-3}) in the net tows (Figure 3.11). The biovolume of small particles varied seasonally, being only 2-3 times higher in the spring (April, May and July 2002, April and May 2003) than during winter months. The seasonality of large particles was much stronger, with two orders of magnitude greater biovolume in the spring than the winter. The seasonal peaks of biovolume in the large particles spanned April - August 2002 and April - July 2003. The average individual volume (mm^{-3}) in the 0 - 100m stratum showed a similar seasonality, reflecting the variation of large particle biovolume (Figure 3.12). Exclusion of the surface 25m of OPC data reduced the small particle biovolumes by about 50mm^3 m^{-3} and the large particle biovolume by a factor of two or three in the spring. However, the same general seasonal pattern persisted.

3.3.4 Comparison of OPC and Net data

Because of the potentially confounding effects of pteropods in the net data and phytoplankton in the OPC data, the Spearman rank correlations of OPC data against net data were calculated both inclusive and exclusive of the 0 - 25m depth stratum in the OPC data, and with and without pteropods in the net samples. The OPC biovolume and abundance data were significantly correlated with the net biomass and abundance data (Tables 3.3 and 3.4). In addition, the average individual biovolume in the OPC samples was significantly correlated with the average individual dry weight in the net samples (Table 3.5). Exclusion of pteropods from the net data and the top 25m of the OPC data slightly reduced the strength of the correlation, but it remained statistically significant. The biovolume in OPC and net samples both followed a similar seasonal pattern (Figure 3.13) and were significantly correlated ($r=0.44$, $p<0.05$, $df= 18$)

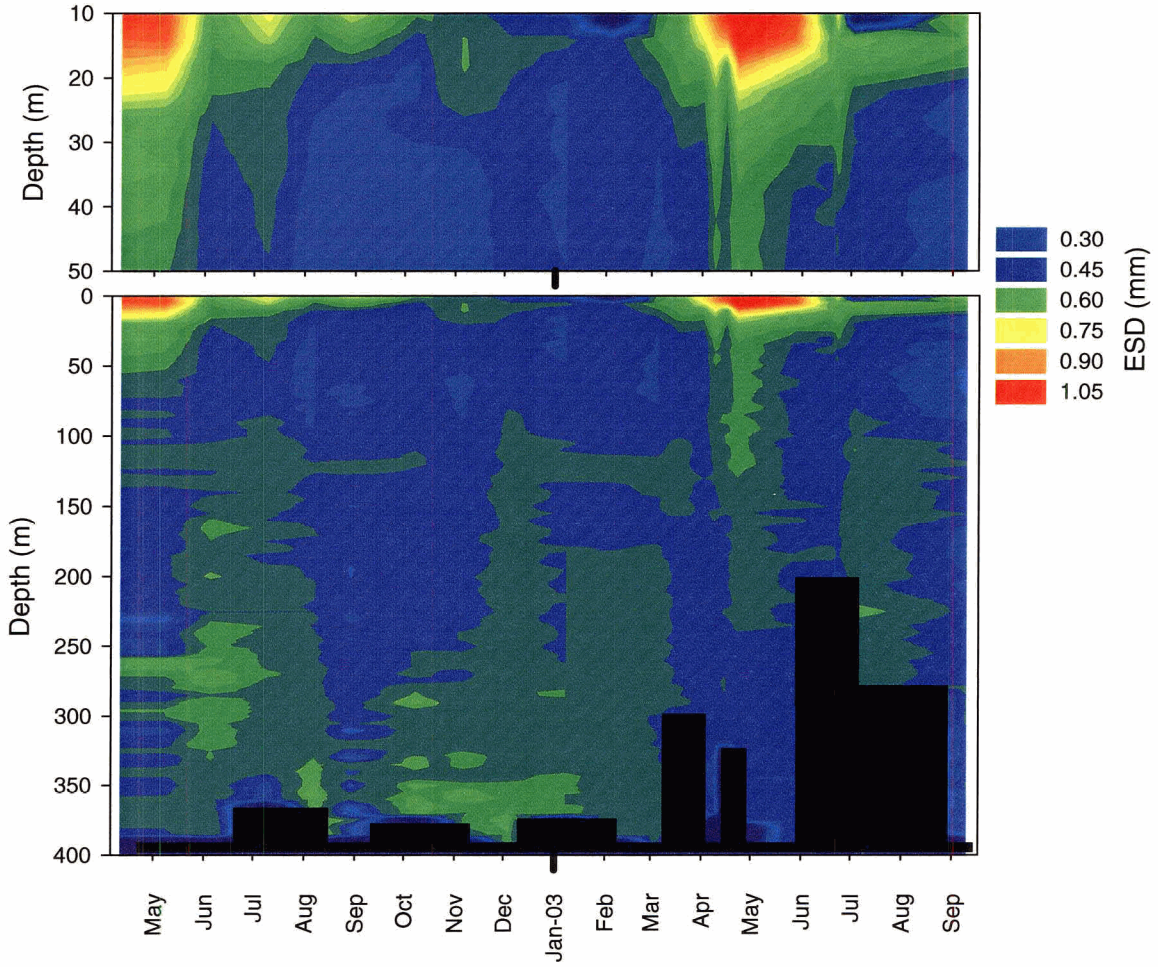

Figure 3.10. Contour plot of average particle size (Equivalent Spherical Diameter - mm) from vertical OPC casts between April 2002 and September 2003. Vertical resolution is 5m. Top panel 0 to 50m (depth scale exaggerated for detail). Bottom panel: 0 - 400m from Apr. Note that the highest average size values occur in the surface 0 - 25m. Black areas indicate no data available for that depth.

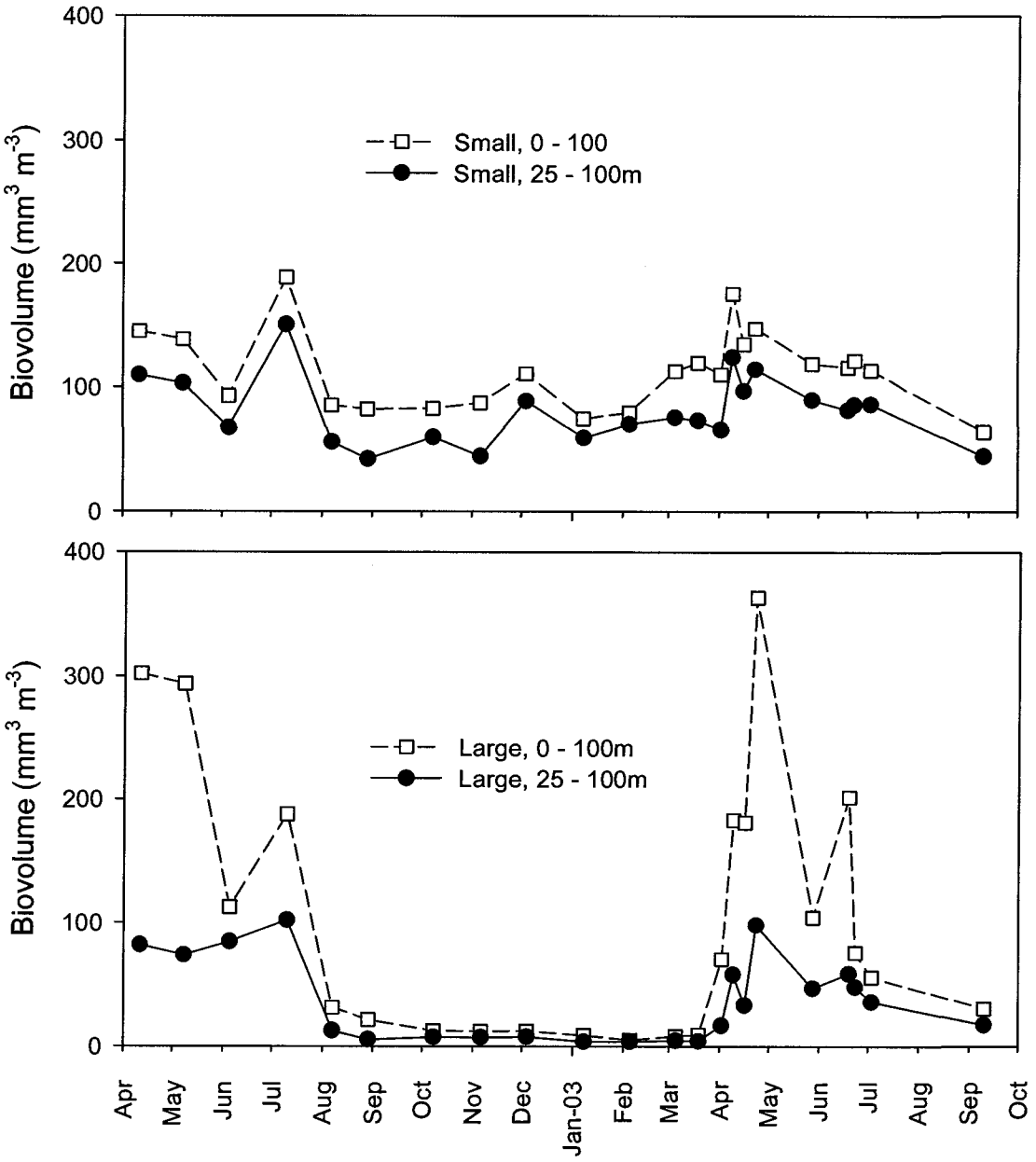

Figure 3.11. Time series of small and large zooplankton biovolume (mm^3 m^{-3}) from near-surface OPC casts. To show the effect of phytoplankton on the OPC biovolume estimates, the surface zooplankton biovolume was calculated from both the 0 - 100m and the 25 - 100m strata. Top panel: small particles (<1.0 mm). Bottom panel: large particles (>1.0 mm). (□) = biovolume in the 0 - 100m depth stratum, (●) = biovolume in the 25 - 100m stratum.

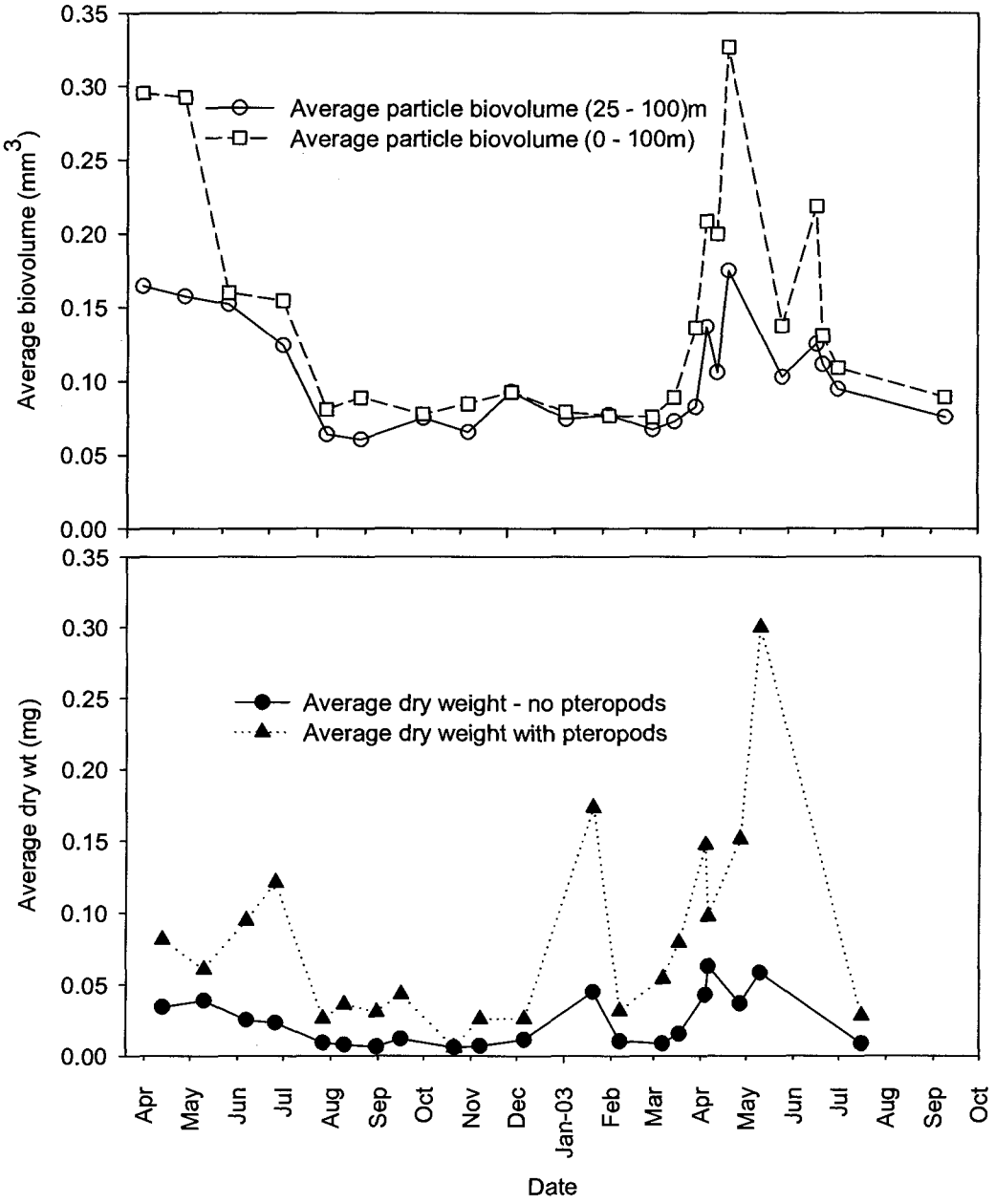

Figure 3.12. Time series of average individual dry weights and biovolumes from net and OPC samples between April 2002 to September 2003. Top panel: average particle biovolume in 0 - 100m (□) and 25 – 100m (○). Bottom Panel: Average individual dry weight (in net samples with pteropods included (▲) and excluded (●).

		OPC biovolumes			
		Large (> 1mm)		Small (< 1mm)	
Net dry weights		0 - 100m	25 - 100m	0 - 100m	25 - 100m
Large	With pteropods	0.61**	0.43*		
	No pteropods	0.64**	0.44*		
Small	With pteropods			0.47*	0.46*
	No Pteropods			0.50*	0.41

Table 3.3. *r* values from the Spearman's rank correlation between zooplankton biovolume (mm m^{-3}) in OPC samples versus biomass (mg m^{-3}) in net samples. Zooplankton in each cast were split into either the small or large size class. To determine the effect of pteropods and phytoplankton on the correlation, *r* values were re-calculated with and without pteropods in the net data and inclusive and exclusive of the top 25m of OPC data. 20 net casts were used in each correlation (*df*=18). * indicates significance at $p < 0.05$, ** indicates significance at $p < 0.01$.

	OPC: abundance			
	Large (> 1mm)		Small (< 1mm)	
Nets: abundance	0 - 100m	25 - 100m	0 - 100m	25 - 100m
Large	0.66**	0.52*		
Small			0.22	0.27

Table 3.4. *r* values from Spearman rank correlation of abundance (# m^{-3}) in 0 - 100m and 25 - 100m OPC samples against abundance in net samples. 20 OPC and 20 net casts were used in each correlation (*df*=18). * indicates significance at $p < 0.05$, ** indicates significance at $p < 0.01$.

	OPC: average biovolume	
Nets: average dry weight	0 - 100m	20 - 100m
With pteropods	0.69**	0.71***
No pteropods	0.68**	0.60**

Table 3.5. *r* values from Spearman rank correlation of the average biovolume (mm^3) of individual particles in OPC samples (0 - 100m and 25 - 100m) against average individual dry weight (µg) in net samples with and without pteropods between April 2002 and September 2003. ** indicates a significant correlation at $p < 0.01$, *** indicates a significant correlation at $p < 0.0025$, df=18.

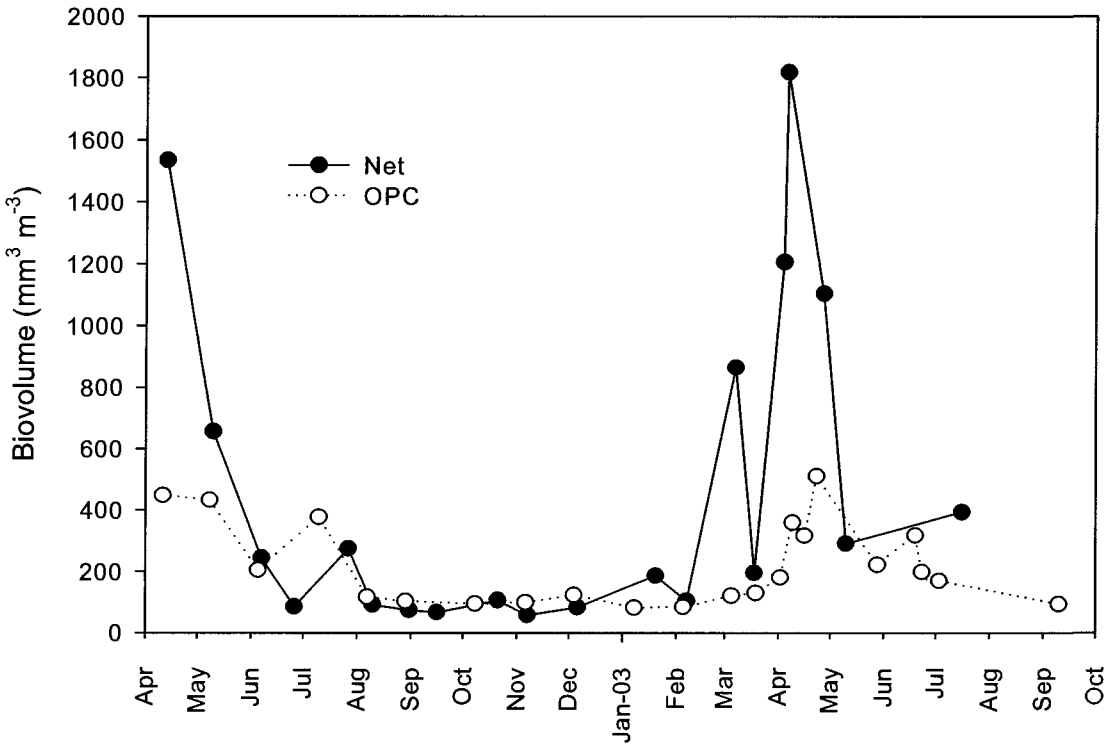

Figure 3.13. Biovolume in OPC and net samples in the Strait of Georgia between April 2002 and September 2003. ○ = OPC samples, ● = net samples.

3.3.5 Biovolume size distribution

Because of the potential contamination of the upper 25m of the water column by high concentrations of non-zooplankton particles, the 25 - 400m biovolume size distribution was plotted instead of 0 - 400m (Figure 3.14). The bulk of the particle biovolume consisted of small to medium-sized particles (0.65-1.0mm in length, or $\sim 2^{-2}$ to 2^{-1} mm^3 biovolume), and occurred almost year round. Larger particles were more seasonal in occurrence and had greater biovolume during the spring and summer months. This pattern is also reflected in Figure 3.15 which shows a similar trend to the pattern of biovolume found in the net samples.

This pattern was reflected in the seasonal changes in the slope of the normalized biovolume size distribution. The slopes of both the net and the OPC biovolume size distributions were most negative in winter months, before becoming shallower during the spring bloom, and more negative again several months after the end of the bloom. The average slope of the 0 - 400m NBSD from the OPC data was -1.03 ± 0.04, which was not significantly different than -1.0 (t-test, $p = 0.14$, $df = 21$). The average slope of biovolume distribution from the net samples was -1.29 ± 0.6 and was not significantly steeper than -1.0 (t-test, $p = 0.15$, $df = 19$). The average slopes of the biovolume distributions for the 0 - 25, 25 - 100, 100 - 200 and 200 - 400m OPC strata are presented in Table 3.6.

The slope of the NBSD also varied seasonally (Figure 3.15). In the 0 - 25 and 25 - 100m strata and the net samples, the NBSD slopes were shallower in the spring and summer and steeper in the winter and fall. In the 100 - 200m stratum, the NBSD slopes were close to -1.0 for most of the year, except for a brief period in June of 2002 and 2003 when the slope was shallow. In the 200 - 400m stratum, the slope was relatively shallow between June and September of both years, then steeper between February and May 2003.

3.3.6. Cumulative probability distribution

Figure 3.17 shows the cruise by cruise change in the CPD residuals in four depth strata. Negative (black) residuals at any size in Figure 3.17 indicate that the proportion of particles in that size for that cruise was less than the average proportion in that size over all cruises, or $\log(Prob_{cruise}/Prob_{average})$ is less than 0. The change in the magnitude of the residuals in different sizes over time shows how the NBSD evolved, likely as a result of growth in the zooplankton. The following section outlines the general trends observed in each depth stratum.

Series	Mean Slope	Standard Deviation	Different from -1.0 ?	*p* value	Degrees of freedom
Net					
0 - 100m	-1.29	0.57	No	0.12	19
OPC					
0 - 400m	-1.03	0.12	No	0.15	21
25 - 400m	-1.06	0.13	No	0.11	21
0 - 25m	-0.91	0.30	No	0.13	21
25 - 100m	-1.22	0.17	Yes	<0.0001	21
100 - 200m	-0.96	0.14	No	0.18	21
200 - 400m	-0.98	0.20	No	0.76	19

Table 3.6. Average slopes of the normalized biovolume distributions for net and OPC data from STRATOGEM samples taken between April 2002 and September 2003. OPC Biovolume distributions were calculated in four different depth strata, as well as over the whole water column. These average slopes were tested (using a t-test) for significant departure from the -1.0 slope that has been measured empirically in other studies (e.g. Sprules *et al.,* 1983; Rodriguez and Mullin, 1986; Gaedke, 1992).

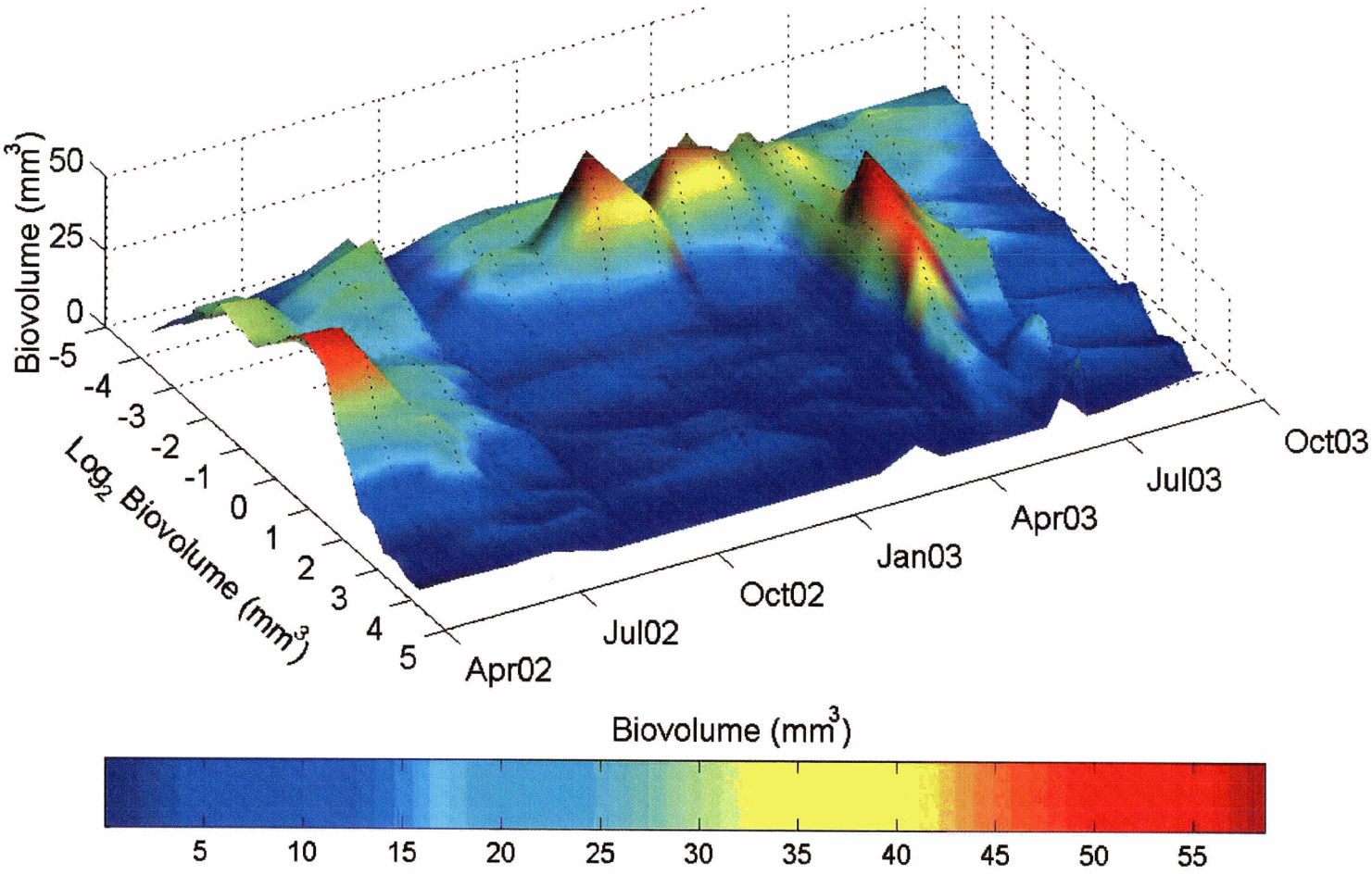

Figure 3.14. Depth-averaged (25 – 400m) biovolume size distribution for particles between 0.25 and 6.0mm from vertical OPC casts in the SoG between April 2002 and September 2003 in the SoG series. Color bar indicates biovolume (mm^3 m^{-3}).

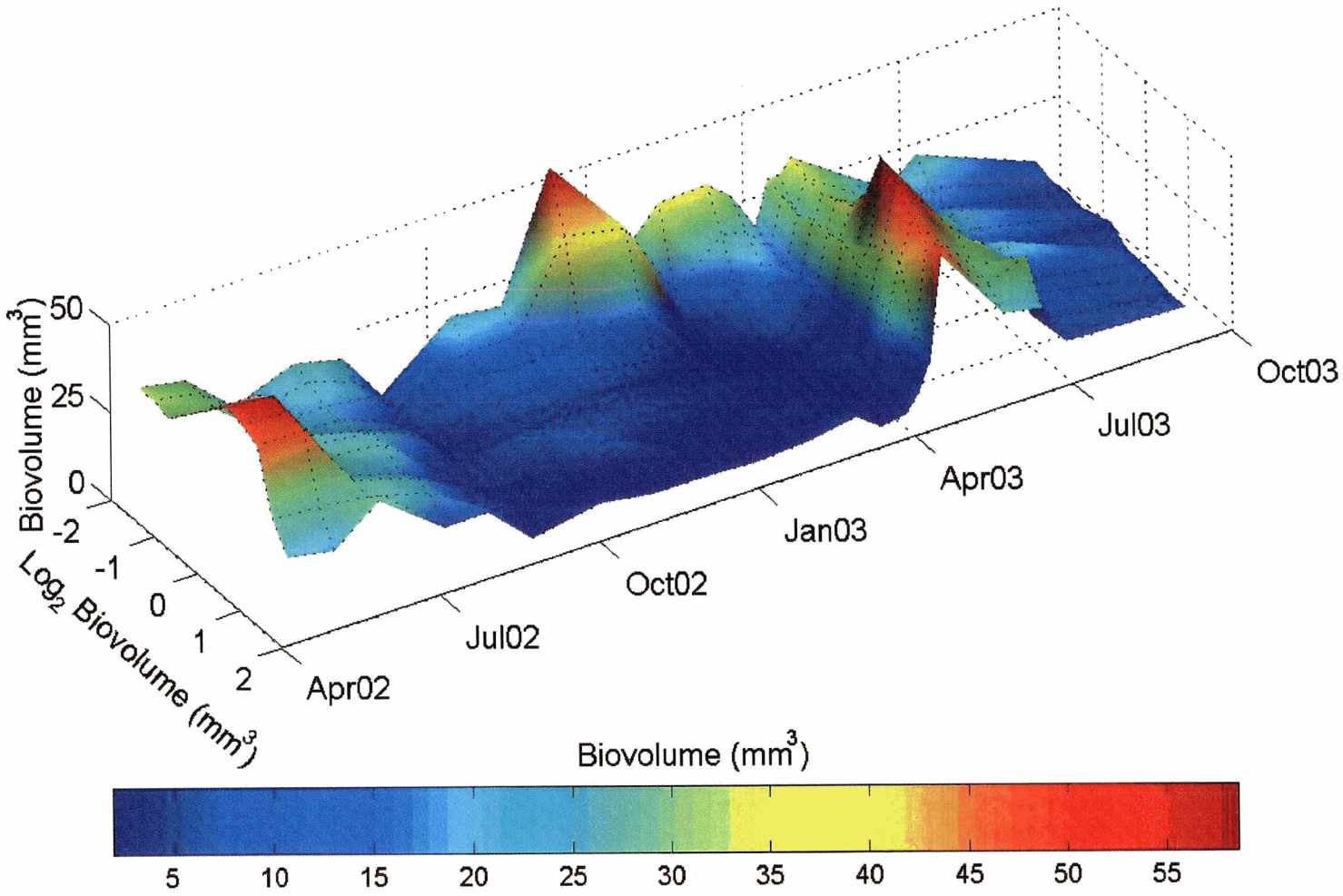

Figure 3.15. Depth-averaged (25 – 400m) biovolume size distribution for particles between 0.625 and 3.0mm from vertical OPC casts in the SoG between April 2002 and September 2003 in the SoG series. Color bar indicates biovolume (mm^3 m^{-3}).

The most dramatic patterns occurred in the surface layer (0 - 25m). In April 2002, the size distribution was dominated by the 1 - 2mm size classes. By June, the residuals in all size classes (except the largest) were negative and between July 2002 and February 2003 the residuals for most particles dropped dramatically. In early March 2003, a pulse of small (0.3-0.4mm) particles appeared and moved slowly up through the size distribution and reached the large (4mm) particles by mid-April. Following this peak, there was a sudden drop in the residuals of all particles, followed by a gradual decrease in all size classes through to June 2003. In July and September 2003 there was a brief increase in the residuals of large particles.

A similar pattern of a spring pulse followed by winter lows was mirrored in the 25 - 100m depth stratum, though with decreased intensity. The two main differences at this depth were a sudden increase in large particles in December 2002, as well as a pulse of 0.6 - 0.8mm particles which moved *down* the size distribution (i.e. from large to small sizes) between December 2002 and March 2003.

Between 100 and 200m, the spring pulse pattern was weaker, though the winter pulse in the small sizes was still present. Below 200m, the spring pulse was confined to a sudden increase in large particle residuals in late May/early June. After June 2002, the residuals remained high in large sizes (> 2mm) well into the winter.

For all depths below the surface 25m, the pulse of biomass moving through the distribution is less apparent (Figure 3.15), but still visible. The greatest change occurred in June of both years, when the residuals of sizes from 1 to 4mm increased by a factor of 10 or more. The backwards pulse in the small size classes was also still apparent.

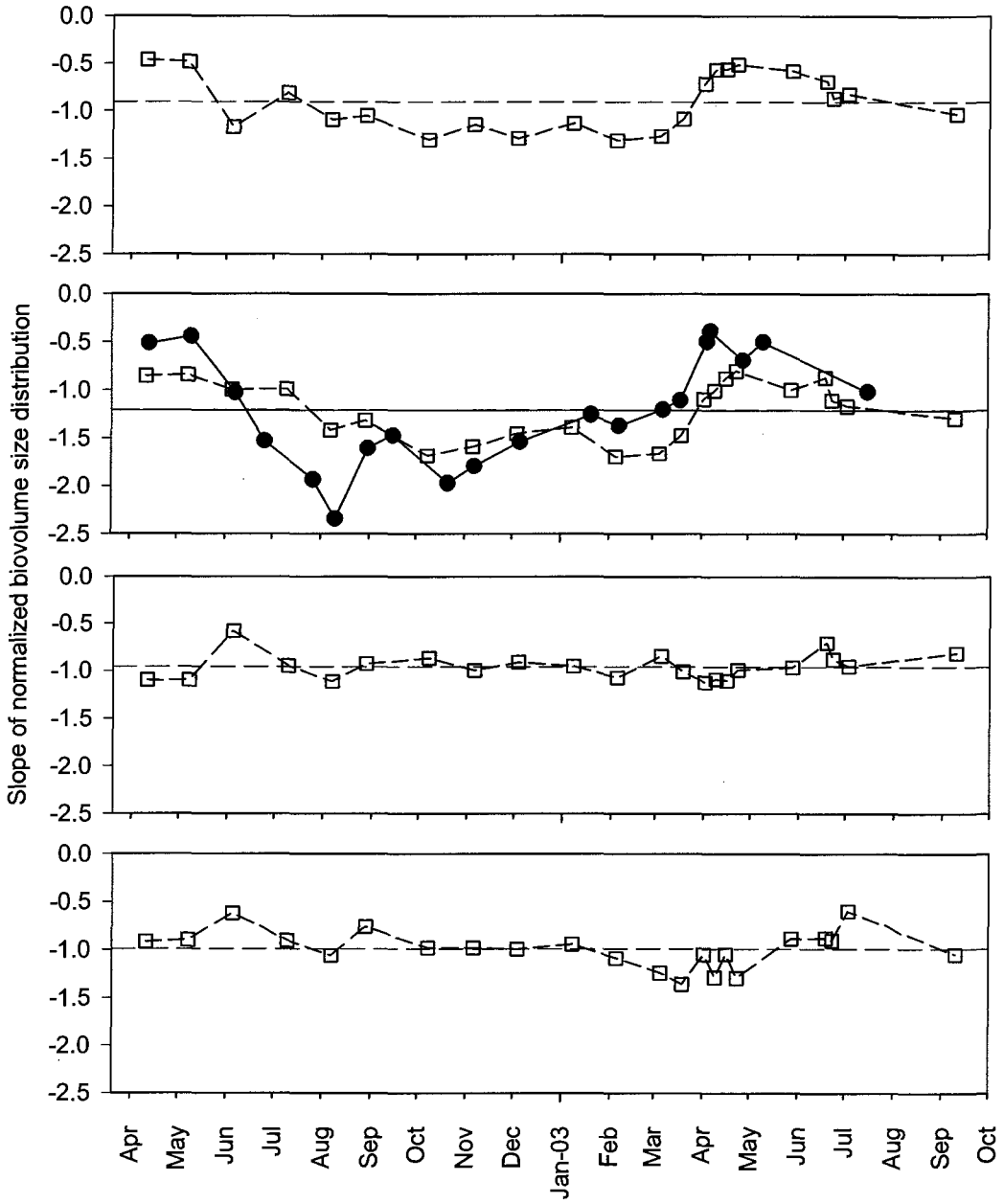

Figure 3.16. Seasonal variation in the slope of the normalized biovolume size distribution for vertical OPC data (subdivided into four depth strata) and net hauls taken between April 2002 and September 2003 in the SoG. Top panel: 0 - 25m OPC data. Second panel: 25 - 100m OPC data and 0 - 100m net hauls (□ = OPC, ● = Nets). Third panel: 100 - 200m OPC data. Bottom panel: 200 - 400m OPC data. Note that NBSD slopes in the surface are shallower in the spring than in the winter and that net and OPC NBSD slopes follow a similar pattern of variation.

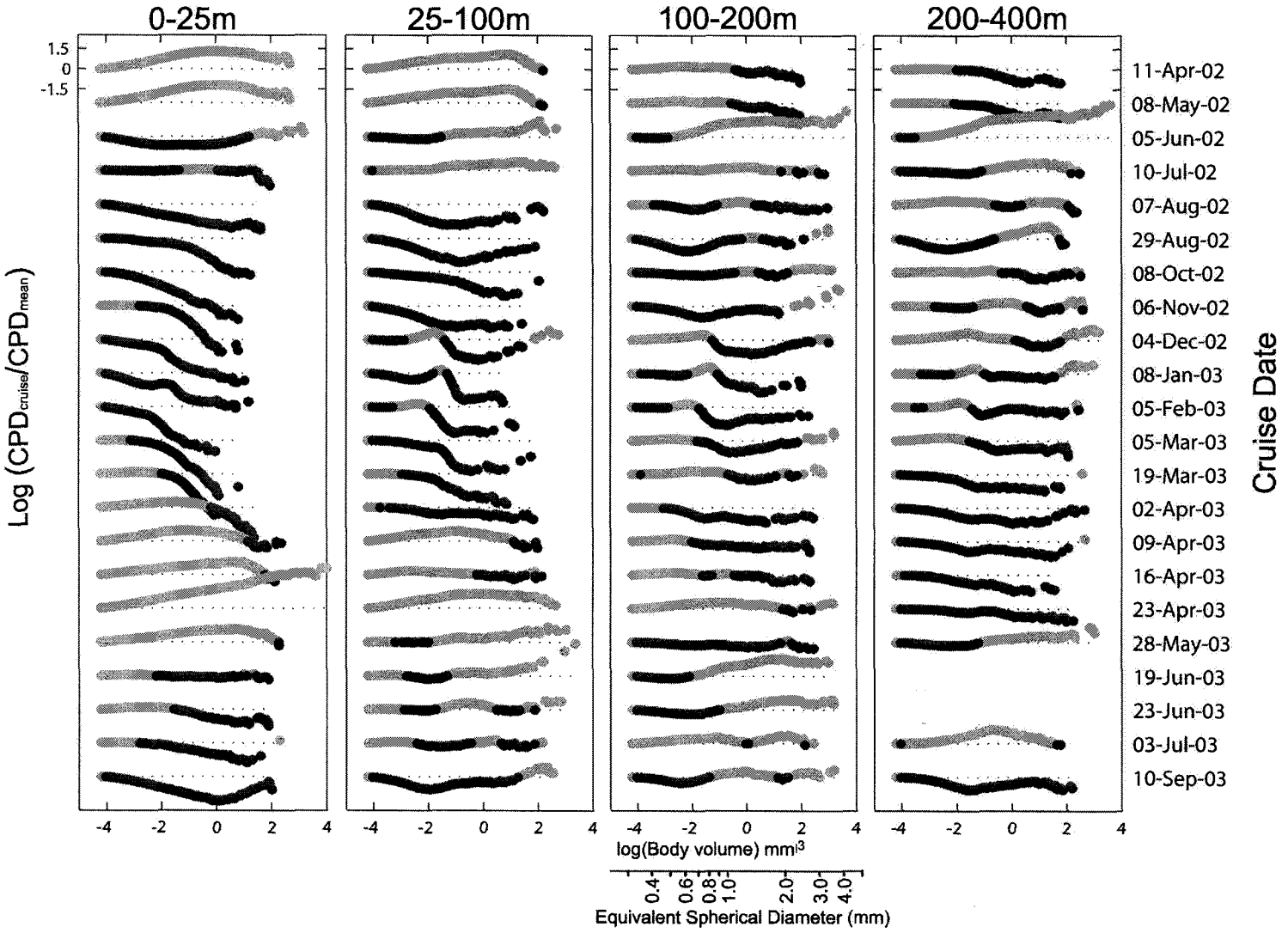
0-25m
25-100m
100-200m
200-400m
1.5
0
-1.5
Log (CPDcruise/CPDmean)
-4
-2
0
2
4
log(Body volume) mm3
0.4
0.6
0.8
1.0
2.0
3.0
4.0
Equivalent Spherical Diameter (mm)
11-Apr-02
08-May-02
05-Jun-02
10-Jul-02
07-Aug-02
29-Aug-02
08-Oct-02
06-Nov-02
04-Dec-02
08-Jan-03
05-Feb-03
05-Mar-03
19-Mar-03
02-Apr-03
09-Apr-03
16-Apr-03
23-Apr-03
28-May-03
19-Jun-03
23-Jun-03
03-Jul-03
10-Sep-03
Cruise Date

Figure 3.17. Residuals of the cumulative probability distribution (CPD) $\log(CPD_{cruise}/CPD_{average})$ in stratified depth bins for each cruise between April 2002 and October 2003. A residual of 1 in any size class indicates that the proportion in that class is 10^1 times greater than the average proportion in all cruises. A -1 indicates that it is 10^{-1} as great. Left to right: 0 - 25m, 25 – 100m, 100 - 200m and 200 - 400m depth bins. Black indicates negative residuals, grey indicates positive. Missing values in June and July 2003 in the 200 - 400m depth bin indicate insufficient data. For each cruise, Y axis range is -1.5 to 1.5.

3.4.0 Discussion

3.4.1 General findings

This study is the first to present a detailed analysis of the seasonal variation in the size distribution of the zooplankton community in the SoG. The pulse of biovolume moving from smaller to larger sizes through the NBSD occurred as expected from the model of Platt and Denman (1978) and occurred at the same time as *Neocalanus plumchrus* were growing to CV stage. The slope of the NBSD, when averaged over the duration of the study, was not significantly different to the -1.0 slope that has been empirically measured in other studies. The variation in the slope of the NBSD with both depth and time suggests that both the structure and trophic dynamics within the community are closely tied to the life-cycle of *N. plumchrus*.

3.4.2 Zooplankton community composition and size distribution

The zooplankton community structure reflected the strongly seasonal life cycles of the dominant zooplankton taxa found in the SoG. The familiarity of these patterns (Legare, 1957; Fulton, 1973; Harrison 1983) is less significant than the fact that the OPC data closely reflected this seasonality as well. The significant correlations between OPC and net data indicate that both sets of samples were measuring similar variations in the zooplankton community, in terms of biovolume, total numbers and average sizes. In addition, the depth distribution of large particles and average sizes of particles in the OPC data closely reflected the expected migration and overwintering patterns of *N. plumchrus* CV's (Fulton, 1973; Harrison, 1983; Campbell, 2003).

Several zooplankton species were more abundant in the net tows than expected, including *Metridia pacifica*, *Euphausia pacifica* and two pteropod species (*Clione limacine* and *Limacina helicina*). All four of these species are known to undergo diel vertical migrations (Batchelder, 1985; Bollens, 1992; Dadon and Cidre, 1992). In coastal and pelagic waters, *Metridia* and other diel migratory species have been reported to reduce their diel migratory behavior in the spring and summer (Dagg, 1985; Mackas *et al.*, 1993), either to feed or because the depth of the photic zone is shallower. If this were the

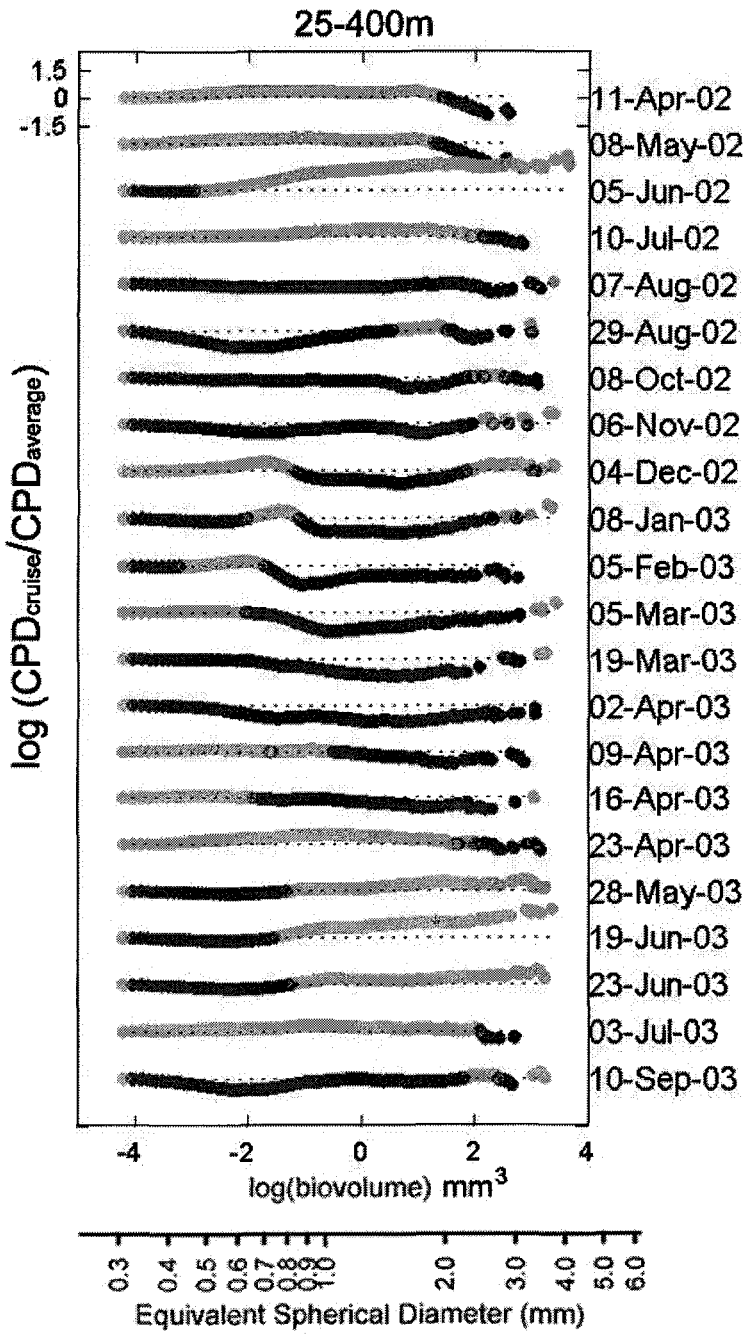

Figure 3.18. Residuals of the cumulative probability distribution (CPD) $\log(CPD_{cruise}/CPD_{average})$ for depths 25 - 400m. A residual of 1 in any size class indicates that the proportion of particles in that class is 10^1 times greater than the average proportion in all cruises. A -1 indicates that it is 10^{-1} as great. Black indicates negative residuals, grey indicates positive. For each cruise, Y axis range is -1.5 to 1.5. A residual of 1 in any one size class indicates that the proportion in that size class is ten times greater than the average proportion in all cruises. For each cruise, Y axis range is -1.5 – 1.5.

case in the present study, it would have the effect of increasing the near-surface biomass.

Because the data for this study were all collected during the day and in the surface 0 - 100m, a resumption of the usual migratory behavior following the bloom could have led to the sudden reduction in their near-surface biomass following the bloom. The variations observed in the two pteropod species are likely related, as *C. limacina* are known to prey on *L. helicina* (Bryan and Slattery, 1996; Conover and Lalli, 1972). It is therefore possible that *L. helicina* changed its migratory behavior in 2003 due to the presence of *C. limacina.*

Although zooplankton sampling has been conducted in the SoG for more than half a century (e.g. Legare, 1957) most of the research has focused on a single species, *N. plumchrus*, rather than on community composition dynamics. The data presented here demonstrate the need for more research on the structure and dynamics of the zooplankton community in the SoG. While *N. plumchrus* is obviously an important component of the community, other species may also play a major role in transferring food energy from phytoplankton to larger size classes. For instance, the duration and magnitude of the spring bloom in the SoG is often said to be controlled by the relative timing of *N. plumchrus* nauplii (Parsons *et al.,* 1969; Yin *et al.*, 1997). However in 2003, the dry weight of *M. pacifica* was almost equal to that of *N. plumchrus*, despite its smaller body size. *M. pacifica* therefore could have had a large controlling influence on phytoplankton that year. Furthermore, surface chlorophyll *a* fluorescence in the SoG remained elevated for much of the summer in 2002, a year in which *M. pacifica* was nearly absent. While these data are insufficient to quantify the effect that *M. pacifica* has on phytoplankton during the spring, they do hint that the community composition dynamics in the SoG are more complex than is generally assumed.

3.4.3 Comparison of OPC and net data

The 25 - 400m biovolume distribution from the OPC data shows that in the spring, biovolume was roughly evenly distributed between logarithmically increasing size

classes, as hypothesized by Sheldon (1972). In the winter, however, small to medium-sized particles dominated the OPC samples. This pattern reflects the size distribution found in the near-surface net tows, as well as what is known about the ecology of larger zooplankton species (particularly the copepod *Neocalanus plumchrus*) in the SoG. (Fulton, 1973; Harrison, 1983). In general, there was a robust agreement between the net and OPC data in terms of biovolume, abundance and the slope of the zooplankton size distribution.

Recent work by Nogueira *et al* (2004) on the Iberian Shelf has shown that Net and OPC estimates of the abundance and/or biomass of small (< 0.5mm) zooplankters were not significantly correlated, where estimates for larger (0.5-2.0mm) zooplankters were. The data in the present study show a similar pattern, with a stronger correlation between net and OPC data for larger (as opposed to smaller) particles. From this, one may conclude either that one of the two sampling instruments is inferior for sampling small particles, or that the two tools simply measure zooplankton differently.

In fact there is good evidence to suggest that OPCs and traditional plankton nets do measure different things. The means by which they acquire their estimates is different (particle detection vs. direct trapping of the organisms) and the basic units in which those estimates are expressed are also different (length vs. mass). As a consequence, it is somewhat of a fallacy to say that the two tools are interchangeable, even if they do provide similar estimates of zooplankton abundance or biomass. Furthermore, OPC data have certain qualities which make them more desirable for some applications than are net data (and vice versa). To illustrate this point, in the following sections the OPC data are analyzed to reflect the seasonal variation in the size distribution of zooplankton in a way that would be extremely difficult using traditional net samples.

3.4.4 Seasonality in the cumulative probability distribution

The cumulative probability distribution residuals demonstrate two things. The first is that the methods used in this study accurately tracked the expected cycle of growth and migration of *N. plumchrus* throughout the 18 months of the study. The second is that the

size distribution and dynamics of the zooplankton were different at different depths. While it has long been known that growth tends to be concentrated at the surface, the way that energy propagates through the system has not been well characterized, nor have depth-related differences been easy to observe. These data vividly depict the evolution of the zooplankton size distribution at different depths in a way that has not been possible using net samples.

The largest fluctuations in the CPD residuals occurred in the surface 0 - 25m and 25 - 100m layers. Keeping in mind that the 0 - 25m OPC data was possibly contaminated by phytoplankton, the variation observed in the surface strata follows both the net tow data and what is known about zooplankton seasonality in the SoG. Past research in the SoG has noted that a large amount of zooplankton biomass and production is concentrated in the surface layers during the spring, likely as a response to increased food availability (Legare, 1957; Fulton, 1973; Harrison, 1983). It is therefore expected that the greatest growth and reproduction should occur in this layer (Parsons, 1973). In these surface strata, the CPD residuals fit the *N. plumchrus* cycle, although other large zooplankton species such as *E. pacifica* and *C. limacina* likely contributed to the observed pattern. In February 2003, the pulse starting in the smaller size classes coincided with the rise of *Neocalanus* nauplii (Fulton, 1973; Campbell, 2003), though this pattern could also have been due to the presence of smaller species including stage 3 and 4 *M. pacifica*, *P. moultoni, O. similis,* and *C. anglicus,* as seen in the net samples. The February pulse moved from smaller to larger size classes until the spring bloom in April 2003, at which time there was a sudden increase in the residuals in all sizes corresponding to the appearance of *N. plumchrus*, *E. pacifica* and *L. helicina* in the net samples.

Following the bloom, the residuals of large species gradually dropped, as did their biomass in the net samples. This was likely due to both the ontogenetic migration of *N. plumchrus* from surface waters and a resumption of the normal diel migratory behavior of species such as *M. pacifica* and *E. pacifica*. The time scale of this surface pulse was of the same order (25 days) as predicted by Denman *et al.* (1989) for phytoplankton biomass to progress up the size distribution into *N. plumchrus*-sized zooplankton.

In deeper waters (100 - 200m and 200 - 400m), the strength of the spring pulse was progressively weaker. This suggests again that much of the growth of zooplankton is focused in surface waters. At these depths a pulse of biovolume appears suddenly in larger size classes in June 2002 and remains until January 2003, likely due to *N. plumchrus* returning to its over-wintering depth. This pattern could also be due to larger species such as *E. pacifica* resuming their normal pattern of migration following the spring bloom. The slow decline in the residuals of large particles over this time could be due to mortality, as noted by Campbell (2003). When the effects of ontogenetic migration are removed by averaging the OPC samples over all depths, the observed pulse of biovolume moving through the distribution is still present.

A brief pulse appeared to move backwards through smaller size classes in the 100 - 400m depth strata, as well as the whole water column residuals between December 2002 and February 2003. The reason for this pulse is uncertain, but may be linked to the appearance of later-stage *N. plumchrus* nauplii, which may show up in the OPC as particles of ~0.6mm ESD. Calibration of the OPC with cultures of *N. plumchrus* nauplii would be necessary to confirm this.

The use of the cumulative probability distribution in this study obscured the variation in the small zooplankton. Because the cumulative probability is calculated as the proportion of particles of greater or equal size to any given size class, the probability of other particles being greater than or equal to the smallest size class is always 1. The results in this analysis are therefore biased towards observations of change in larger size classes. Despite this, the CPD residuals were still effective for showing a pulse of biovolume moving from ~0.8mm - 4.0mm sized particles using the CPD residuals.

3.4.5 Seasonality in the slope of the normalized biovolume size distribution

The average slope of the NBSD measured in this study matched the -1.0 slope found empirically in other studies (Sprules, 1983; Rodriguez and Munuwar, 1986; Gaedke, 1992). This indicates that the OPC may be used to measure the NBSD with comparable

results to studies that used much more labor-intensive techniques (e.g. Rodriguez and Munuwar, 1986; Gaedke 1992; Nogueira *et al*, 2004). Furthermore, it confirms that on average and at most depths, the biovolume of zooplankton in the SoG is evenly distributed between logarithmically increasing size classes (Sheldon, 1972). However, the seasonal variation around the -1.0 slope indicates that this even distribution is the exception rather than the rule.

The NBSD slopes show a similar pattern to the CPD residuals, again reflecting the ontogenetic migration of *N. plumchrus* and the commencement of the spring bloom in March and April of both years. Of particular note is the decrease in the NBSD slope in February 2003 in the 25 - 100m stratum, which coincides with the rise of *N. plumchrus* nauplii, as well as the presence of small zooplankton species in the net tows. During the April bloom, the slope becomes rapidly shallower in the surface, reflecting the growth of larger species, then becomes gradually shallower over several months. In June and July of 2002 and 2003, the NBSD slope became shallower, likely due to the return of *N. plumchrus* CV's to their overwintering depth.

The NBSD slopes in mid-water depths varied little around the -1.0 slope, reflecting the lower levels of biovolume variation seen in the contour plots. That mid-water depths tend to hold less biomass than the surface and at depth has been reported previously in net-tow studies (Legare, 1957; Fulton, 1972; Harrison, 1983) and with recent acoustic profiler work (Ruthie Yahel, University of Victoria, *pers comm*). The present data suggest that mid-water depths are also areas of relatively constant trophic structure and even distribution of biovolume amongst all size classes. This idea requires further testing with net samples and more thorough OPC sampling.

3.4.6 Interpretation of the seasonal variation in the NBSD using size-distribution theory

Beyond demonstrating the utility of the OPC for monitoring *N. plumchrus* migration, the NBSD slope data can also be used to infer how the Trophic Transfer Efficiency (TTE) of the zooplankton community varies seasonally. Using the conceptual framework of biomass size distribution theory, it is possible to hypothesize what kinds of processes

might be at the root of this seasonal variation. Equation 3.3 provides a way to relate the slope of the NBSD to individual growth and population level growth rates g and u:

$$\frac{\partial \ln(\bar{\beta})}{\partial \ln(\bar{w})} \cong \frac{\bar{u}}{\bar{g}} \qquad (3.3)$$

Individual growth rates of zooplankton depend primarily on temperature and body size (Vidal, 1982; Huntley and Lopez, 1992; Hirst and Scheader, 1997; Savage *et al.*, 2004) and, to a lesser extent, on food quality (Rinke and Petzold, 2003). Considering the contour plot of temperature (Figure 3.2), the average temperature change in the 0 - 100m stratum between March and April 2003 (the period of the most dramatic biological change in the SoG) was on the order of just 1 degree; between 8 and 9 °C. The empirical model of Huntley and Lopez (1992) states that growth varies logarithmically with temperature. From Figure (2) and equation (13) in Huntley and Lopez (1992) it is possible to infer that this observed 1 °C change in temperature would result in a change in growth rate on the order of 0.05 d^{-1}. Thus, if the population-level growth rate were very low (on the order of 0.05 d^{-1}), then temperature alone could have caused the observed change in the NBSD slope. However, values of u(w) reported by Edvardsen *et al* (2001) lie between -0.1 and -0.4. Although the values of u(w) in the present study remain uncertain, it is still worth investigating how $u(w)$ may have changed throughout the year in order to explain the observed change in the NBSD slope.

Food quality and quantity (at non-starvation levels) are believed to have a secondary impact on individual zooplankton growth rates (Vidal, 1980). However, a change in zooplankton diet, perhaps in response to a change in the composition of the primary producers, could have caused an increase in the population growth rate $u(w)$. Primary production in the SoG switches from dinoflagellates and protozoa in the fall and winter to diatoms in the spring (Takahashi *et al.*, 1978). Some copepod species have been shown to have a higher conversion efficiency and fecundity when reared on higher quality food such as diatoms (Twombly and Burns, 1996; Ray *et al.*, 2001; Jones *et al.*, 2002; DeMott and Tessier, 2002; Klein Breteler *et al.*, 2004). Higher fecundity translates into a greater transfer of food energy into individual adults.

Supposing that food quality was an important determinant of the community size structure in the SoG, then there should also be a link between the nutritional value of the preferred food for zooplankton and the slope of the zooplankton NBSD. While field data of this sort are extremely rare, mesocosm experiments could prove useful in providing a controlled environment in which to explicitly test this hypothesis. The quality of phytoplankton as a food source may also have consequences at higher trophic levels, by providing more large zooplankton as food for larval and juvenile fish. These zooplankton, because they feed on a higher quality food, may in turn represent a more nutritious food source themselves. As a result, it could be hypothesized that years with shallow NBSD slopes may correspond to years of higher growth rates among larval fish, perhaps evidenced by greater length-at-age and wider otolith increments, (Secor *et al.,* 1989), or subsequently higher rates of recruitment.

An increase in the size of predators relative to their prey could also have caused a shallower NBSD slope by increasing the trophic transfer efficiency and allowing higher biomass of larger zooplankters to be supported. Jennings *et al.* (2002) observed that one fundamental assumption of size distribution theory is that the ratio of predator size to prey size is constant (Platt and Denman, 1977, 1978; Silvert and Platt, 1978). However, Dickie *et al.* (1987) found that the relative size distributions of predators and their prey are important factors influencing the size distribution of zooplankton in a community. Filter-feeding zooplankton have been shown to influence the shape of lake plankton size distributions as they feed directly on smaller phytoplankton sizes, bypassing a trophic step (Tittel *et al.,* 1998; Gaedke *et al.*, 2004). Havens (1998) found that a planktonic community dominated by larger zooplankton species also had higher TTEs than those dominated by smaller species. In the present study, the spring bloom heralded the arrival of large grazers and filter feeders such as *E. pacifica*, *N. plumchrus* and gelatinous zooplankton. This change in the average size of secondary consumers could have changed the overall feeding efficiency of zooplankton community and contributed to the shallow springtime NBSD slopes. This hypothesis could (indeed should) be tested by measuring the size ratio of zooplankton to their food source throughout the year and relating it to the slope of the NBSD (Havens, 1998).

The measurement of the size distribution of zooplankton-sized particles with an OPC will prove to be a useful tool in monitoring the ecology of zooplankton. The size-based patterns that can be measured can provide important information that may be of value to both fisheries managers and plankton ecologists. The slope of the biovolume spectrum can provide a snapshot of the trophic dynamics of the zooplankton community, which has always been challenging for oceanographers to observe with any degree of consistency. This information can also be related in a meaningful way to other variables (such as chlorophyll *a* fluorescence and temperature) and effectively monitored over extended periods to try and interpret the proximal factors influencing interannual fluctuations in zooplankton abundance and community structure. With persistent observation (e.g. such as might be collected via sub-sea cabled observatories), sufficient data may be generated with which researchers may make inferences and predictions about zooplankton communities based on OPC data. This is not to suggest that the OPC will replace net sampling, but that it will provide novel analytical and experimental approaches that are simply not feasible with net samples. While the need for net sampling of zooplankton will likely always remain, this study has demonstrated that the OPC will provide new and insightful ways with which to monitor and model zooplankton community dynamics.

4.0 GENERAL CONCLUSIONS

4.1 Fine-Scale Sampling With the OPC

The data presented in the first chapter of this thesis show how the OPC can be used at high resolutions. The OPC can resolve variations in the abundance and size distribution of zooplankton communities with fewer samples and at higher frequencies than traditional net samples. It also takes fewer OPC samples than net samples to approximate the mean abundance of zooplankton in a community. This work shows how zooplankton sampling may be optimized to gain the most out of OPC and net data. If a study is focused on small-scale variation in community size-structure, then high-resolution OPC data can be supplemented with relatively few net samples to measure the general community structure. In addition, this work provides an indication of the sampling effort required to approximate zooplankton abundance within a given time period. Finally, this study demonstrates the extent to which phytoplankton can contaminate OPC samples. Further work is needed to determine whether this contamination can somehow be measured and corrected.

Perhaps because of the contamination by phytoplankton in this study, it was difficult to truly test the OPC's ability to resolve any specific variation in the abundance or size distribution of zooplankton. In order to do so, it would be necessary to have an a-priori knowledge of how the zooplankton should vary over a specific distance or time scale. There are numerous fine-scale processes that could be used to test the OPC at fine spatiotemporal scales in the future. Potential studies of behavioral processes include characterizing the size-specific differences in the diel vertical migration behavior of zooplankton, locating (and sizing) mono-specific swarms and observing active tidal transport processes. Abiotic processes of potential interest include the aggregation and size-structure of zooplankton in Langmuir circulation cells, the distribution of zooplankton along tidal and estuarine fronts, and relating changes in the structure of zooplankton communities to small-scale variation in their food environment. However, the difficulty in working at these scales remains in having an independent measure of the zooplankton community against which to compare the OPC data. The use of an acoustic

profiler (Sameoto *et al.*, 1993) or a continuous plankton recorder (Grant *et al.*, 2000) might be useful in this context.

Despite 30 years of research using fine-scale automated sampling devices (Mackas and Boyd, 1971), it remains a challenge to analyze the high resolution multi-dimensional data generated by the OPC. Zooplankton ecologists will want to borrow from phytoplankton ecologists and physical oceanographers, who have been analyzing fine-scale spatiotemporal patterns in the oceans for many years. At the same time, the irregular nature of ecological zooplankton data will require innovative approaches to their analysis. One area of research that may assist with this are the techniques of spatial analysis used in plant ecology (Legendre, 1993; Legendre and Legendre, 1998), which deal with defining patterns in two or more dimensions. Randomization and Monte Carlo techniques as used in this study will also be useful in relating physical and biological variables (Manly, 1991).

4.2 Seasonality in the Size Distribution of Zooplankton in the Strait of Georgia

The data presented in Chapter 3 represents the first measurements of the way the zooplankton community size distribution in the Strait of Georgia varies seasonally. The general pattern is dominated by the growth and ontogenetic migration of *N. plumchrus*. The growth of *N. plumchrus* nauplii to CV stage in the surface was tracked as a pulse of biovolume moving through the Normalized biovolume size distribution (NBSD) from small to large size classes. The change in the slope of the NBSD size distribution also corresponded with the growth and migration of *N. plumchrus* and imply that the trophic structure and trophic transfer efficiency of the zooplankton community varies both seasonally and with depth. On average, the slope of the NBSD was close to the -1.0 value for the normalized biovolume distribution measured empirically in other studies.

This study demonstrates that the OPC can be used effectively to monitor detailed variation in the zooplankton size distribution with similar success to other techniques. However, this work also highlights the importance of linking the "ecological context" of a zooplankton community to the interpretation of size-distribution data. It also

highlights the need for more work on the community composition dynamics and species succession of zooplankton in the SoG.

This work presents the hypothesis that seasonal variation in size the community-level growth rate $u(w)$, due either to a change in food quality or the relative sizes of predators and their prey could be linked for the observed variation in the slope of the NBSD. Testing this hypothesis would require field observations of both factors, neither of which are particularly easy to measure. However, it may be feasible to include variation in the loss rate into a size-based model such as the one derived by Benoit and Rochet (2004). This model could be used to test which of these two factors is more likely to cause the seasonal variation observed in this study.

Chapter 3 shows how OPC data may be a useful tool for rapidly assessing the dynamic 'state' of zooplankton communities and how they change over time. This may prove to be useful in fisheries oceanography for linking the dynamics of fish and zooplankton communities. For instance, the years in which the zooplankton community has a shallower size distribution (i.e. higher trophic transfer efficiency) may prove to be years in which there is a greater food source for pelagic fish species. A first approximation at answering this question might be made by comparing the slope of the zooplankton NBSD in the summer to estimates of zooplankton production and measures of larval fish growth and survival. Much work has been done on measuring the biomass distribution of plankton communities that range in size from nano-bacteria to meso-zooplankton. It may be possible to extend this range to include larval and adult fish. However, much field and theoretical work needs to be done in order to determine whether it is feasible to link zooplankton and fish community dynamics using size-distribution theory.

Because size has been shown to be such an important scaling factor across ecosystems (Savage *et al.,* 2004), the temptation to derive size-distribution models for everything from bacteria to whales may be strong. However not all biological processes exhibit a continuous relationship with size (Yen, 2002). For aquatic organisms, the transition from laminar to turbulent flow with increasing body size represents a drastic change in

lifestyle, especially in terms of how they interact with their environment (Weissburg, 2000). The behavioral and physiological changes that occur in the transition from a viscous to a turbulent regime would be difficult to include in a size-distribution model. It is therefore important that the detail of whole-ecosystem size-spectrum models be kept to realistic proportions. Biomass size-distribution theory was originally intended as a 'first order approximation' of the organization and flow of biomass in planktonic ecosystems. The addition of too much complexity to this simple and elegant model may have the unintended result of rendering it useless for more than a narrow set of circumstances.

4.3 Caveat on the Using the OPC in High Productivity Waters

This study has shown that OPC data collected under high productivity conditions (e.g. during spring blooms) should be treated with caution, as demonstrated by the strong link between water column transmissivity and the average particle sizes measured by the OPC (Appendix 1). This relationship indicates the need for either better *in-situ* correction factors or post-sampling processing in highly productive waters. One possible solution is to ensure that each OPC cast is accompanied by observations of transmissivity and fluorescence. Judicious exclusion of data from high turbidity water can help to reduce the inclusion of erroneous size measurements.

Cloudy water was found in this study to skew the size distribution measured by the OPC. This is the first time that the amount of error introduced into *in-situ* OPC measurements by cloudy water has been related to the water transmissivity (Appendix 1). Other correction factors have been derived to deal with phytoplankton contamination of OPC samples (Sprules *et al.*, 1997; Zhang *et al.*, 2001), but these studies were in controlled laboratory environments. The observation that the average size measured by the OPC is correlated with the transmissivity of the water indicates that there may be a way to create a correction of not only the estimated abundance of zooplankton in a phytoplankton-contaminated sample, but its size-distribution as well.

Finally, OPC data will always need to be validated against an independent measure estimate of the size-distribution or abundance of zooplankton in a community. As Video

plankton recorders become more widely available, we may see the development of a combination OPC-VPR: an OPC to count and size the plankton, a VPR to identify what species were actually encountered.

4.4 Future Developments

The main advantage of the OPC is that it is faster and cheaper to analyze size-distribution data than traditional plankton samples. The primary limitation to the quantity of data the OPC can obtain is the effort required to launch and fund ship-based oceanographic expeditions. However, oceanography is still constrained by the need for people to go out in ships, which have become increasingly costly to operate, and which will always be limited by weather conditions to some extent. This situation is beginning to change, however, as technology becomes available which allows researchers to collect extensive, high resolution data sets without needing to be constantly in contact with their instruments. Autonomous Underwater Vehicles can collect a wide variety of data over distances of thousands of kilometers without the need for ship-based assistance (Eriksen *et al.,* 2001). Future oceanographic research will see the expansion of cabled underwater observatories, along the lines of the VENUS and NEPTUNE projects that are currently in development on the west coast of North America (e.g. Dewey and Tunnicliffe, 2003). Zooplankton sampling instruments such as the OPC, as well as environmental sensors such as CTDs and nutrient analyzers will make daily measurements of the physical and biological environment. The complex and multi-disciplinary data these systems generate will require excellent cooperation between oceanographers of different flavors.

The OPC itself is also evolving. At the time of this writing, a new generation of OPC – the Laser OPC - is being marketed and tested (Herman, 2001). The Laser OPC will allow for finer scale size and spatial measurements, while remaining accurate in particle concentrations 100 times greater than current OPC technology. It will also permit shape recognition for particles under 1.5mm, which may assist with the filtering of detrital particles. As a result, it will be possible to more accurately measure the size distribution of zooplankton at finer scales. The amount of data generated by the laser OPC may present an analytical problem. Indeed, one of the difficulties with the first-generation

OPC remains the density of data that it generates. In processing these data for presentation and storage, researchers can unknowingly bias their results or ignore important information. It will therefore be important for biological oceanographers to develop data handling protocols which allow them to address many different kinds of questions from one data set while retaining the integrity of their data.

In summary, the OPC has potential to take biological oceanography in new directions, both theoretically and in the field. The ease with which its data can be collected and compared to model predictions makes it practical to develop sampling strategies which are optimized to address fine-scale ecological questions. In addition, the size-structured data collected by the OPC is well-suited to answering general questions on the flow of energy in zooplankton ecosystems.

LITERATURE CITED

Ahrens MA and Peters RH (1991b). Patterns and limitations in limno-plankton size distributions. Canadian Journal of Fisheries and Aquatic Sciences, 48: 1967-1978.

Arai MN and Mason JC (1982). Spring and summer abundance and vertical distribution of hydromedusae of the central Strait of Georgia, B.C.. Syesis 15:7-15.

Arai MN and Brinkman -Voss A (1980). *Hydromedusae of British Columbia and Puget Sound.* Canadian Bulletin of Fisheries and Aquatic Sciences, (no. 204), 200 p.

Ambler JW (2002). Zooplankton swarms: characteristics, proximal cues and proposed advantages. Hydrobiologia, 480: 155-164.

Anderson, JJ; Devol, AH (1973). Deep water renewal in Saanich Inlet, an intermittently anoxic basin. Estuarine, Coastal and Shelf Science, 1: 1-10.

Atkinson, A (1996). Subantarctic copepods in an oceanic, low chlorophyll environment: Ciliate predation, food selectivity and impact on prey populations. Marine Ecology Progress Series, 130: 85-96.

Barnes H (1950). A statistical study of the variation in vertical plankton hauls, with special reference to the loss of the catch with divided hauls. Journal of Marine Research, 429-445.

Barnes H and Marshall SM (1958). On the variability of replicate plankton samples and some applications of 'contagious' series to the statistical distribution of catches over restricted time periods. Journal of the Marine Biological Association of the UK, 30:233-263.

Batchelder H (1985). Seasonal abundance, vertical distribution, and life history of *Metridia pacifica* (Copepoda: Calanoida) in the oceanic subarctic Pacific. Deep-Sea Research, 32: 949–964.

Baumgautener MF (2003). Comparisons of *Calanus finmarchicus* fifth copepodite abundance estimates from nets and an optical plankton counter. Journal of Plankton Research, 25:855-868.

Benoit E and Rochet MJ (2004). A continuous model of biomass size distributions governed by predation and the effects of fishing on them. Journal of Theoretical Biology, 226: 9-21.

Boden BP and Kampa EM (1963). An aspect of euphausiid ecology revealed by echo-sounding in a fjord. Crustaceana, 9:155-173.

Bollens SM, Frost BW and Lin TS (1992). Recruitment, growth, and diel vertical migration of *Euphausia pacifica* in a temperate fjord. Marine Biology, 114:219-228.

Boyd CM (1973). Small-scale spatial patterns of marine zooplankton examined *in-situ* with an electronic zooplankton counting device. Netherlands Journal of Sea Research, 7:103-111.

Brander KM, Milligan SP and Nichols JH (1993). Flume tank experiments to estimate the volume filtered by high-speed plankton samplers and to assess the effect of net clogging. Journal of Plankton Research, 12:385-401.

Bryan PJ and Slattery M (1996). Reproductive behavior of the gymnosomatous pteropod *Clione antarctica.* Invertebrate Reproduction and Development, 29: 143-148.

Campbell RW (2003). (*PhD Thesis*) Overwintering Ecology and Ecophysiology of *Neocalanus plumchrus*. University of Victoria.

Cassie RM (1963). Microscale distribution of zooplankton. Oceanography and Marine Biology: Annual Review, 1:223-252.

Clarke GL and Bumpus DF (1939). Brief account of a plankton sampler. Internationale Revue der Gesamten Hydrobiologie und Hydrographi, 39:190-192.

Conover RJ and Lalli CM (1972). Feeding and growth in *Clione limacina* (Phipps), a pteropod mollusc. Journal of Experimental Marine Biology and Ecology, 9: 279–302.

Cozar A, Garcia C and Galvez JAX (2003). Analysis of plankton size distributions irregularities in two subtropical shallow lakes (Esteros del Ibera, Argentina). Canadian Journal of Fisheries and Aquatic Sciences, 60: 411-420.

Dagg MJ (1985). Effects of food limitation on diel migratory behavior in marine zooplankton. *In Food limitation and the structure of zooplankton communities* Ergebnisse der Limnologie/ Advances in limnology. Stuttgart. 21: 247-255.

Dadon JR and Cidre LLde (1992). The reproductive cycle of the thecosomatous pteropod *Limacina retroversa* in the western South Atlantic. Marine Biology, 114: 439-442.

Davis CS, Gallager SM, Marra M and Stewart WK (1996). Rapid visualization of plankton abundance and taxonomic composition using the Video Plankton Recorder. Deep-Sea Research Part II – Topical studies in oceanography, 43:1947-1970.

DeBruyn AMH, Marcogliese DJ and Rasmussen JB (2002). Altered body size distributions in a large river fish community enriched by sewage. Canadian Journal of Fisheries and Aquatic Sciences, 59: 819-828.

De Robertis A, Eiane K and Rau GH (2001). Eat and run: anoxic feeding and subsequent aerobic recovery by *Orchomene obtusus* in Saanich Inlet, British Columbia, Canada. Marine Ecology-Progress Series, 219: 221-227.

DeMott WR and Tessier AJ (2002). Stoichiometric constraints vs. algal defenses: Testing mechanisms of zooplankton food limitation. Ecology, 83: 3426-3433.

Denman KL and Mackas DL (1978). Collection and analysis of underway data and related physical measurements. In: JH Steele (ed) *Spatial pattern in plankton communities*. Plenum, New York, p 277-327.

Denman KL, Freeland HJ and Mackas DL (1989). Comparisons of time scales for biomass transfer up the marine food web and coastal transport processes. Canadian Special Publications in Fisheries and Aquatic Science, 108: 255-264.

Dewey R and Tunnicliffe V (2003). VENUS: Future Science on a Coastal Mid-Depth Observatory. Paper presented at the 3rd International Workshop on Scientific Use of Submarine Cables and Related Technologies, Tokyo, Japan.

Dickie LM, Kerr SR and Boudreau PR (1987). Size dependent processes underlying regularities in ecosystem structure. Ecological Monographs, 57: 223-250.

Doty MS and Oguri M (1956). The island mass effect. Journal du Conseil International du Exploration de la Mer, 22: 3–37.

Dower JF and Mackas DL (1996). "Seamount effects" in the zooplankton community near Cobb Seamount. Deep-Sea Research Pt I, 43:v 837-858.

Edvardsen A, Zhou M, Tande KS and Zhu Y (2001). Zooplankton population dynamics: Measuring in situ growth and mortality rates using an Optical Plankton Counter. Marine Ecology Progress Series, 227: 205-219.

Eriksen CC, Osse TJ, Light RD, Wen T, Lehman TW, Sabin PL, Ballard JW and Chiodi AM (2001). Seaglider: A long-range autonomous underwater vehicle for oceanographic research IEEE Journal of Oceanic Engineering, 26: 424-436.

Fiksen O, Carlotti F (1998). A model of optimal life history and diel vertical migration in *Calanus finmarchicus*. Sarsia, 83: 129-147.

Flater, D (1998). Xtide: Harmonic tide clock and tide predictor. http://www.flaterco.com/xtide.

Fleminger A and Clutter RI (1963). Avoidance of towed nets by zooplankton. Limnology and Oceanography, 10: 96-104.

Fraser JH (1966). Zooplankton sampling. Nature, 211: 915-916.

Foote KG (2000). Optical methods. *In* R. P. Harris, P. H. Wiebe, J. Lenz, H. R. Skjoldal, & M. Huntley (Eds.), *ICES zooplankton methodology manual* (pp. 259–295). London: Academic Press.

Foote KG and Stanton TK (2000). Acoustical methods. *In* R. P. Harris, P. H. Wiebe, J. Lenz, H. R. Skjoldal, & M. Huntley (Eds.), *ICES zooplankton methodology manual* (pp. 223–258). London: Academic Press.

Fulton J (1973). Some aspects of the life history of *Calanus plumchrus* in the Strait of Georgia. Journal of the Fisheries Research Board of Canada, 30: 811-815.

Gaedke U (1992). The size distribution of plankton biomass in a large lake and its seasonal variability. Limnology and Oceanography, 37: 1202-1220.

Gaedke U (1993). Ecosystem analysis based on biomass size distributions: A case study of a plankton community in a large lake. Limnology and Oceanography, 38: 112-127.

Gaedke U, Seifried A and Adrian R (2004). Biomass size distributions and plankton diversity in a shallow eutrophic lake. International Review of Hydrobiology, 89: 1-20.

Gallienne CP and Robins DB (1998). Trans-oceanic characterization of zooplankton community size structure using an optical plankton counter. Fisheries Oceanography, 7: 147-158.

Gallienne CP, Robins DB and Wood-Walker RS (2001a). Abundance, distribution and size-structure of zooplankton along a 20° west meridional transect of the northeast Atlantic Ocean in July. Deep-Sea Research Pt I, 48: 925-949

Gallienne CP and Robins DB (2001b) Is *Oithona* the most important copepod in the world's oceans? Journal of Plankton Research, 23: 1421-1432.

Garcia CM, Echevarria F and Niell FX (1995). Size structure of plankton in a temporary, saline inland lake. Journal of Plankton Research, 17: 1803-1817.

Gardner GA (1977). Analysis of zooplankton population fluctuations in the Strait of Georgia, B.C.. Journal of the Fisheries Research Board of Canada, 34: 1196-1206.

Gargett AE, Stucchi D and Whitney F (2003). Physical processes associated with high primary production in Saanich Inlet, British Columbia. Estuarine and Coastal Shelf Science, 56: 1141-1156.

Gasol JM, Guerrero R and Pedros-Alio C (1991). Seasonal variations in size structure and prokaryotic dominance in sulfurous Lake Ciso. Limnology and Oceanography, 36: 860-872.

Gismervik I, Olsen Y and Vadstein O (2002). Micro- and mesozooplankton response to enhanced nutrient input - a mesocosm study. Hydrobiologia, 84: 75-87.

Goldblatt R, Mackas DL and Lewis AG (1999). Mesozooplankton community characteristics in the NE subarctic Pacific. Deep-Sea Research, 46: 2619-2644.

Grant S, Ward P, Murphy E, Bone D and Abbott S (2000). Field comparison of an LHPR net sampling system and an optical plankton counter (OPC) in the Southern Ocean. Journal of Plankton Research, 22: 619-638

Haberman KL, Ross RM, Quetin LB (2003). Diet of the Antarctic krill (*Euphausia superba* Dana): II. Selective grazing in mixed phytoplankton assemblages. Journal of Experimental Marine Biology and Ecology, 283: 97-113.

Hamner WM and Shneider D (1986). Regularly spaced rows of medusae in the Bering Sea – role of Langmuir circulation. Limnology and Oceanography, 31: 171-177.

Harris RP, Irigoien X, Head RN, Rey C, Hygum BH, Hansen BW, Niehoff B, Meyer-Harms B and Carlotti F (2000). Feeding, growth, and reproduction in the genus *Calanus* Ices Journal of Marine Science, 57: 1708-1726.

Harrison PJ, Fulton JD, Taylor FJR and Parsons TR (1983). Review of the biological oceanography of the Strait of Georgia: pelagic environment. Canadian Journal of Fisheries and Aquatic Sciences, 40: 1064 - 1094.

Haury LR, McGowan JA and Wiebe PH (1978). Patterns and processes in the time-space scales of plankton distributions. In: JH Steele (ed) Spatial pattern in plankton communities. Plenum, New York, p 277-327

Havens KE (1998). Size structure and energetics in a plankton food web. OIKOS, 81: 346-358.

Hays GC (1995). Ontogenetic and seasonal variation in the diel vertical migration of the copepods *Metridia lucens* and *Metridia longa*. Limnology and Oceanography, 40: 1461-1465.

Heath MR (1995). Size spectrum dynamics and the planktonic ecosystem of Loch Linnhe. ICES Journal of Marine Science, 52: 627-642.

Heath MR (2001). Calibration of towed OPC data from taxanomic analysis of net sample. Pp 12-15 *in* No. 17. Report of the GLOBEC Workshop on Optical Plankton Counters, 17-20 June 2001, Tromsø, Norway.

Herlinveaux RH (1962). Oceanography of Saanich Inlet in Vancouver Island, British Columbia. Journal of Fishery Research Board Canada, 19: 1–37.

Herman AW (1988). Simultaneous measurement of zooplankton and light attenuance with a new optical plankton counter. Continental Shelf Research, 8: 205-221.

Herman AW (1992). Design and calibration of a new Optical Plankton Counter capable of sizing small zooplankton. Deep-Sea Research, 39:395-415.

Herman AW, Cochrane, NA and Sameoto DD (1993). Detection and abundance estimation of euphausiids using an optical plankton counter. Marine Ecology Progress Series, 94: 165-173

Herman AW (2001). A review of OPC and an introduction to the next generation of OPC: laser OPC. pp 3-6 *In* No. 17. Report of the GLOBEC Workshop on Optical Plankton Counters, 17-20 June 2001, Tromsø, Norway.

Hirst AG and Sheader M (1997). Are *in-situ* weight-specific growth rates body-size independent in marine planktonic copepods? A re-analysis of the global syntheses and a new empirical model. Marine Ecology Progress Series, 154: 155-165

Holligan PM, Harris RP, Newell RC, Harbour DS, Head RN, Linley EAS, Lucas MI, Tranter PRG and Weekley CM (1984). Vertical-distribution and partitioning of organic-carbon in mixed, frontal and stratified waters of the English Channel. Marine Ecology Progress Series, 14: 111-127.

Hopkins TL (1963). The variation in the catch of plankton nets in a system of estuaries. Journal of Plankton Research, 21: 39-47.

Huntley ME and Hobson LA. (1978). Medusa predation and plankton dynamics in a temperate fjord, British Columbia. Journal of the Fisheries Research Board of Canada, 35:257-261.

Huntley ME and Lopez MDG (1992). Temperature-dependent production of marine copepods: A global synthesis. American Naturalist, 140: 201-242.

Huntley ME, Zhou M and Nordhausen W (1995). Mesoscale distribution of zooplankton in the California Current in late spring, observed by optical plankton counter. Journal of Marine Research, 53:647-674.

Jennings S, Pinnegar JK, Polunin NVC and Warr KJ (2002). Linking size-based and trophic analyses of benthic community structure. Marine Ecology Progress Series, 226: 77-85.

Isaacs JD and Schwartz RA (1965). Migrant sound scatterers –interaction with sea floor. Science, 150:1810-1813

Jones RH, Flynn KJ and Anderson TR (2002). Effect of food quality on carbon and nitrogen growth efficiency in the copepod Acartia tonsa. Marine Ecology Progress Series, 235: 147-156.

Katz J, Donaghay PL, Zhang J, King S and Russell K, (1999). Submersible holocamera for detection of particle characteristics and motions in the ocean. Deep-Sea Research I 46: 1455–1481.

Kerr SR (1974). Theory of size distribution in ecological communities. Journal of the Fisheries Research Board of Canada, 31: 1859-1862.

Klein Breteler WCM, Koski M, Rampen S (2004). Role of essential lipids in copepod nutrition: no evidence for trophic upgrading of food quality by a marine ciliate Marine Ecology Progress Series, 274:199-208.

Knox C, (1966). Holographic microscopy as a technique for recording dynamic microscopic objects. Science, 153: 989–990.

Kobayashi T, Shiel RJ and Gibbs P (1998). Size structure of river zooplankton: seasonal variation, overall pattern and functional aspects. Marine and Freshwater Research, 49: 547-552.

Koeller PA, Barwell-Clarke JE, Whitney F and Takahashi M (1979). Winter condition of marine plankton populations in Saanich Inlet, B.C., Canada. .3 – Meso-zooplankton. Journal of Experimental Marine Biology and Ecology, 37: 161-174.

Kott M (2001). *Elements of mathematical ecology*. Cambridge University Press, Cambridge.

Labat J, Mayzaud P, Dallot S, Errhif A, Razouls S, and Sabini S (2002). Mesoscale distribution of zooplankton in the Sub-Antarctic Frontal system in the Indian part of the Southern Ocean: a comparison between optical plankton counter and net sampling. Deep-Sea Research, 49: 735-749

Langmuir I (1938). Surface motion of water induced by wind. Science, 87:119-123.

Larson RJ (1987). Trophic ecology of planktonic gelatinous predators in Saanich Inlet, British Columbia: Diets and prey selection. Journal of Plankton Research, 9:811-836.

Lawrence SG, Malley DF, Findlay WJ, MacIver MA and Delbsere IL (1987). Method for estimating dry weight of freshwater planktonic crustaceans from measures of length. Canadian Journal of Fisheries and Aquatic Sciences, 44 (Supplement 1): 264-274.

Lazzaretto I, Franco F and Battaglia B (1994). Reproductive behavior in the harpactacoid copepod *Tigriopus fulvus*. Hydrobiologia, 293: 229-234.

LeBlond PH (1983). The Strait of Georgia: functional anatomy of a coastal sea. Canadian Journal of Fisheries and Aquatic Sciences, 40 (7): 1033 – 1063.

Legare JEH (1957). The qualitative and quantitative distribution of plankton in the Strait of Georgia in relation to certain oceanographic factors. Journal of the Fisheries Research Board of Canada, 14: 521-552.

Legendre P and Fortin MJ (1989). Spatial pattern and ecological analysis. Vegetatio, 80: 107-138.

Legendre, P (1993). Spatial autocorrelation: trouble or a new paradigm? Ecology, 74: 1659-1673.

Legendre P and Legendre L. (1998). Numerical ecology (2nd English edition). Elsevier, Amsterdam.

Li M, Gargett and Denman K (2002). What determines seasonal and interannual variability of phytoplankton and zooplankton in strongly estuarine systems? Application to the semi-enclosed estuary of Strait of Georgia and Juan de Fuca Strait. Estuarine and Coastal Shelf Research, 50: 467-488.

Lindeman RL (1942). The trophic-dynamic aspect of ecology. Ecology, 23: 399-418.

Liu SH, Sun S, Han BP (2003). Diel vertical migration of zooplankton following optimal food intake under predation. Journal of Plankton Research, 25: 1069-1077.

Longhurst AR, Reith AD, Bower RE and Seibert DLR, (1966). A new system for the collection of multiple serial plankton samples. Deep-Sea Research, 13:213–222.

Mackas DL (1984). Spatial autocorrelation of plankton community composition in a continental shelf ecosystem. Limnology and Oceanography, 29: 451-47.

Mackas DL, Denman KL and Abbott MR (1985). Plankton patchiness, Biology in the physical vernacular. Bulletin of Marine Science, 37: 652-674.

Mackas DL and Burns KE (1986). Poststarvation feeding and swimming activity in *Calanus pacificus* and *Metridia pacifica*. Limnology and Oceanography, 31: 383–392.

Mackas DL, Sefton H, Miller CB and Raich A. (1993). Vertical habitat partitioning by large calanoid copepods in the oceanic Subarctic Pacific during spring. Progress in Oceanography, 32: 259-294.

Mackas DL, Goldblatt R and Lewis AJ. (1998). Interdecadal variation in developmental timing of *Neocalanus plumchrus* populations at Ocean Station P in the subarctic North Pacific. Canadian Journal of Fisheries and Aquatic Sciences, 55: 1878-1893.

Mackas DL and Tsuda A (1999). Mesozooplankton in the eastern and western subarctic Pacific: community structure, seasonal life histories, and interannual variability. Progress in Oceanography 43: 335-363.

Mackas DL and Galbraith MD (2002). Zooplankton distribution and dynamics in a North Pacific eddy of coastal origin: 1. Transport and loss of continental margin species. Journal of Oceanography, 58: 725-738.

Mackie GO and Mills CE (1983). Use of the *Pisces IV* submersible for zooplankton studies in coastal waters of British Columbia. Canadian Journal of Fisheries and Aquatic Science, 40: 763–776.

Manly BFJ (1991). *Randomization and Monte Carlo methods in biology*. Chapman and Hall, London.

Mantel NA (1967). The detection of disease clustering and a generalized regression approach. Cancer Research, 27: 209-220.

Masson, D (2002). Deep Water Renewal in the Strait of Georgia. Estuarine, Coastal and Shelf Science, 54: 115–126.

Miller CB, Frost BW, Batchelder HP, Clemons MJ and Conway RE (1984). Life histories of large, grazing copepods in a subarctic ocean gyre: *Neocalanus plumchrus*, *Neocalanus cristatus*, and *Eucalanus bungii* in the northeast Pacific. Progress in Oceanography, 13:201-243.

Motoda S (1953). New plankton samplers. Bulletin of the Faculty of Fisheries Hokkaido University, 3: 181–186.

Nair VR, Achuthankutty CT and Skreekumarin Nair SR (1983). Zooplankton variability in the Zuari estuary, Goa. Mahasagar-Bulletin of the National Institute of Oceanography, 16: 235-242.

Nansen F (1915). Closing-nets for vertical hauls and for horizontal towing. Publications de Circonstance — Conseil Permanent International pour l'Exploration de la Mer 67: 1–8.

Nichols JH and Thompson AB (1991). Mesh selection of copepodite and nauplius stages of four calanoid copepod species. Journal of Plankton Research, 12:661-671.

Nogueira E, Gonzalez-Nuevo G, Bode A, Varela M, Moran XAG, Valdes L (2004). Comparison of biomass and size spectra derived from optical plankton counter data and net samples: application to the assessment of mesoplankton distribution along the Northwest and North Iberian Shelf. ICES Journal of Marine Science, 61: 508-517.

Olsen Y, Reinertsen H, Vadstein O, Andersen T, Gismervik I, Duarte C, Agusti S, Stibor H, Sommer U, Lignell R, Tamminen T, Lancelot C, Rousseau V, Hoell E and Sanderud KA (2001). Comparative analysis of food webs based on flow networks: effects of nutrient supply on structure and function of coastal plankton communities. Continental Shelf Research, 21: 2043-2053.

Osgood KE (1997). Seasonal variation in a deep aggregation of *Calanus pacificus* in the Santa Barbara Basin. Marine Ecology Progress Series, 148:56-69.

Parsons TR, Stephens K and LeBrasseur RJ (1969). Production studies in the Strait of Georgia. Part 1. Primary production under the Fraser River plume, February to May, 1967. Journal of Experimental Marine Biology and Ecology, 3: 27-38.

Parsons TR, LeBrasseur RJ and Barraclough WE (1970). Levels of production in the pelagic environment of the Strait of Georgia, B.C. – A review. Journal of the fisheries Research Board of Canada. 27:1251-

Pinca S and Huntley ME (2000). Spatial organization of particle size composition in an eddy-jet system off California. Deep-Sea Research Part 1: Oceanographic Research Papers. 47:973-996.

Pinel-Alloul (1995). Spatial heterogeneity as a multiscale characteristic of zooplankton community. Hydrobiologia. 300/301: 17-42.

Platt T and Denman K (1977). Organization in the Pelagic Ecosystem. Helgol Wiss Meeresunters, 30: 575-581.

Platt, T. and K. Denman (1978). *In* The Structure of Pelagic Marine Ecosystems. Marine ecosystems and fisheries oceanography. p. 60-65173: 60-65. Rapp. P.-V. Reun. CIEM,, v. 173

Quinones RA, Platt T and Rodriguez J (2003). Patterns of biomass-size distributions from oligotrophic waters of the Northwest Atlantic. Progress in Oceanography, 57: 405-427.

Quntana XD, Comin FD and Mareno-Amich R (2002). Biomass-size distributions in aquatic communities in shallow fluctuating Mediterranean salt marshes (Emporda wetlands, NE Spain). Journal of Plankton Research, 24: 1149-1161.

Rand PS and Hinch SG (1998). Spatial patterns of zooplankton biomass in the northeast Pacific Ocean. Marine Ecology Progress Series, 171: 181-186.

Ray S, Berec L, Straskraba M and Jorgensen SE (2001). Optimization of exergy and implications of body sizes of phytoplankton and zooplankton in an aquatic ecosystem model. Ecological Modelling, 140: 219-234.

Rinke K and Petzoldt T (2003). Modelling the effects of temperature and food on individual growth and reproduction of *Daphnia* and their consequences on the population level. Limnologica, 33: 293-304.

Rodriguez J and Mullin MM (1986a). Relationship between biomass and body weight of plankton in a steady state oceanic system. Limnology and Oceanography, 31:361-370.

Rodriguez J and Mullin MM (1986b). Diel and interannnual variation of size distribution of zooplankton biomass. Ecology, 67:215-222.

Sameoto D, Cochrane N and Herman A (1993). Convergence of acoustic, optical and net-catch estimates of euphausiid abundance – use of artificial light to reduce net avoidance. Canadian Journal of Fisheries and Aquatic Sciences, 50: 334-346.

Samson S, Hopkins T, Remsen A, Langebrake L, Sutton T and Patten J (2001). A system for high-resolution zooplankton imaging. IEEE Journal of Oceanic Engineering, 26:671-676.

Samuels WB, Uzzo A and Nuzzi R (1979). Correlations of phytoplankton standing crop, species diversity and dominance with physical-chemical data in a coastal salt pond. Hydrobiologia, 64: 233-237.

Savage VM, Gillooly JF, Brown JH, West GB and Charnov EL (2004). Effects of body size and temperature on population growth. American Naturalist, 163:E429-E441.

Saville, A. (1958). Mesh selection in plankton nets. Journal du Conseil International pour l'Exploration de la Mer, 23: 192-201.

Schweffer M, Rinaldi S, Huisman J and Weissing FJ (2003). Why plankton communities have no equilibrium: solutions to the paradox. Hydrobiologia, 491: 9-18.

Secor DH, Dean JM and Baldevarona RB (1989). Comparison of otolith growth and somatic growth in larval and juvenile fishes based on otolith length/fish length relationship. Reunion du Conseil. International de l'Exploration de la Mer, 191: 431–438.

Sheldon RW, Prakash A and Sutcliffe WH (1972). The size distribution of particles in the ocean. Limnology and Oceanography, 17: 327 -340.

Sheldon RW, Sutcliffe WH. and Pranjape MA (1977). Structure of pelagic food chains and relationship between plankton and fish production. Journal of the Fisheries Research Board of Canada, 34: 2344-2353.

Shin K, Jang MC, Jang PK, Ju SJ, Lee TK and Chang M (2003). Influence of food quality on egg production and viability of the marine planktonic copepod *Acartia omorii*. Progress in Oceanography, 57: 265-277.

Silliman RP (1946). A study of variability in plankton tow-net catches of pacific pilchard (*Sardinops caerulea*) eggs. Journal of Marine Research, 6:74-83.

Silvert W and Platt T (1978). Energy flux in the pelagic ecosystem: a time dependent equation. Limnology and Oceanography, 23: 813-816.

StJohn MA, Harrison PJ and Parsons TR (1992). Tidal-wake mixing – localized effects on primary production and zooplankton distributions in the Strait of Georgia, British Columbia. Journal of Experimental Marine Biology and Ecology, 164: 261-274.

Smith PE, Counts RC and Clutter RI (1968). Changes in filtering efficiency of plankton nets due to clogging under tow. Journal du Conseil, 32: 232-247

Smouse PE, Long JC and Sokal RR (1986). Multiple-regression and correlation extensions of the Mantel test of matrix correspondence. Systematic Zoology, 35:627-632.

Sprules WG, Casselman JM and Shuter BJ (1983). Size distribution of pelagic particles in lakes. Canadian Journal of Fisheries and Aquatic Sciences, 40:1761-1769.

Sprules WG and Munawar M (1986). Plankton size distributions in relation to ecosystem productivity, size and perturbation. Canadian Journal of Fisheries and Aquatic Sciences, 43: 1789 – 1794.

Sprules WG, Brandt SB, Stewart DJ, Munuwar M, Jin EH and Love J (1991). Biomass size spectrum of the lake Michigan pelagic food web. Canadian Journal of Fisheries and Aquatic Sciences, 48:105-115.

Sprules WG, Herman AW and Stockwell JD (1998). Calibration of an optical plankton counter for use in fresh water. Limnology and Oceanography, 43:726-733.

Sprules WG, Morris, TJ and Menza C (2001). OPC coincidence: a simulation approach. pp. 26-33 *In* No. 17. *Report of the GLOBEC Workshop on Optical Plankton Counters*, 17-20 June 2001, Tromsø, Norway.

Takahashi M, Seibant DL and Thomas, WH (1977). Occasional blooms of plankton during the summer in Saanich Inlet B.C., Canada. Deep Sea Research, 24:775-779.

Takahashi M, Berwell-Clarke JE, Whitney F and Koeller PA (1978). Winter condition of marine plankton populations in Saanich Inlet, B.C., Canada. .2 – Microzooplankton. Journal of Experimental Marine Biology and Ecology, 31: 27-37.

Takahashi M, Berwell-Clarke JE, Whitney F and Koeller PA (1979). Winter condition of marine plankton populations in Saanich Inlet, B.C., Canada. .1 – Phytoplankton and its

surrounding environment. Journal of Experimental Marine Biology and Ecology. 31: 283-301.

Thomson RE (1981). Oceanography of the British Columbia Coast. Canadian Special Publication of Fisheries and Aquatic Science 56. 291p.

Timothy DA, Soon MYS and Calvert SE (2003). Settling fluxes in Saanich and Jervis Inlets, British Columbia, Canada: sources and seasonal patterns. Progress in Oceanography, 59:31-57.

Tittel J, Zippel B, Geller W and Seeger J (1998). Relationships between plankton community structure and plankton size distribution in lakes of northern Germany. Limnology and Oceanography, 43: 1119-1132.

Tucker GH (1951). Relation of fishes and other organisms to the scattering of underwater sound. Journal of Marine Research, 10: 215–238.

Twombly S and Burns CW (1996). Effects of food quality on individual growth and development in the freshwater copepod Boeckella triarticulata. Journal of Plankton Research, 18: 2179-2196.

Velez-Belchi P, Allen JT and Strass VH (2002). A new way to look at mesoscale zooplankton distributions: an application at the Antarctic Polar Front. Deep-Sea Research Part II, 49:3917-3929.

Venrick EL (1999). Phytoplankton species structure in the central North Pacific, 1973-1996: variability and persistence. Journal of Plankton Research, 21: 1029-1042.

Vidondo B, Prairie YT, Blanco JM and Duarte CM (1997). Some aspects of the analysis of size distributions in aquatic ecology. Limnology and Oceanography, 42: 184-192.

Vidal J and Whitledge TE (1982). Rates of Metabolism of Planktonic Crustaceans as Related to Body Weight and Temperature of Habitat. Journal of Plankton Research, 4: 77-84.

Waldichuk M (1957). Physical Oceanography of the Strait of Georgia, British Columbia. Journal of the Fisheries Research Board of Canada, 14: 321-486.

Waite A, Fisher A, Thompson PA and Harrison PJ (1997). Sinking rate versus cell volume relationships illuminate sinking rate control mechanisms in marine diatoms. Marine Ecology Progress Series, 157: 97-108.

Weissburg MJ (2000). The fluid dynamical context of chemosensory behavior. Biological Bulletin, 198: 188-202.

Wiebe PH and Holland WR (1968). Plankton patchiness: effects on repeated net tows. Limnology and Oceanography, 13: 315-321.

Wiebe PH, Burt KH, Boyd SH and Morton AW (1976). A multiple opening/closing net and environmental sensing system for sampling zooplankton. Journal of Marine Research, 34: 313–326.

Wiebe PH (1970). Small-scale spatial distribution in oceanic zooplankton. Limnology and Oceanography, 15: 205-217.

Wiebe PH and Benfield MC (2003). From the Hensen net toward four-dimensional biological oceanography. Progress in Oceanography, 56: 7-136.

Winsor CP and Clark GL (1940). A statistical study of variation in the catch of plankton nets. Journal of Marine Research, 3: 1-34.

Yamazaki H, Mackas DL and Denman KL (2002). Coupling small-scale physical processes with biology. In: Robinson AR, McCarthy JJ, and Rothschild BJ (eds) *The Sea.* John Wiley & Sons, Inc., New York.

Yen J (2000). Life in transition: Balancing inertial and viscous forces by planktonic copepods. Biological Bulletin, 198: 213-224.

Yentsch CS and Duxbury AC (1956). Some factors affecting the calibration number of the Clarke-Bumpus quantitative plankton sampler. Limnology and Oceanography, 1: 268-273.

Yin K, Harrison PJ, Goldblatt RH and Beamish RJ (1996). Spring bloom in the central Strait of Georgia: interactions of river discharge, winds and grazing. Marine Ecology-Progress Series 138: 255-263.

Yin K, Harrison PJ, Goldblatt RH, Micheal St J and Beamish RJ (1997). Factors controlling the timing of the spring bloom in the Strait of Georgia estuary, British Columbia. Canadian Journal of Fisheries and Aquatic Sciences, 54: 1985-1995.

Zhang X, Roman M, Sanford A, Adolf H, Lascara C and Burgett R (2000). Can an optical plankton counter produce reasonable estimates of zooplankton abundance and biovolume in water with high detritus? Journal of Plankton Research, 22: 137-150.

Zhou M, Huntley ME (1997). Population dynamics theory of plankton based on biomass distributions. Marine Ecology-Progress Series 159: 61-73.

APPENDIX 1

Relationship between water transmissivity and the average particle size measured by the OPC.

A1.1 Introduction

During field deployments, it was noticed that the OPC measured high average particle sizes in water that had low transmissivity due to phytoplankton. Because the OPC measures the size of particles by the size of the shadow it casts, cloudy water can influence the perceived size of particles. The OPC measures light attenuance every 0.5s, which supposedly allows it to correct the measured size of each particle it encounters in cloudy water. However, from the slight increase in the measured particle sizes, it appeared that this correction factor may not have been effective during some of the STRATOGEM cruises. Several tests were performed to determine the extent of this error.

Because both an OPC and a transmissometer use LED lights to generate their respective measurements, it was thought that a comparison between the OPC's light attenuance (LA) and the % transmissivity (%Tx) from a transmissometer might clarify the problem. A depth profile of the OPC's measurements of LA were compared against a transmissometers measurements of %Tx. Average particle size was plotted against Tx to determine whether there is a measureable relationship between the two. Finally, the correlation coefficient between Tx and depth was calculated for depths between 2 and 100 meters across all casts from the STRATOGEM series. These tests were used to help determine which OPC data should be treated separately in the data analysis in chapter 3.

A1.2 Methods

A1.2.1 Comparison of measures of water cloudiness from the OPC's Light attenuance meter and the transmissometer

The first test was to determine whether the OPC's light attenuance meter measured similar depth-wise variation to a transmissometer. For one cruise in May 2003, light

attenuance from was measured using the OPC for depths from 0 to 100m in 2m depth bins, then plotted against depth. A Loess smoothing line was also plotted through the these values (Polynomial degree = 1, Smoothing coefficient = 0.2). The same procedure was repeated for the transmissometer data.

A1.2.2 Water transmissivity vs. average particle size

To determine whether there was a correlation between water tranmisssivity and the average particle size measured by the OPC, transmissivity was plotted against average particle size for every two meter depth bin (from 0 to 100m) in every cast on taken between March and September 2003 (70 casts total and 350 comparisons). A Loess smoothing curve was plotted through the resulting scatterplot (Polynomial degree = 1, Smoothing coefficient = 0.1), as well as a linear regression line.

To determine when transmissivity became correlated with average particle size, a Monte-Carlo randomization test was performed. First, a subset of the data was taken of all Tx values greater than 97%, along with the corresponding OPC average size data. The Pearson correlation coefficient between this subset of average sizes and transmissivity values was found. Then the average size values were permuted randomly (with replacement) and the correlation coefficient was re-calculated. This permutation was repeated 5000 times. The significance of the correlation between average size and Transmissivity (above 97%) was calculated as the proportion of permuted values that were greater or equal to the true correlation coefficient. This procedure was repeated for all levels of percent transmissivity.

A1.2.3 Correlation between transmissivity and average particle size at different depths

The effect of cloudy water on the OPC was largely restricted to surface waters, but the depth at which the relationship between transmissivity and average size became problematic was uncertain.. In order to determine this, the transmissivity and average size was calculated for every 2m depth bin for all casts taken between March and September 2003. For each depth, the correlation coefficient of transmissivity vs. average size was calculated and the results plotted against depth.

A1.3 Results

A1.3.1 Depth profiles of light attenuance and transmissivity.

The OPC's measure of light attenuance (LA) bore little resemblance to % transmissivity (Tx) (Figure A1.3). In the transmissometer data, the effect of phytoplankton on water clarity is readily visible between 0 and 25m depth. The LA data, on the other hand, is highly variable. There is a strong change of LA with depth, but it is not regular as with the transmissivity data.

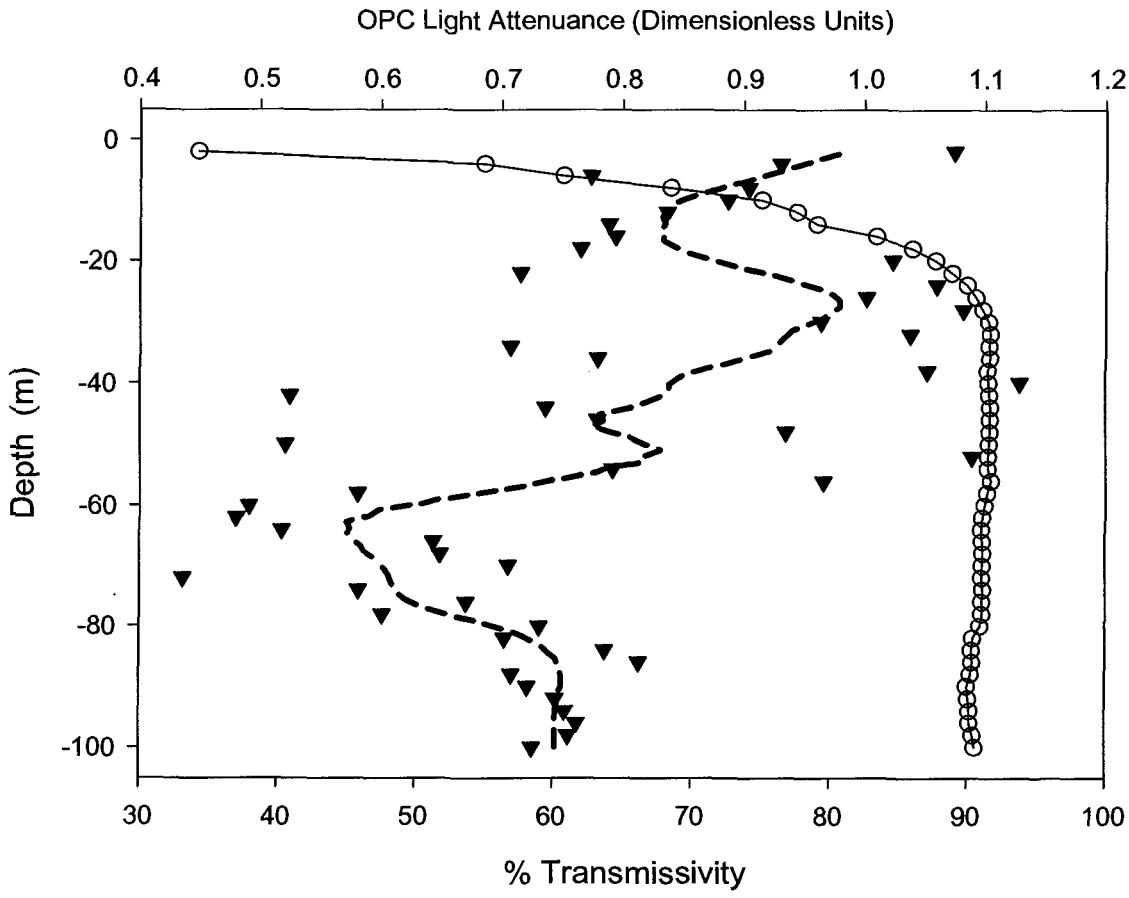

Figure A1.1 Depth profile of light attenuance (▼) percent transmissivity (○) in 2m depth bins. Dashed line is Loess smoothing line (Polynomial degree = 1, smoothing coefficient = 0.2).

A1.3.2 Average particle size vs. transmissivity

There is a clear relationship between average size vs. Tx (Figure A1.2). The equation of the regression line indicates that a 1% decrease in Tx causes a 0.015mm increase in average ESD. However, the Loess smoothing line shows that the relationship was linear. For clear water, (Tx = 94 to 100%), there was no significant relationship between Tx and size, while below 94% Tx there was ($p < 0.001$).

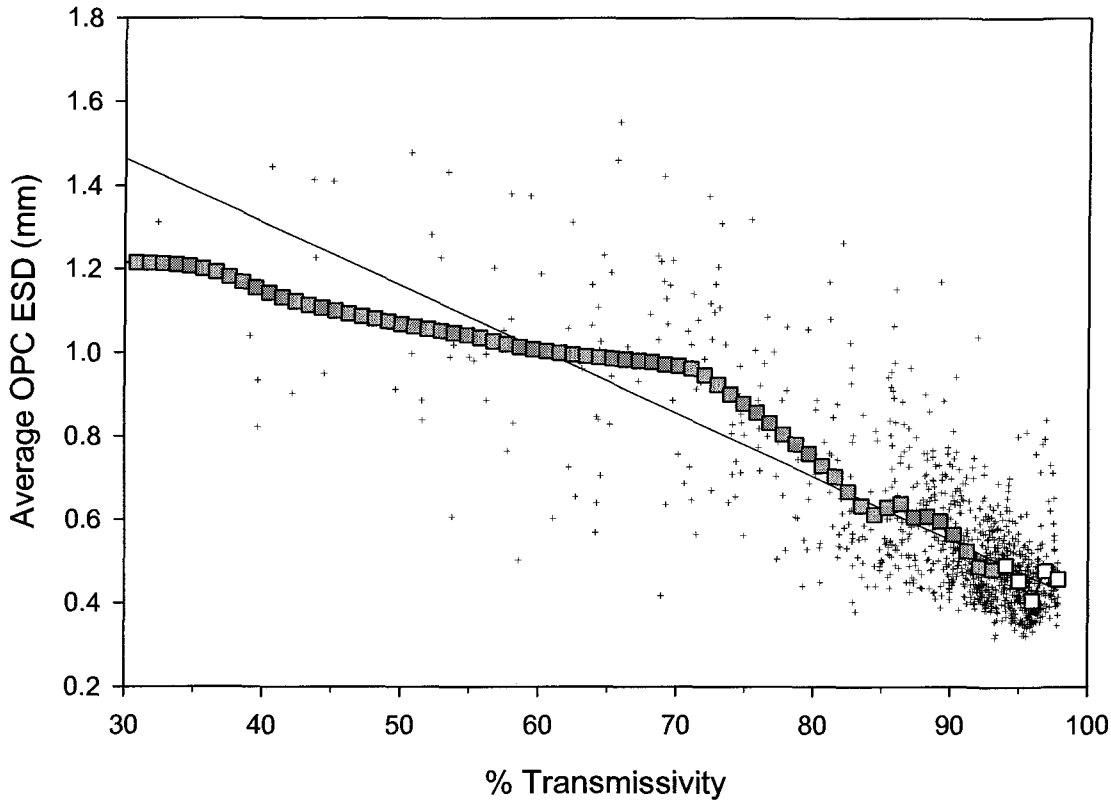

Figure A1.2. Plot of average particle size (mm, measured by the OPC) vs. % Transmissivity (from a transmissometer) for casts taken between March and September 2003 (+ indicates average values for a 2m depth bin). The data from 70 casts and 50 depth bins were plotted, for a total of 350 points. The straight line is a linear least squares regression with 99% confidence intervals (dotted lines). Equation of the regression line is ESD = - 0.015(Tx) + 1.92. Grey squares (■) denote Loess smoothing curve (polynomial degree = 1, smoothing coefficient = 0.1). Open squares indicate Tx values at which there is no significant relationship between Tx and average ESD (Monte-Carlo randomization test).

A1.3.3 Correlation of average size vs. Transmissivity at different depths

The relationship between average size and transmissivity was highly variable, though there appeared to be a falloff in the strength of the correlation with depth. (Figure A1.3). The largest *r* values occurred in the surface depths between 0 and 25m, though the correlation was significant at all depths.

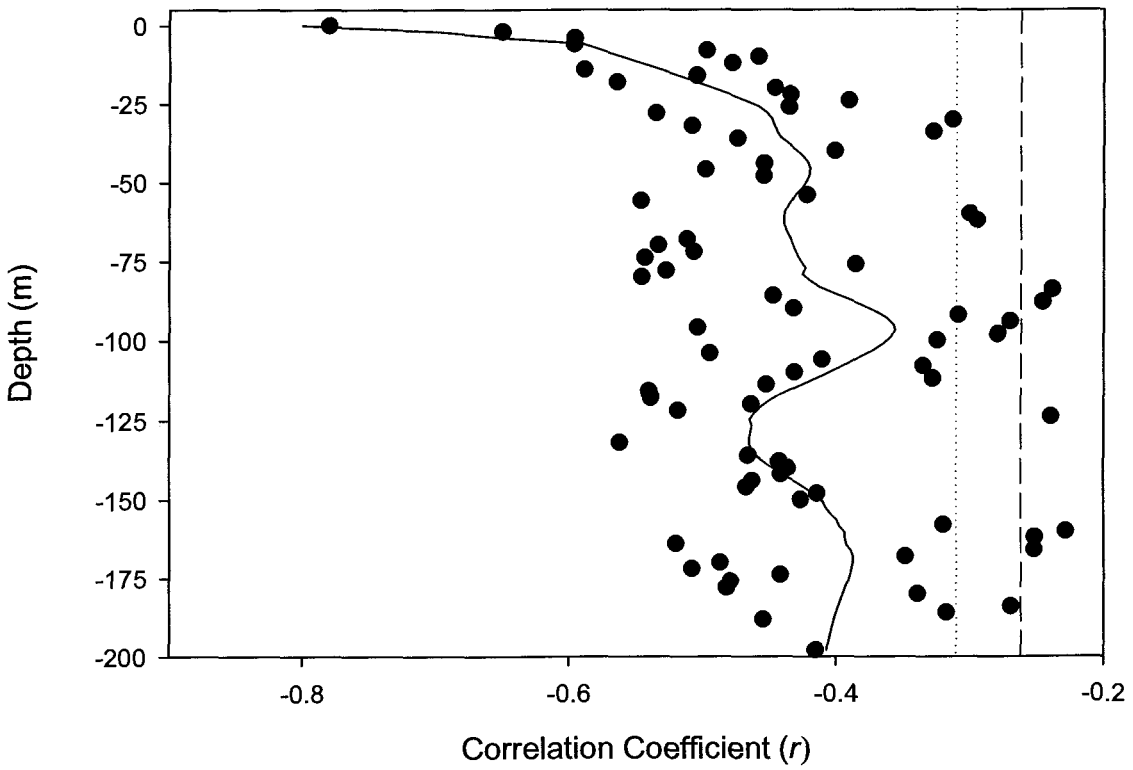

Figure A1.3. Correlation coefficient (*r*) of average particle size vs. transmissivity at different depths for all casts between March and September 2003. Each circle denotes the calculation for a 2m depth bin. Solid line is the Loess smoothing curve (polynomial degree = 1, smoothing coefficient = 0.1). The 1% (dotted line) and 5% (dashed line) significance levels of the correlation are shown.

A.1.4 Discussion

The OPC was affected in the field by low transmissivity water, likely corresponding to high concentrations of phytoplankton. The measurements of light attenuance taken by the OPC do not reflect the same increase in water clarity with depth that the transmissometer data show. Therefore, its use in correcting the measured size of particles in cloudy water is questionable. A clear relationship exists between water transmissivity and average particle size, indicating an upwards bias in the sizes of particles measured by the OPC. This relationship was significant only for Tx values below 94%. Much of the data taken in the STRATOGEM series was in water with lower transmissivity than this. However, the significance of the relationship at these levels may be partially due to the fact that most of the Tx values were between 90 and 100%. The strength of the correlation may therefore be significant but weak.

The falloff with depth of the relationship between Tx and average size indicates that the correlation between Tx and size is most important in surface (0 - 25m) waters. The correlation was significant at all depths, but this may again be simply due to the fact that there were so many data points. In light of this and of the fact that roughly half the samples were taken in water that had transmissivity of less than 94%, it was decided that the best solution would be to choose a cutoff depth of 25m. This effectively excluded all data taken in water of transmissivity 85% or less.

These data show that the OPC does have an inherent weakness. However, they should not be seen as to invalidate the findings of the previous chapters. The synchronicity of the net data with the OPC data suggest that they are still meaningful. Furthermore, the transmissivity data (which are related to chl *a* fluorescence) cannot be considered as independent of zooplankton abundance. It is therefore suggested that the OPC data be interpreted as is, though appropriate precautions should be taken (as in chapter 3) to avoid the inclusion of (potentially confounding) water with low transmissivity.

APPENDIX 2

Appendix 2: Brief description of biomass size-distribution theory

Assume that in a size-structured ecosystem, the biomass of organisms in the weight class $w_1 \rightarrow w_2$ is denoted by

$$\int_{w_1}^{w_2} \beta(w)dw \qquad \text{(A1.1)}$$

where β is the normalized biomass size distribution (Platt and Denman, 1977, 1978), such that β is equal to the biomass in weight class $b(w_1 \rightarrow w_2)$ divided by the weight interval w_2 minus w_1. Weight intervals in this model are logarithmically increasing with size. The derivation of the model describing energy flow through the ecosystem equates the biomass of organisms that *is not lost* through a loss term μ(w) (respiration and non-predation mortality) over an interval *dt:*

$$\int_{w_1}^{w_2} [1 - \mu(w)dt]\beta(w)dw \qquad \text{(A1.2)}$$

against the biomass of organisms which *grew* over the interval *dt:*

$$\int_{w_1+g_1(w_1)dt}^{w_2+g_2(w_2)dt} \beta(w+dt)dw \qquad \text{(A1.3)}$$

where g is the growth rate. In the bounds of integration of equation (3), the terms $w_1 + g_1(w_1)dt$ and $w_2 + g_2(w_2)dt$ describe how the weight interval $w_1 \rightarrow w_2$ changes due to growth over the time interval *dt*. In the model, mortality is assumed to occur before growth. The biomass of organisms in $w_1 \rightarrow w_2$ surviving the time interval *dt* should therefore be equal to the biomass of organisms present in the post-growth weight interval $w_1 + g_1(w_1)dt \rightarrow w_2 + g_2(w_2)dt$.

The quantities from (2) and (3) are assumed to be equivalent and the partial derivatives with respect to *dt* and *dw* are taken to produce:

$$\frac{\partial\beta(w)}{\partial t} = \frac{\partial(g(w,t)\beta(w))}{\partial w} - \mu(w)\beta(w) \qquad \text{(A1.4)}$$

This equation is similar to the McKendrick von Foerster equation for the growth of age-structured populations (e.g. Kott, 2001), as well as the mass balance equation used to described turbulence cascades in physical oceanography.